NGU Report 98.001

Phanerozoic palaeogeography and geodynamics
with Atlantic details

NGU
Norges geologiske undersøkelse
Geological Survey of Norway

Postboks 3006 - Lade
7002 TRONDHEIM
Tlf. 73 90 40 11
Telefaks 73 92 16 20

REPORT

Report no.: 98.001	ISSN 0800-3416	Grading: Open

Title:
Phanerozoic palaeogeography and geodynamics with Atlantic details

Author: Trond H. Torsvik & Elizabeth A. Eide	Affiliates: Mobil, NFR, OD, Phillips, Statoil & UiO

County:	Kommune:
Map-sheet name (M=1:250.000)	Map-sheet no. and name (M=1:50.000)
Deposit name and grid-reference:	Number of pages: 82 Price:140 Map enclosures:

Fieldwork carried out: 1996 and 1997	Date of report: 20.01.98	Project no: 2671.00	Person responsible: Odleiv Olesen

Summary:

In this report we synthesize palaeogeographic reconstructions over the last 500 million years. These reconstructions are global and should be regarded as first-order approximations. Reconstructions are essentially derived from 5 sources: (1) palaeomagnetic data, (2) magnetic anomaly data, (3) hot spot tracks, (4) biogeographic-tectonic data and (5) continental 'coast-line' fitting. Palaeomagnetic data provide quantitative information on palaeolatitude and palaeo-rotation of a continent, while palaeolongitude is unconstrained. The Palaeozoic reconstructions are essentially grounded in palaeomagnetic data combined with biogeographic-tectonic data.

The Late Palaeozoic to Early-Mid Mesozoic reconstructions are based on a combination of palaeomagnetic, magnetic anomaly data and 'coast-line' fits. Finally, Cretaceous and younger reconstructions (130-10.5 Ma) are 'absolute' reconstructions in a hot-spot/magnetic anomaly reference scheme. The latter reconstructions rely on the assumption that hot-spots are stationary or move at rates that are insignificant compared with plate-tectonic movements.

Data analyses, reconstructions and most figures were produced with the GMAP software of Torsvik & Smethurst (1998) which is located on http://www.ngu.no/geophysics or http://dragon.ngu.no.

Keywords: Geophysics	Palaeomagnetism	Hot-Spots
Palaeogeography	Magnetic anomalies	Geodynamics
North Sea	Offshore	Onshore

CONTENTS

1. INTRODUCTION

Palaeogeographic reconstructions have been an integral part of global tectonic research since the discovery of sea-floor magnetic anomalies and the advent of the plate tectonic paradigm. The display of reconstructions in sequential 'time slices' is a comprehensive method to view biogeographic, geologic and palaeogeographic information and is extremely useful to understand local and regional geologic relationships, as well as the fundamental driving forces of the Earth's core and mantle.

The reconstructions of Chris Scotese and co-workers and the palaeogeographic atlases propagated by Peter Ziegler and his group aided in promoting the concept and accessibility of these types of data and their displays within many tectonic research fields. The current work, which combines our own revised GMAP palaeogeographic reconstruction and analysis software with a new compilation of biogeographic and geologic data, is an advanced and expanded reconstruction package. We combine the capacity to analyse palaeogeographic data in the framework of palaeomagnetic, hot-spot and/or magnetic anomaly reference frames. Interpretations of the reconstructions derived from these datasets lead us to conclude that measurable 'misfits' exist between oft-reported reconstructions for the Late Palaeozoic and Mesozoic North Atlantic. We maintain that these misfits may be analysed quantitatively and can be attributed to known episodes of extension in specific regions of the North Atlantic zone; however we still require better Mesozoic palaeomagnetic data from the North Atlantic bordering continents before these misfits can be fully assessed.

This palaeogeographic atlas is a sub-product of the project 'Onshore-Offshore Tectonic Correlation in Western Norway' and is the first in an ongoing effort to constrain and understand large-scale plate rotations and collision-rift events in a rigorous plate tectonic framework. In this account, the Atlantic bordering continents are the main focus and as an example we do not discuss detailed aspects of the Tethys or Alpine evolution. Improvements and refinements to this palaeogeographic atlas will be developed in future co-operative projects.

2. PALAEOZOIC RECONSTRUCTIONS

The Early Palaeozoic continental plates comprised the independent plates of Laurentia, Baltica, Siberia and North China, as well as the Gondwana 'associates' which were fully assembled by Late Precambrian (c. 550 Ma) times (Meert & Van der Voo 1997). The

Laurentian plate included North America, Greenland and the 'European' elements of Scotland and North Ireland, all of which ultimately collided with Baltica and Avalonia during Silurian times (Figs. 1-5).

Baltica broadly comprised Eastern Europe (west of the present-day Urals) and Scandinavia; on most palaeogeographic maps, the NE margin of Baltica includes Novaya Zemlya. Other maps have depicted the northern and central parts of Taimyr as part of Baltica during the Palaeozoic (Ziegler 1990, Pickering & Smith 1995, Nikishin et al. 1996) or alternatively, have portrayed Taimyr as a separate microcontinent that ultimately collided with Siberia in Late Permian-Early Triassic times and became an extension of the polar Urals. However, recent evidence may indicate that Baltica actually extended NE from Novaya Zemlya through to, Taimyr in the Early Palaeozoic (Fig. 1) : the identification of Baikalian (Baltica)-age deformation (620-575 Ma) in parts of Taimyr (Gee 1996) and documented compatibility between Late Ordovician (mid-Ashgill) fauna from central Taimyr and Baltica (Cocks and Mudzalewskaya 1998) suggest that links may have existed between Baltica and north-central Taimyr from Late Precambrian time onward.

Other, smaller continental fragments also participated in the Palaeozoic chorus of the North Atlantic and are presently dispersed about the Tornquist margin of Baltica; these include Eastern Avalonia (including England) and the European massifs of Armorica, Bohemia and Iberia. The Tornquist margin presently records Late Ordovician amalgamation and Devono-Carboniferous collisions between Baltica and the massifs that are now constituents of Variscan Europe (Ziegler 1990, Franke 1989, Matte 1991). Palaeomagnetic data from many of the European massifs are sparse, but palaeomagnetic palaeolatitude estimates, fauna and facies data show that the European massifs and Avalonia bordered the northern areas of Gondwana during the Early Ordovician (Fig. 1).

Avalonia separated first from Gondwana (Fig. 2) and was eventually welded along the southern Baltic and eastern Laurentian margins. The Armorican, Iberian, Central and Bohemian Massifs were probably peripheral to Gondwana during lower-mid-Ordovician times (Figs. 1-3). Bohemia (Tait et al. 1995) rifted away from Gondwana by Caradoc-Ashgill times (Fig. 3), whilst existing, but old, data indicate that the Armorican and Iberian Massifs maintained close affinities to Gondwana at this stage.

2.1 Early Ordovician

In Early Ordovician times, Laurentia, Siberia and the North China Block occupied equatorial latitudes (Fig. 1) and were all dominated by warm-water carbonates. A passive or transform Tornquist margin of Baltica faced the Avalonia-European Massifs-Northwest Gondwana conglomerate in high southerly latitudes (>60°S). Arenig-Llanvirn (cf. time-scale in Table 1) platform trilobites (Fig. 1) indicate the existence of a separation between the low-latitude continents Laurentia, Siberia and the North China Block, the intermediate-latitude Baltica, and the high-latitude areas of NW Gondwana/Avalonia/Armorica (Cocks & Fortey 1990).

Siberia was geographically inverted and the present-day Taimyr perimeter faced the strongly overturned Caledonian margin of Baltica. Converging palaeolatitudes during the Arenig (compare Figs. 1 & 2) suggest 'closure' of an intervening oceanic domain with palaeo-northward subduction of Baltic continental crust in an ocean-ocean/arc zone between Baltica and Siberia. This subduction event, with local arc development, was later followed by uplift and retrograde metamorphism of eclogites and obduction of Early Ordovician ophiolites across what is now the western margin of Baltica (Torsvik et al. 1995). A c. 2000 km wide Tremadocian Ocean between Baltica and Siberia (Fig. 1) was considerably narrowed at the Llanvirn-Llandeilo boundary (Fig. 2).

2.2 Middle Ordovician

Ordovician break-up of Gondwana commenced with rapid rifting of Avalonia away from Gondwana's NW margin during Arenig times (Fig. 2) and resulted in reduction of the width of the Iapetus Ocean across the British sector from 5000 to 3000 kilometres (Torsvik & Trench 1991). An Early Ordovican Avalonian arc-subduction zone (Fig. 1) may have been shut down as Avalonia rifted away from NW Gondwana; northward movement of Avalonia was facilitated and enhanced by development of a spreading regime between Gondwana and Avalonia (Fig. 2). A NW-directed subduction zone(s), along or adjacent to the Laurentian margin, is likely to have been established sometime during the Ordovician (Coakley & Gurnis 1995), although the polarity of subduction along Laurentia during the Ordovician remains contentious (Bock et al. 1996). A southward-dipping subducted margin (e.g. Pickering & Smith 1995) along Laurentia during the Early Ordovician (Fig. 1) would require a polarity 'flip' to the NW-dipping configuration envisioned at Mid-Ordovician time (Fig. 2).

2.3 Late Ordovician

As Avalonia drifted northwards and opened the Rheic Ocean (Figs. 2 & 3), Baltica continued to move northward with simultaneous counter-clockwise rotation; the latter vorticity peaked at c. 2 deg/Ma in Caradoc times (Fig. 3). Closure of the Tornquist Sea between Baltica and Avalonia is indicated by subduction of oceanic crust (Fig. 3) beneath Eastern Avalonia (Noble et al. 1993) and faunal mixing between Avalonia and Baltica (Cocks & Fortey 1982, 1990, McKerrow et al. 1991). The Tornquist Sea had closed sufficiently to form 'Balonia' (Baltica + Eastern Avalonia) by latest Ordovician (Fig. 4) or earliest Silurian times (Torsvik et al. 1993). Elimination of the Tornquist Sea and production of the North German Polish Caledonides involved a strong component of palaeo-East-West closure and was probably dominated by dextral amalgamation of the two continents (Torsvik & Trench 1991). The timing of this closure may correspond to the early Ashgill Shelvian Orogeny in Britain (Toghill 1992). It is noteworthy that Caledonian Nappes in western Norway (excepting the Jotun Nappe), emplaced on Baltica during Mid-Silurian times, primarily record Ordovician cooling ages (Andersen et al., 1997) that peak at 450-440 Ma (Figs. 6a & d). These cooling ages are broadly similar to Taconic (c. 450 Ma) deformation on the Laurentian margin and the age of magmatic-arc activity in Eastern Avalonia (Fig. 3).

Balonia was situated at low latitudes by the end of the Ordovician (Fig. 4); this latitudinal shift was marked by the first appearance of warm-water Bahamian type reefs in Late Ordovician and Mid-Silurian times, respectively, on Baltica and Eastern Avalonia. Conversely, parts of Gondwana were glaciated in the Late Ordovician (Scotese & Barret 1990) (Fig. 4). Siberia moved eastward with respect to Baltica either during or shortly after the Caradoc. As noted earlier during Ordovician to Early Silurian times (Figs. 2-4), Baltica rotated counter-clockwise (vorticity peak during the Caradoc; Fig. 3) as it moved northward. This rotation-translation probably gave rise to a deep-seated, strike-slip regime in the narrowing oceanic tract between Baltica and Siberia (Torsvik et al. 1995). The strike-slip origin postulated for the extensive allochthonous tracts of Late Ordovician (Ashgill) granites in Mid-Norway (Nordgulen 1993) may have originated in this type of mega-strike-slip regime.

2.4 Silurian

The 420-430 Ma palaeomagnetic poles from Baltica, Scotland and North America (Torsvik et al. 1993, 1996) are virtually identical in a Bullard et al. (1965) fit (BFIT) and indicate that Baltica collided, probably obliquely, with Laurentia and caused the Scandian Orogeny in western Norway

during Mid-Late Silurian times (Fig. 5). In western Norway (Sunnfjord), the continental collision can locally be dated by the stratigraphic and deformational history (Torsvik et al. 1997; Andersen et al. 1998). In this area, the Solund-Stavfjord Ophiolite (443±3 Ma, Dunning & Pedersen 1988) was obducted above continental margin deposits of Wenlock age (428-424 Ma) (Fig. 6d). The Wenlock deposits overlie Precambrian rocks which record an earlier 'Taconian-aged' (446-449 Ma) cooling event. These cooling ages are marginally older or overlap with the Solund-Stavfjord Ophiolite, a preserved remnant of the Iapetus oceanic lithosphere (Fig. 5), which probably evolved in a Caledonian marginal basin (Furnes et al. 1990).

Prior to their Silurian collision, Laurentia was nearly stationary at the equator whereas Baltica had a rapid northward-directed latitudinal velocity component of up to 8-10 cm/yr (Fig. 5 & 6c). Whole-scale palaeo-westward subduction of Baltic continental crust gave rise to extreme crustal thickening in the Caledonian Belt, exemplified by the preserved high-pressure terranes in western Norway (Andersen et al. 1991, Dewey et al. 1993, Eide & Torsvik 1996). Sinistral transpressive deformation prevailed (Hutton 1987) and Scandian thrust-related orogenesis continued into Devonian times in northern areas of Norway. The age of Late Caledonian eclogite metamorphism in the lower plate have often been cited to c. 425 Ma; the high-pressure metamorphism is interpreted to signify the 'main' collision between Baltica-Laurentia. An analysis of the most reliable metamorphic ages, however, show a large metamorphic age spread between 400 and 450 Ma (Figs. 6b). Moreover, eclogite ages from the upper plate (allochthonous rocks on the Western Gneiss Region) yield a generally higher range of ages (420-470 Ma; Fig. 6a). Thus, data from both plates demonstrate variable ages of metamorphism, probably indicative both of subduction-collision diachroneity (early metamorphism of nappe-eclogites and later metamorphism of Western Gneiss Region eclogites) and of their differential exhumation and final emplacement (Fig. 6c). These data also imply that the oft-quoted '425 Ma' collision-metamorphism event necessarily oversimplifies the operative tectonic processes of the times.

2.5 Devonian and Carboniferous

The Scandian event was followed by Emsian extensional collapse at least in the southwestern parts of Norway, but from central Scotland to New York, compressional events continued in the form of the Emsian/Eifellian Acadian Orogeny (McKerrow 1988). The extensional collapse in western Norway is recorded by uplift-cooling ages implying

temperatures of ca. 320-430°C within the Western Gneiss Region (lower plate), that peak between 390-400 Ma (Fig. 6b).

During Late Silurian and Early Devonian times, Euramerica (probably comprising Laurentia, Avalonia, Baltica and Barentsia) rotated counter-clockwise while undergoing southward-directed movement that narrowed its oceanic separation from both the European Massifs and Gondwana. In Mid-Devonian times (Fig. 7) Euramerica stretched from low northerly latitudes (Taimyr-Barenstia) to intermediate high southerly latitudes (North America). Siberia was still geographically inverted while Kazakhstan probably approached the Baltic margin of Euramerica (Fig. 7). Siberia essentially stayed northeast of Baltica until their terminal collision in Late Permian-Early Triassic times (see later).

Parts of the 'Devonian' in East Greenland have recently been demonstrated to be of Lower Carboniferous age (pole B in Fig. 8; dated to 336 Ma ($^{40}Ar/^{39}Ar$ plagioclase, Hartz et al. 1997) & 342 Ma (Ub/Pb zircon, Hartz, in progress)). The Devonian and the Lower Carboniferous are separated by a major unconformity; this Lower Carboniferous unconformity in Greenland has regional links to episodes of inversion and block faulting known in central England, Scotland, Spitsbergen and to a newly identified Early Carboniferous unroofing event in Western Norway (Eide et al. 1998).

Devonian and Carboniferous poles (Fig. 8) from Laurentia (North America/Scotland) and Baltica can be matched in a BFIT. The Lower Carboniferous (pole B) and an Upper Devonian Givetian pole from East Greenland (pole A in Fig. 8a-b) overlap with Laurentia and Baltica poles after reconstructing the Labrador Sea (Hartz et al. 1997). The collective data imply a near-equatorial position for Greenland during Late Devonian and Early Carboniferous times (Figs. 7-8c). We do, however, note a minor but systematic easterly offset of both Greenland poles compared with reference poles (Fig. 8a-b); the overall misfit of these poles is minimized in a BFIT. Both fits may indicate that the amount of pre-drift, Labrador Sea extension has previously been underestimated. The fits can alternatively be improved by invoking Late Devonian to Early Carboniferous local, counterclockwise block rotations of the East Greenland "Devonian" basin. Since Baltica had docked obliquely against Laurentia from the south (Torsvik et al. 1996), the resulting transpression could, via strain partitioning, have caused local rotations, folding, and left-lateral faulting by continued northward translation of Baltica relative to Laurentia. Such local block rotations may verify a linkage to other left-lateral faults within the Caledonian orogen such as the Great Glen Fault in Scotland and/or the Møre-Trøndelag Fault Zone in west-central Norway (Fig. 8).

2.6 Permian and formation of Pangea

During the Palaeozoic all continents converged to form the Supercontinent Pangea by Permian or earliest Mesozoic times. Formation of Pangea completed a c. 500 Ma Supercontinental cycle that had commenced with break-up of the old Rodinia Supercontinent at c. 750-725 Ma (Torsvik et al. 1996). In southern Norway, the rocks in the Oslo region experienced a continuous series of events related to final amalgamation of Pangea. The highlights of Late Palaeozoic activity in the Oslo region are considered to include N-S compression and related dextral transpression and transtension as Variscan tectonics advanced northward through continental Europe. Dextral transtension led to development of a purely extensional regime in the Oslo Rift system and the culmination of rifting and peak magmatic activity in the Oslo Graben in Early Permian times (Ramberg 1976, Ramberg & Larsen 1978, Sundvoll & Larsen 1994, Olaussen et al. 1994).

Details about the geometry of Pangea (see discussion on configuration A, B or C in Van der Voo 1993) and the final assembly timing are matters of dispute, most notably with respect to the relative position of Gondwana-Euramerica in the configuration (see Muttoni et al., 1996; Torcq et al. 1997). While most authors would argue for a transition from Pangea B to A during Permian times, Torcq et al. (1997) maintain Pangea B well into the Triassic (Fig. 9); if the latter is correct, it would require massive dextral shear (c. 3500 km) between Gondwana and Euramerica during the early Triassic (<244 Ma) and would have obvious implications for interpretations of the resulting geology along the plate margins.

An additional problem in Late Palaeozoic and Early-Mid Mesozoic reconstructions relates to the detailed palaeomagnetic fits between the various continental elements. In a number of critical regions and time periods, palaeomagnetic data are either unavailable, or have questionable reliability, in addition to the fact that palaeomagnetic data cannot resolve palaeo-longitude. Other data sources must thus be used to supplement the palaeomagnetic record. Two principal relative continental fits (sometimes modified with palaeomagnetic data) that allow extrapolation backwards to Permian Pangea reconstructions are the BFIT, essentially based on 'coast-line' fitting (500 foot contour interval) and the fit based on magnetic anomaly fits (the oldest anomaly is c. 166 Ma). Magnetic anomaly fits must principally be considered *minimum* fits since they do not account for pre-drift extension. However, with outstanding palaeomagnetic and magnetic anomaly data it is possible, in principle, simply to calculate pre-drift extension from the net difference between the two fits. The net difference between a

palaeomagnetic fit before drift and the fit commencing with the first magnetic anomaly (at c. 166 Ma) would thus represent the amount of pre-drift extension.

The Permian and Early Mesozoic backward extrapolated magnetic anomaly fits of Lottes and Rowley (1990, LRFIT) have been used extensively in the literature but, as pointed out by the original authors as well as Van der Voo (1993), the LRFIT is inconsistent with high-quality Permian data from Baltica-Europe and Laurentia. Indeed, the BFIT fit is superior for Permian and older times (Fig. 10a; see also Figs. 5 & 8) compared to the LRFIT with respect to the Greenland-Europe-Laurentia positions. In Fig. 10, *insitu* Laurentia mean palaeomagnetic poles are plotted as solid circles whilst reconstructed (i.e. closing the North Atlantic) Laurentia poles (LRFIT or BFIT) are shown as open circles (all with error ellipses). Baltica (/Europe) are shown as open squares. Note, for example, that the Permian pole for Baltica only overlaps with the Laurentia pole after using a BFIT for the North Atlantic. The Laurentia pole in a LRFIT is not concordant with the Baltic pole (Fig. 10a). In Early Jurassic times, the distinction between the BFIT and LRFIT is less clear (all fits overlap at the 95% confidence level); taken at face value, however, the BFIT is better since the mean poles are almost identical (Fig. 10b). On the other hand, by the Early Cretaceous, the LRFIT is the better of the two (Fig. 10c). These comparisons imply that the North Atlantic fits changed from a BFIT ('coastlines') to a LRFIT ('magnetic anomaly') type during the Mesozoic. These modifications were probably manifested by the Permian-Early Triassic and Mid-Jurassic-Early Cretaceous rifting events documented in the North Sea and the Rockall areas.

Differences between the BFIT and the LRFIT are demonstrated in Fig. 11, and both relative reconstructions are supposed to be representative for Permian times. In the BFIT (Fig. 11a) we notice a tighter fit toward Greenland for areas west of the British Isles/Rockall zone and a rather looser fit in the Arctic areas (Spitsbergen-Greenland) compared to the LRFIT for the same time period (Fig. 11b). Therefore, the transition from a BFIT to a LRFIT in Mesozoic times must require some 200 km of E-W extension (probably asymmetric) west of the British Isles/Rockall area, probably accompanied by some 100 km of extension in the North Sea. The latter are not accounted for in Figure 11.

3. MESOZOIC AND CENOZOIC RECONSTRUCTIONS

3.1 Triassic

The Supercontinent Pangea (Fig. 12) was equatorially centred during Mid-Late Permian times subsequent to its northward movement during Mid-Devonian through

Carboniferous times (Figs. 7-8). In this construction the southern parts of Euramerica (Laurentia + Eurasia) straddled the equator while the Gondwanan part of Pangea stretched to high southerly latitudes. The latter is readily noticed in the stratigraphic record by the presence of glaciogenic deposits in southern Gondwana (Fig. 12a). We prefer the Pangea reconstruction shown in Fig.12a (BFIT for the North Atlantic; see discussion above), but notice that the polar Urals (collision between Siberia and Eurasia) were probably not finally sutured until the Early Triassic (Fig. 12c). Some dextral shear between Gondwana and Euramerica may still have been in progress; continued collisional shear may provide the link to Permian-Early Triassic rifting in the North Sea/Rockall area.

The overall Pangea configuration lasted at least to the Mid-Jurassic, but underwent minor modification due to pulsed extensional episodes (e.g. from BFIT to LRFIT type). In the North Sea and within the central parts of Pangea, we recognise two major rift-phases, i.e. in Permian-Early Triassic and Mid-Jurassic-Early Cretaceous times. Permo-Triassic E-W extension was probably significantly greater and more regionally important than the Mesozoic extension (Færseth et al. 1995). In onshore areas in western Norway, Permian-aged low-angle fault-rejuvenation (Torsvik et al. 1992, Osmundsen 1996, Eide et al. 1997) and coast-parallel dykes (Færseth et al. 1976, Løvlie & Mitchell 1982, Torsvik et al. 1997) further attest to the importance of Late Palaeozoic rifting in the region (Fig. 13). New ^{40}Ar-^{39}Ar ages from the youngest Permo-Triassic dyke-activity in the coastal areas (Eide et al. 1998; Torsvik et al. 1998) give ages between 243-235 Ma; this we consider to date the terminal phase of the Permian-Early Triassic rift event.

Northwest Europe occupied latitudes between 15 and 30°N in early Triassic times, i.e. essentially within the northern arid belt of Pangea (Fig. 13). The main Zechstein evaporite belt was located between 15 and 20°N. Pangea moved northwards during the Triassic (Figs. 13 and 14a) and we maintain a BFIT configuration for North America-Greenland-Eurasia also at this time. Due to uncertainties in the Triassic and parts of the Jurassic palaeomagnetic database for North America, we use a newly constructed apparent polar wander path for Eurasia (Fig. 14b) for parts of the Mesozoic (Torsvik, in progress). We use this latter path to position the continents on the correct latitudes at 225 Ma, 175 Ma and 150 Ma (Figs. 14a & 17).

3.2 Jurassic

The oldest identified magnetic anomaly is of mid-Jurassic age (c. 166 Ma, Central Atlantic) but the break-up of Pangea is likely to have started at c. 175 Ma (Figs. 15 & 16). From this time period and onward, we use magnetic anomalies extensively for relative plate fits (Table 4), while we use palaeomagnetic data for the latitudinal positions of the continents. In the Atlantic region, sea-floor spreading began in the Central Atlantic (Fig. 15), was followed by the South Atlantic (c. 133 Ma), the Labrador Sea (c. 95-46 Ma) and finally, by the East North Atlantic, which opened at c. 56 Ma.

A relative reconstruction (c. 175 Ma) at the dawn of Pangea break-up, based on magnetic anomalies/backward extrapolation (Tables 3 & 4), is illustrated in Figure 16, but we have earlier noted that Laurentia-Eurasia is better constrained with the BFIT at this time (Fig. 10); hence, in the latitudinally controlled reconstruction at 175 Ma (Fig. 17a), we maintain a BFIT for the northern continents (North America-Greenland-Eurasia). The transition from BFIT to LRFIT type is probably gradual and related to the Permo-Triassic and Mesozoic rifting events, but for the Late Jurassic (c. 150 Ma) reconstruction we have switched to a magnetic anomaly fit (Fig. 17b).

The Mid-Jurassic is associated with two major global events that led to the break-up of Pangea, (1) initiation of NW-SE directed sea-floor spreading in the Central Atlantic and (2) rifting of the south-Gondwana elements (Antarctica-Australia-Madagascar-India) from Pangea (Gondwana dispersal) (Fig. 17a-b). Important E-W or NW-SE (Færseth 1996), mid-Jurassic-early Cretaceous rifting in the North Sea area (Fig. 18) is time-equivalent with this global dispersal of Pangea. Mid-Jurassic rifting in the North Sea/NW Europe is associated with a major extrusive centre (Forties) and local volcanics; the latter, probably of syn-rift origins, are also present in onshore areas in Scandinavia, e.g. Sunnhordland (162±4 Ma) and SW Sweden (Gobnehall 179±4 Ma; Fig. 18). In addition, important reactivation of low-angle fault systems in western Norway is noted in the Late Jurassic and Early Cretaceous (Figs. 19 & 20). Onshore dykes and fault-rock development (reactivation of older lineaments) demonstrate the intimate tectonic links between onshore and offshore rift evolution (Torsvik et al. 1992, 1997; Eide et al. 1997, 1998; Dore et al. 1997).

3.3 Cretaceous

From early Cretaceous times (130 Ma) we use hot-spots from the Atlantic and the Indian Ocean (Müller et al. 1993, Table 2) combined with magnetic anomalies (Table 3) for

total reconstructions (Figure 21 and onwards). We assume that hot-spots are stationary or move at insignificant speeds relative to plate-tectonic speeds. If this assumption is correct, hot-spot references and their corresponding reconstructions offer a unique contribution to palaeoreconstructions because they give palaeologitudinal control on plate positions, in contrast to reconstructions based on palaeomagnetic data alone. It should be noted though, that the 'stationarity' of hot-spots is disputed (e.g. Tarduno & Cottrell 1997).

During most of the Early and Mid-Mesozoic, the Pangean elements moved northwards and by the Early Cretaceous, south Scandinavia stretched southward to approximately 45°N according to hot-spot/magnetic anomaly (HOTMAG) reconstructions. In Europe, we lack high-quality paleomagnetic data at that time, but using North American (120-128 Ma) poles, we do notice a minor discrepancy between the PALMAG and the HOTMAG reconstructions (essentially a problem of palaeorotation) (Fig. 21). It should also be mentioned that hot-spot tracks between 130-84 Ma is based on only two Atlantic hot-spots, i.e. Tristan da Cunha and the Great Meteor.

During the Early Cretaceous most of the plate activity occurred amongst the former Gondwana elements of Pangea (Figs. 21-23). The south Atlantic opened at c. 133 Ma and in the West North Atlantic, the Labrador Sea started to open at c. 95 Ma (Fig. 23).

In the Indian Ocean, India (together with e.g. the Seychelles; not shown on maps) separated from Africa-Madagascar at 90-80 Ma; this separation has been linked to initiation of the Marion hot-spot. A reconstruction of Madagascar (Torsvik et al. 1998) using palaeomagnetic data from the break-up related Marion volcanics, agrees perfectly with the HOTMAG reconstruction (compare hot-spot and palaeomagnetic latitudes of Madagascar in Fig. 24). This Marion hot-spot 'burner' drove the separation of India-Seychelles group from Madagascar in Cretaceous time. The India-Seychelles amalgam continued to drift northward until the two of them separated over the Reunion hot-spot (Figs. 24- 25); interaction with Reunion produced the massive Deccan traps at the K-T boundary (c. 65 Ma). The subsequent collision of India with Eurasia in Palaeocene time followed rapid NNE-directed motion of India (Figs. 25 and 26-28) as the eastern Tethys was consumed. From about 68 to 43 Ma, the rates of India's northward drift ranged from 18 to 9.5 cm/yr; full-scale collision with Eurasia is marked by the dramatic decrease in rate of India's speed (to ca. 5 cm/yr) relative to Asia at ca. 43 Ma (Fig. 25).

3.4 Tertiary

By Late Cretaceous times, North Atlantic spreading was well underway, but Greenland remained close to Europe as spreading initiated in the Labrador Sea. East North Atlantic spreading between Greenland and Europe was initiated at around 56 Ma, whilst Labrador spreading ceased at around 46 Ma (Figs. 26-28).

Cretaceous and Tertiary 'absolute' movements and average velocities of two selected localities from Greenland (75°N & 320°E) and 'Eurasia' (Oslo:60°N & 010°E) in a hot-spot/magnetic anomaly reference frame are illustrated in Fig. 31. NNE-directed movement of both Greenland and Eurasia is evident in Early-Mid Cretaceous times. Velocities for Eurasia were moderate and peaked at 2.5 cm/yr in the Late Cretaceous (90-60 Ma; Fig. 31b). Conversely, Greenland velocities were consistently higher, peaking at 4.2 cm/yr in early Tertiary times, i.e. during opening of the East North Atlantic (Fig 31a). Both Greenland-'Eurasia' show an interesting directional shift, from NNE to NNW, in Late Cretaceous time (Fig. 31a). This shift is time-equivalent with opening of the Labrador Sea where spreading stopped at c. 46 Ma; however, the NNW track shows that the overall movement of Greenland-Eurasia was not governed by Labrador ridge-push but rather by 'external' forces. Ridge push would not have allocated the NNW-directed movement, and a global force contributing to the overall NNW-directed shift in both plates may be commencement of subduction in the Pacific. Greenland continued tracking NNW until recent times, i.e. independent of shut down of sea-floor spreading in the Labrador Sea at c. 46 Ma. Conversely, the Eurasian track rotated clockwise after opening of the East North Atlantic (Fig. 31a). Both Greenland and Eurasia show reduced velocities during the Tertiary. Present-day velocities for both plates in a hot-spot reference frame (calculated from the NUVEL-1 model; Gripp & Gordon 1990) are 1.86cm/yr and 0.93 cm/yr, respectively (Fig. 31b).

4. SUMMARY

Calculations of palaeolatitude and velocities for Baltica/Eurasia, combining hot-spot reference data (0-130 Ma) and palaeomagnetic data, are shown in Fig. 32. Baltica occupied high southerly latitudes in the early Ordovician (Fig. 1) and following high northward velocities (c. 8-11 cm/yr), collided with Laurentia during the mid-Silurian (c. 425 Ma). These velocities are not unrealistic when compared with the only 'modern' analogue, the India-Eurasia collision in Tertiary times (Fig. 25). The Baltica-Laurentia collision hallmarks included high, pre-collision plate velocities, whole-scale subduction of Baltic continental crust and ensuing rapid Late Silurian-Lower Devonian exhumation of an orogen that contains high- and ultra-high pressure metamorphic rocks (Andersen et al. 1991; Dewey et al. 1993; Eide & Torsvik 1996). The Himalayan region is the archetypal continent-continent collision zone and has four basic features in common with the Baltica-Laurentia collision in mid-Silurian times (Figs. 5-6): 1) high pre-collision plate velocities; 2) whole-scale subduction of the continental crust of the colliding plate; 3) rapid exhumation of an orogen that includes high-pressure metamorphic rocks and 4) partial to complete delamination of the thermal boundary layer beneath the over-thickened continental crustal package (Eide & Torsvik 1996).

Extensional and erosional unroofing along the central parts of the Caledonian Baltica-Laurentia orogen eventually resulted in formation of high-angle faults in the exhumed middle and upper crustal complexes. These faults subsequently controlled the formation of the Devonian Old Red Basins of Western Norway (Osmundsen 1996) and were rooted in an array of lower-angle, extensional detachments that presently floor the eastern margins of the Devonian Basins (Andersen & Jamtveit 1990).

The amalgamated Euramerica drifted northwards during most of the remaining part of the Palaeozoic and was finally embedded as part of Pangea. The final Pangea assembly in Permo-Triassic times probably concluded with dextral shear between Euramerica and Gondwana. This shearing was contemporaneous with Permian-early Triassic rifting in the North Sea and the Rockall area.

The Pangean Supercontinent drifted northwards during Triassic-early Jurassic times until break-up began in the Mid-Jurassic. The SE-NW opening of the Central Atlantic probably started at c. 175 Ma whilst the oldest preserved magnetic sea-floor anomaly is c. 166 Ma. Pre-rift extension in mid-Jurassic time and syn-rift extension in late Jurassic time in the North Sea probably developed within a SE-NW extensional field. This broadly Jurassic extensional period in the North Atlantic correlates globally with the break-up of Pangea (Fig.

32). The other areas of focused extension included the opening of the Central Atlantic and sea-floor spreading along the southern margin of Pangea.

5. REFERENCES

Andersen, T.B. & Jamtveit, B., 1990. Uplift of deep crust during orogenic extensional collapse: A model based on field studies in the Sogn-Sunnfjord region, W.. Norway. Tectonics, 9, 1097-1111.

Andersen, T.B., Skjerlie, K.P. & Furnes, H. 1990. The Sunnfjord Melange, evidence of Silurian ophiolite accretion in the West Norwegian Caledonides. Journal Geological Society London, 147, 59-68.

Andersen, T.B., Jamtveit, B., Austrheim, H. & Dewey, J.F., 1991. Subduction and eduction of continental crust; major mechanisms during continental collision and orogenic extensional collapse. Terra Nova, 3, 303-310.

Andersen, T.B., Berry, H.N., Lux, D.R. & Andresen, A. 1998. The tectonic significance of pre-Scandian $^{40}Ar/^{39}Ar$ phengite cooling ages in the Caledonides of western Norway. Journal Geological Society London (in press).

Berggren, W.A., D.P. McKenzie, J.G. Sclater, & J.E. van Hinte, 1975. World-wide correlation of Mesozoic magnetic Anomalies and its implications: Discussion & reply, Geol. Soc. Am. Bull., 86, 267-272.

Bock, B., McLennan, S.M. & Hanson, G.N., 1996. The Taconian orogeny in southern New England:Nd-isotope evidence against addition of juventile components. Can. J. Earth Sci., 33, 1612-1627.

Bullard, E.C., Everett, J.E. & Smith, A.G., 1965. The fit of the continents around the Atlantic. R. Soc. Lond. Phil. Trans. Ser. A., 258, 41-51.

Cande, S.C. & Kent, D.V., 1995. Revised calibration of the geomagnetic polarity timescale for the Late Cretaceous and Cenozoic. J. Geophys. Res., 100, 6093-6095.

Cande, S., LaBrecque, J.L., and Haxby, W.B., 1988, Plate kinematics of the South Atlantic: Chron 34 to present, J. Geophys. Res., 93(B11): 13479-13492.

Coakley, B. & Gurnis, M., 1995. Far-field tilting of Laurentia during the Ordovician and constraints of the evolution of a slab under an ancient continent. J. Geophys. Res., 100, 6313-6327.

Cocks, L.R.M. & Fortey, R.A., 1982. Faunal evidence for oceanic separations in the Palaeozoic of Britain. J. Geol. Soc. Lond., 139, 465-478.

Cocks, L.R.N. & Fortey, R.A., 1990. Biogeography of Ordovician and Silurian faunas. In McKerrow, W.S. & Scotese, C.F. (eds.) Palaeozoic palaeogeography and biogeography. Geol. Soc. Lond. mem. 12, 97-104.

Cocks, L.R.M. & Modzalevskaya, T.L., 1998. Late Ordovician brachiopods from Taimyr, arctic Russia, and their palaeogeographical significance (in press).

Dewey, J.F., Ryan, P.D. & Andersen, T.B., 1993. Orogenic uplift and collapse, Crustal thickness, fabrics and metamorphic changes:The role of eclogites. Geol. Soc. Lond. Spec. Publ. 76, 325-343.

Dore, A.G., Lundin, E.R., Fichler, C. & Olesen, O., 1997. Patterns of basement structure and reactivation along the NE Atlantic margin. J. Geol. Soc. Lond., 154, 85-92.

Dunning, G.R. & Pedersen, R.B., 1988. U/Pb ages of ophiolites and arc-related plutons of the Norwegian Caledonides:implications for the development of Iapetus. Contr. Min. Petrol., 98, 13-23.

Eide, E.A. & Torsvik, T.H., 1996. Paleozoic Supercontinent assembly, Mantle flushing and genesis of the Kiaman Superchrons. Earth Planetary Science Letters, 144, 389-402.

Eide, E.A. & Torsvik, T.H., 1998. A synopsis of onshore results from the Onshore-Offshore Tectonic Link project. NGU Report 98.004.

Eide, E.A., Torsvik, T.H. & Andersen, T.B., 1997. Absolute dating of brittle fault movements:Late Permian and late Jurassic extentional fault breccias in western Norway. Terra Nova, 9, 135-139.

Eide, E.A., Torsvik, T.H., Andersen, T.B. & Arnaud, N, 1998. Carboniferous folding in Western Norway: Constraints from K-feldspar $^{40}Ar/^{39}Ar$ thermochronology and implications for North Sea structural settings (in prep.)

Franke, W., 1989. Tectonostratigraphic units in the Variscan Belt of central Europe. In R.D. Dallmeyer (Ed.) Terranes in the circum-Atlantic Paleozoic orogens. Geol. Soc. America Spec. Paper, 230, 67-90.

Fullerton, L.W., W.W. Sager, & D.W. Handschumacher, 1989. Late Jurassic and early Cretaceous tectonic evolution of the eastern Indian Ocean off northwest Australia, J. Geophys. Res., 94, 2937-2953.

Furnes, H., Skjerlie, K.P., Pedersen, R.B., Andersen, T.B., Stillman, C.J., Suthren, R., Tysseland, M. & Garmann, L.B. 1990. The Solund-Stavfjord Ophiolite Complex and

associated rocks, west Norwegian Caledonides: Geology, geochemistry and tectonic environment. Geological Magazine, 28, 209-224.

Færseth, R.B., Macintyre, R.M. & Naterstad, J. 1976. Mesozoic alkaline dykes in the Sunnhordland region, western Norway: ages, geochemistry and regional significance. Lithos, 9, 331-345.

Færseth, R.B., Gabrielsen, R.H. & Hurich, C.A. 1995. Influence of basement in structuring of the North Sea basin, offshore southwest Norway. Norsk Geologisk Tidsskrift, 75, 105-119.

Færseth. R.B., 1996. Interaction of Permo-Triassic and Jurassic extensional fault-blocks during the development of the northern North Sea. J. Geol. Soc. Lond., 153, 931-944.

Gee, D.G., 1996. Barentia and the Caledonides of the High Arctic. Geol. Fore. Forh., 118, 32-33.

Gradstein, F.M., Agterberg, F.P., Ogg, J.G., Hardenbol, J., Van Veen, P., Thierry, J. & Huang, Z., 1995. A Triassic, Jurassic and Cretaceous time scale. In Geochronology, Time Scales and Global Stratigraphic Correlation (Ed. Berggren, W.A., Kent, D.V.., Aubry, M.P. & Hardenpol, J.), 54, Sp. Publ. SEPM, Tulsa, Oklahoma, 95-126.

Gripp, A.E. & Gordon, R.G., 1990. Current plate velocities relative to hotspots incorporation the NUVEL-1 global plate motion model. Geophys. Res. Lett., 17, 1109-1112.

Handschumacher, D.W., W.W. Sager, T.W.C. Hilde, & D. Bracey, 1988. Pre-Cretaceous tectonic evolution of the northern Pacific plate and extension of the geomagnetic reversal timescale with implications for the origin of the Jurassic "Quiet Zone", Tectonophysics, 155, 365-380.

Harland, W.B., Armstrong, R.L., Cox, A.V., Craig, L.E., Smith, A.G. & Smith, D.G., 1990. A Geological Time Scale 1989. Cambridge Univ. Press, Cambridge, UK.

Hartz, E.H., Torsvik, T.H. & Andresen,A., 1997. Special report: A Carboniferous Age for the East Greenland 'Devonian' Basin: Palaeomagnetic and isotopic constraints on age, stratigraphy and plate reconstructions. Geology, 25, 675-678.

Herron, E.M., S.C. Cande, & B.R. Hall, 1981. An active spreading center collides with a subduction zone - geophysical survey of the Chile margin triple junction, Geological Society of America Memior, 154, 683-701.

Hutton, D.H.W., 1987. Strike-slip terranes and a model for the evolution of the British and Irish Caledonides. Geol. Mag., 124, 404-425.

Kent, D.V., & F.M. Gradstein, 1985. A Jurassic to recent chronology, in The Geology of North America, vol. M- The western Atlantic region, edited by B.E. Tucholke & P.R. Vogt, pp. 45-50, Geological Society of America, Boulder, CO.

Klitgord, K.D. and Schouten, H. 1986, Plate kinematics of the central Atlantic, in Vogt, P.R. and Tucholke, B.E., eds., The Western North Atlantic Region, GSA DNAG vol. M, pp. 351-378.

Lawver, L.A., Müller, R.D., Srivastava, S.P., and Roest, W., 1990, The Opening of the Arctic Ocean, in Geologic History of the Polar Oceans: Arctic Versus Antarctic, U. Bleil and J. Thiede (eds.), from the NATO Symposium (October, 1988) in Bremen, West Germany, pp. 29-62.

Lawver, L.A., and Scotese, C.R., 1987, A revised reconstruction of Gondwanaland, in McKenzie, G.D., ed., Gondwana Six: Structure, Tectonics, and Geophysics, AGU Geophysical Monograph 40 , 17-24.

LePichon, X. and J.-M. Gaulier, 1988, The rotation of Arabia and the Levant fault system, Tectonophysics, 153: 271-294.

Lonsdale, P., 1988. Paleogene history of the Kula plate: Offshore evidence and onshore implications, Geol. Soc. Am. Bull., 100 , 733-754.

Lottes, A.K. & Rowley, D.B. 1990. Reconstruction of the Laurasian and Gondwanan segments of Permian Pangea. In W.S. McKerrow & C.R. Scotese (Eds.) Palaeogeography and Biogeography, Geol. Soc. Lond. Mem. 12, 383-395.

Løvlie, R. & Mitchell, J.G. 1982. Complete remagnetization of some Permian dykes from western Norway induced during burial/uplift. Physics Earth Planetary Interiors, **30**, 415-421.

Mammerickx, J., & G.F. Sharman, 1988. Tectonic evolution of the north Pacific during the Cretaceous Quiet Period, J. Geophys. Res., 93, 3009-3024.

Matte, P., 1991. Accretionary history and crustal evolution of the Variscan belt in western Europe. Tectonophysics, 196, 309-337.

Mayes, C.L., Lawver, L.A., and Sandwell, D.T., 1990, Tectonic history and new isochron chart of the South Pacific, Journal of Geophysical Research, 95(B6), pp. 8543-8567.

McKerrow, W.S., 1988. The development of the Iapetus Ocean from the Arenig to the Wenclock. In Harris, A.L. & Fettes, D.J. (Eds.) The Caledonian-Appalachian Orogen. Geol. Soc. Special Public. Lond., 38, 405-412.

McKerrow, W.S., Dewey, J.F. & Scotese, C.F., 1991. The Ordovician and Silurian development of the Iapetus Ocean. Spec. paper in Palaeontology, 44, 165-178.

Meert, J.G. and Van der Voo, R., 1997. The assembly of Gondwana 800-550 Ma. J. Geodyn., 23, 223-235.

Müller, R.D, Royer, J-Y. & Lawver, L.A., 1993. Revised plate motions relative to the hotspots from combined Atlantic and Indian Ocean hotspot tracks. Geology, 21, 275-278.

Müller, R.D., Sandwell, D.T., Tucholke, B.E., Sclater, J.G., and Shaw, P.R., 1990, Depth to basement and geoid expression of the Kane Fracture Zone: a comparison, Marine Geophysical Researches, 13: 105-129.

Muttoni, G, Kent, D.V. & Channel, J.E.T., 1996. Evolution of Pangea:palaeomagnetic constraints from the Southern Alps, Italy. Earth. Planet. Sci. Lett., 140, 97-112.

Nikishin, A.M., Ziegler, P.A., Stephenson, R.A., Cloetingh, S.A.P.L., Furne, A.V., Fokin, P.A., Ershov, A.V., Bolotov, S.N., Korotaev, M.V., Alekseev, A.S., Gorbachev, V.I., Shipolov, E.V., Lankreijer, A., Bembinova, E.Yu & Shalimov, I.V., 1996. Late Precambrian to Triassic history of the East European Craton: dynamics of sedimentary basin evolution. Tectonophys., 268, 23-63.

Noble, S.R., Tucker R.D. & Pharaoh, T.C., 1993. Lower Palaeozoic and Precambrian igneous rocks from eastern England, and their bearing on late Ordovician closure of the Tornquist Sea: constraints from U-Pb and Nd isotopes. Geol. Mag., 130, 835-846.

Nordgulen, Ø., 1993. The Caledonian Bindal Batholith: regional setting based on geological, geochemical and isotopic data. Unpublished Dr. Scient thesis, Department of Geology,University of Bergen.

Ogg, J.G., 1995. Magnetic polarity time scale of the Phanerozoic, in: Global Earth Physics: A Handbook of Physical Constants, T.J. Ahrens, ed., pp. 240-270, American Geophysical Union, Washington, D.C., 1995.

Olaussen S., Larsen B. T. & Steel R., 1994. The Upper Carboniferous-Permian Oslo Rift: Basin fill in relation to tectonic development. In: Pangea: Global Environments and Resources. Can. Soc. Petrol. Geol. Mem. 17, 175-197.

Osmundsen, P-T. 1996. Late-orogenic structural geology and Devonian basin formation in Western Norway: A study from the hanging wall of the Nordfjord-Sogn Detachment in the Sunnfjord Region. Unpublished Dr. Scient thesis, University of Oslo, Norway.

Pickering, K.T. & Smith, A., 1995. Review Article: Arcs and backarc basin in the Early Palaeozoic Iapetus Ocean. The Island Arc, 4, 1-67.

Ramberg, I.B., 1976. Gravity interpretation of the Oslo Graben and associated igneous rocks. Nor. geol. unders. Bull., 325, 193pp.

Ramberg, I.B. & Larsen, B.T., 1978. Tectonomagmatic Evolution. In Dons. J.A. & Larsen, B.T. (eds.) The Oslo paleorift. A review and Guide to Excursions. Nor. geol. unders. Bull., 337, 55-73.

Roest, W.R. & Srivastava, S.P., 1989, Seafloor spreading in the Labrador Sea: a new reconstruction, Geology, 17: 1000-1004.

Royer, J.-Y., & R. Schlich, 1988. The southeast Indian Ridge between the Rodriquez Triple Junction & the Amsterdam & Saint-Paul Islands - Detailed kinematics for the past 20 Ma, J. Geophys. Res., 93, 13524-13550.

Royer, J.Y. and Sandwell, D.T., 1989, Evolution of the Eastern Indian Ocean Since the Late Cretaceous: Constraints from Geosat Altimetry, J. Geophys. Res., 94(B10): 13,755-13,782.

Royer, J.-Y., Müller, R.D., Gahagan, L.M., Lawver, L.A., Mayes, C.L., Nürnberg, D. & Sclater, J.G., 1992. A global isochron chart: University of Texas Institute for Geophysics Technical Report No. 117.

Scotese, C.R. & Barrett, S.F., 1990. Gondwana's movement over the South Pole during the Palaeozoic: evidence from lithological indicators of climate. In McKerrow, W.S. & Scotese, C.R. (eds.) Palaeozoic Palaeogeography and Biogeography, Geol. Soc. Lond. Memoir, 12, 75-85.

Srivastava, S.P. and Roest, W.R., 1989, Seafloor spreading history II-IV, in East Coast Basin Atlas Series: Labrador Sea, J.S. Bell (co-ordinator). Atlantic Geoscience Centre, Geologic Survey of Canada, Map sheets L17-2 - L17-6.

Srivastava, S.P., and Tapscott, C.R., 1986, Plate kinematics of the North Atlantic, in Tucholke, B.E., and Vogt, P.R., eds., The Geology of North America: The Western Atlantic Region, DNAG Series, vol. M, Geol. Soc. of America, pp. 379-404.

Stock, J., and Molnar, P., 1987, Revised history of early Tertiary plate motion in the south-west Pacific, Nature, 325: 495-499.

Sturt, B.A. & Roberts, D., 1991. Tectonostratigraphic relationships and obduction histories of Scandinavian ophiolitic terranes. In Tj. Peters et al. (Eds.) Ophiolite genesis and evolution of the oceanic lithosphere, Ministry of Petroleum and minerals, Sultanate of Oman, Kluwer Amsterdam, 745-769.

Sundvoll B. & Larsen B. T., 1994. Architecture and early evolution of the Oslo Rift. Tectonophys. 240, 173-189.

Tait, J., Bachtadse, V. & Soffel, H.C., 1995. Upper Ordovician palaeogeography of the Bohemian Massif: implications for Armorica. Geophys. J. Intern., 122, 211-218.

Tarduno, J.A. & Cotrell, R.D., 1997. Paleomagnetic evidence for motion of the Hawaiian hotspot during formation of the Emperor seamounts. Earth Planet. Sci. Lett., 153, 171-180.

Toghill, P., 1992. The Shelvian event, a late Ordovician tectonic episode in Southern Briatian (Eastern Avalonia). Proc. Geol. Ass., 103, 31-35.

Torcq, F., Besse, J., Vaslet, D., Marcoux, J., Riicou, L.E., Halawani, M. & Basahel, M., 1997. Paleomagnetic results from Saudi Arabia and the Permo-Triassic Pangea configuration. Earth. Planet. Sci. Lett., 148, 553-567.

Torsvik, T.H. & Trench, A., 1991. Short Paper: The Ordovician history of the Iapetus Ocean in Britain: New palaeomagnetic constraints. J. Geol. Soc. Lond., 148, 423-425.

Torsvik, T.H. & Eide, E..A., 1998. NGUISO: Database and analysis package for Norwegian isotope geochronology. NGU Report 98.003.

Torsvik, T.H. & Smethurst, M.A., 1998. GMAP v. 32: Geographic mapping and palaeoreconstruction package. NGU report 98.002.

Torsvik, T.H., Trench, A., Svensson, I. & Walderhaug, H.J., 1993. Palaeogeographic significance of mid-Silurian palaeomagnetic results from southern Britain - major revision of the apparent polar wander path for eastern Avalonia. Geoph. J. Intern., 113, 651-668.

Torsvik, T.H., Andersen T.B., Eide, E.A. & Walderhaug, H.J., 1997. The age and tectonic significance of dolerite dykes in Western Norway. J. Geol. Soc. Lond., 154, 961-973.

Torsvik, T.H., Sturt, B.A., Swensson, E., Andersen, T.B., Dewey, J.F. 1992. Palaeomagnetic dating of fault rocks: Evidence for Permian and Mesozoic movements and brittle deformation along the extensional Dalsfjord Fault, western Norway. Geophysical Journal International, 109, 565-580.

Torsvik, T.H., Eide, E.A., Meert, J.G., Smethurst, M.A. & Walderhaug, H.J., 1998. The Oslo Rift:New palaeomagnetic and $^{40}Ar/^{39}Ar$ age constraints. Geophys. J. Intern. (in review).

Torsvik, T.H., Smethurst, M.A., Van der Voo, R., Trench, A., Abrahamsen, N. & Halvorsen, E., 1992. Baltica. A synopsis of Vendian-Permian palaeomagnetic data and their palaeotectonic implications. Earth Sci. Rev., 33, 133-152.

Torsvik, T.H., Tait, J., Moralev, V.M., McKerrow, W.S., Sturt, B.A. & Roberts, D., 1995. Ordovician palaeogeography of Siberia and adjacent continents. J. Geol. Soc. Lond., 152, 279-287.

Torsvik, T.H., Smethurst, M.A., Meert, J.G.,Van der Voo, R. & McKerrow, W.S., Brasier, M.D. Surt, B.A. & Walderhaug. H.J., 1996. Continental break-up and collision in the

Neoproterozoic and Palaeozoic: A tale of Baltica and Laurentia. Earth Science Reviews, 40, 229-258.

Torsvik, T.H., Tucker, R.D., Eide, E.A., Aswal, L.D., Rakotosolofo, N. & de Wit, M.J., 1998. Madagascar Cretaceous volcanism and the Marion hot-spot postulate. Geology (in review).

Tucker, R.D. & McKerrow, W.S., 1995. Early Palaeozoic chronology: a review in light of new U-Pb zircon ages from Newfoundland and Britain. Canadian Journal of earth Sciences, 32, 368-379.

Tucker, R.D., Bradley, D.C., Ver Straeten, C.A., Harris, A.G., Ebert, J.R. & McCutcheon, S.R., 1998. New U-Pb zircon ages and the duration and division of Devonian time. Earth Plan. Sci. Lett. (in review).

Van der Voo, R., 1988. Palaeozoic palaeogeography of North America, Gondwana, and intervening displaced terranes: comparisons of palaeomagnetism with palaeoclimatology and biogeographical patterns. Geol. Soc. Am. Bull., 100, 311-324.

Van der Voo, R., 1993. Paleomagnetism of the Atlantic, Tethys and Iapetus Oceans. Cambridge University Press, New York, 411pp.

Ziegler, P.A., 1982, Geological atlas of Western and Central Europe, Shell Int. Petr. Maatschappij B.V. 130 p.

Ziegler, P.A., 1990. Geological atlas of Western and Central Europe 1990. Shell, 239 pp.

TABLES

Table 1
Updated geological time-scale used in the present study. Sources: Harland et al. (1990), Tucker & McKerrow (1995), Tucker et al. (1998), and Gradstein et al. (1995).

PERIOD	EPOCH	EPOCH/AGE	AGE (end in Ma)
Quaternary	Holocene		0
	Pleistocene		0.01
Neogene	Pliocene	Piacenzian	1.8
		Zanclean	3.6
	Miocene	Messinian	5.3
		Tortonian	7.1
		Serravallian	11.2
		Langhian	14.8
		Burdigalian	16.4
		Aquitanian	20.5
Paleogene	Oligocene	Chattian	23.8
		Rupelian	28.5
	Eocene	Priabonian	33.7
		Bartonian	37
		Lutetian	41.3
		Ypresian	49
	Paleocene	Thanetian	54.8
		Selandian	57.9
		Danian	61
Cretaceous	Late	Maastrichtian	65
		Campanian	71.3
		Santonian	83.5
		Coniacian	85.8
		Turonian	89
		Cenomanian	93.5
	Early	Albian	98.9
		Aptian	112.2
		Barremian	121
		Hauterivian	127
		Valanginian	132
		Ryazanian	136.5
Jurassic	Late	Volgian	142
		Kimmeridgian	150.7
		Oxfordian	154.1
	Middle	Callovian	159.4
		Bathonian	164.4
		Bajocian	169.2
		Aalenian	176.5
	Early	Toarcian	180.1
		Pliensbachian	189.6

		Sinemurian	195.3
		Hettangian	201.9
Triassic	Late	Rhaetian	205.7
		Norian	209.6
		Carnian	220.7
	Middle	Ladinian	227.4
		Anisian	234.3
	Early	Olenekian	241.7
		Induan	244.8
Permian	Late	Tatarian	248.2
		Ufimian-Kazanian	252.1
		Kungurian	256
		Artinskian	260
	Early	Sakmarian	269
		Asselian	282
Carboniferous	Late	Gzelian	290
		Kasimovian	296.5
		Moscovian	311
		Bashkirian	311
	Early	Serpukhovian	323
		Visean	327
		Tournaisian	342
Devonian	Late	Fammenian	354
		Frasnian	364
	Middle	Givetian	370
		Eifelian	380
	Early	Emsian	391
		Praghian	400
		Lochkovian	412
Silurian	Late	Pridoli	417
		Ludlow	419
		Wenlock	423
	Early	Llandovery	428
Ordovician	Late	Ashgill	443
		Caradoc	449
	Middle	Llandeilo	458
		Llanvirn	464
	Early	Arenig	470
		Tremadoc	485
Cambrian	Late		495
	Middle		505
	Early	Lenian	518
		Atdabanian	524
		Tommotian	530
		Nemakitian-Daldynian	534
Vendian			545

Table 2
Absolute Hot Spot reference reconstruction's (10.5-130 Ma) & total reconstruction poles based on magnetic anomaly fit & palaeomagnetic data (150-248 Ma). Hot-spot fits after Müller et al (1993). Magnetic anomalies are listed in Table 2.

Rotation Pole & Angle

Continent	Latitude	Longitude	Angle	Comment
10.5 Ma				
North America	43.6	120.7	1.39	a5-10.4ma
Africa	59.3	328.4	-1.89	
Madagascar	59.3	328.4	-1.89	
Australia	23.7	40.6	-7.27	
South America	59.4	314.2	1.8	
India	36.1	21.9	-5.81	
Antarctica	64.9	102	-1.56	
Greenland	43.6	120.7	1.4	asNAMSpreadStop
Eurasia	80.4	215.3	-1.3	anomaly fit
Iberia	80.4	215.3	-1.3	as Eurasia
Arabia	49.7	338.8	-5.7	anomaly fit
Spitsbergen	80.4	215.3	-1.3	as Eurasia
Barentsia	80.4	215.3	-1.3	as Eurasia
20.5 Ma				
North America	35	112.2	3.38	a6-20.5ma
Africa	50.9	315.5	-4.36	
Madagascar	50.9	315.5	-4.36	
Australia	27.1	31.4	-13.23	
South America	65.8	340.2	3.21	
India	40.6	4.3	-10.71	
Antarctica	85.3	37.3	-2.87	
Greenland	35	112.2	3.4	asNAMstopSPREAD
Eurasia	63.9	262.9	-3.02	anomaly fit
Iberia	63.9	262.9	-3	as Eurasia?
Arabia	44.5	357.6	-8.8	anomaly fit
Spitsbergen	63.9	262.9	-3.02	as EurasiaASIA
Barentsia	63.9	262.9	-3.02	as Eurasia
35.5 Ma				
North America	44	109.1	6.48	a13-35.5ma
Africa	40.3	317	-7.91	
Madagascar	40.3	317	-7.91	
Australia	22.7	30.1	-22.47	
South America	72.1	4	6.37	
India	30.9	17.4	-19.33	

Antarctica	72.6	5.7	-3.91	
Greenland	44	109.1	6.48	asNAMstopSPREAD
Eurasia	45.6	256.3	-3.4	anomaly fit
Iberia	45.6	256.3	-3.4	as Eurasia?
Arabia	39.9	347.4	-12.8	anomaly fit
Spitsbergen	45.6	256.3	-3.4	as Eurasia
Barentsia	45.6	256.3	-3.4	as Eurasia
42.7 Ma				
North America	47.7	110.2	8.44	a18-42.7ma
Africa	37.7	318.8	-9.65	
Madagascar	37.7	318.8	-9..65	
Australia	24	27.8	-26	
South America	74.2	12.9	8.36	
India	31.3	16.9	-23	
Antarctica	75.6	359.5	-4.07	
Greenland	38.2	108.7	8.5	anomaly fit interpolated
Eurasia	35.7	263.1	-3.6	anomaly fit interpolated
Iberia	35.7	263.1	-3.6	as Eurasia
Arabia	38.2	344.5	-14.5	anomaly fit
Spitsbergen	35.7	263.1	-3.6	as Eurasia
Barentsia	35.7	263.1	-3.6	as Eurasia
50.3 Ma				
North America	46.8	112.7	11.27	a21-50.3ma
Africa	32.8	319.2	-12.09	
Madagascar	32.8	319.2	-12.09	
Australia	23.3	25.9	-27.67	
South America	76	50.6	10.28	
India	27.9	11.1	-29.06	
Antarctica	71.1	342.4	-5.22	
Greenland	32.5	110.6	10.7	anomaly fit
Eurasia	24.8	273.6	-4.6	anomaly fit
Iberia	24.8	273.6	-4.6	as Eurasia?
Arabia	34.57	340.3	-16.72	anomaly fit
Spitsbergen	24.8	273.6	-4.6	as Eurasia
Barentsia	24.8	273.6	-4.6	as Eurasia
58.6 Ma				
North America	46.2	115.8	14.51	a25-58.6ma
Africa	30.1	318.3	-13.89	
Madagascar	30.1	318.3	-13.89	
Australia	23	26.2	-27.86	
South America	74.1	68	12.74	
India	24.7	6.2	-37.29	
Antarctica	73.8	320.3	-6.28	
Greenland	38.1	103.1	14.5	anomaly fit

Eurasia	26	269.7	-5.5	anomaly fit
Iberia	26	269.7	-5.5	as Eurasia?
Arabia	32.4	337.3	-18.3	anomaly fit
Spitsbergen	26	269.7	-5.5	as Eurasia
Barentsia	26	269.7	-5.5	as Eurasia
68.5 Ma				
North America	46	119.5	18.65	aa31-68.5ma
Africa	26.4	319.1	-16.23	
Madagascar	26.4	319.1	-16.23	
Australia	18.3	26.8	-28.72	
South America	73.2	87.5	15.9	
India	19.1	3.4	-53.37	
Antarctica	67.6	336.4	-7.49	
Greenland	34.5	106.8	16.9	anomaly fit
Eurasia	17.6	282.9	-7.3	anomaly fit
Iberia	17.6	282.9	-7.3	as Eurasia?
Arabia	29	335.5	-20.6	anomaly fit
Spitsbergen	17.6	282.9	-7.3	as Eurasia
Barentsia	17.6	282.9	-7	as Eurasia
73.6 Ma				
North America	49.3	119.6	21.11	a33y-73.6ma
Africa	22.3	320.4	-17.8	
Madagascar	22.3	320.4	-17.8	
Australia	18	26.7	-29.61	
South America	72.6	93	18.31	
India	18.7	2.5	-58.12	
Antarctica	64.9	343	-7.79	
Greenland	39.3	107.8	19.2	anomaly fit
Eurasia	2.6	104.8	7.8	anomaly fit
Iberia	2.6	104.8	7.8	as Eurasia?
Arabia	25.3	335.2	-22	anomaly fit
Spitsbergen	2.6	104.8	7.8	as Eurasia
Barentsia	2.6	104.8	7.8	as Eurasia
80.2 Ma				
North America	53.4	117	24.58	a33o-80.2ma
Africa	18	321.1	-19.98	
Madagascar	18	321.1	-19.98	
Australia	18.3	26.7	-30.16	
South America	72.3	93.7	21.9	
India	18.1	1.8	-63	
Antarctica	65.7	343.9	-8.04	
Greenland	27.7	109.8	19.9	anomaly fit
Eurasia	11.9	99.3	9.2	anomaly fit
Iberia	11.9	99.3	9.2	as Eurasia?

Arabia	21.3	334.3	-24.1	anomaly fit
Spitsbergen	11.9	99.3	9.2	as Eurasia
Barentsia	11.9	99.3	9.2	as Eurasia
84 Ma				
North America	54.5	111.2	25.81	a34-84ma
Africa	19	319.1	-21.53	
Madagascar	19	319.1	-21.53	
Australia	18.7	27.4	-29.49	
South America	71.6	82.4	22.87	
India	17.1	2.3	-65.48	
Antarctica	72.4	327.5	-8.21	
Greenland	30.1	105.5	21.2	anomaly fit
Eurasia	13.3	91.3	10.4	anomaly fit
Iberia	13.3	91.3	10.4	as Eurasia?
Arabia	21.9	331.9	-25.5	anomaly fit
Spitsbergen	13.3	91.3	10.4	as Eurasia
Barentsia	13.3	91.3	10.4	as Eurasia
90 Ma				
Africa	19.4	318.1	-23.31	
Madagascar	19.4	318.1	-23.31	
Australia	22.4	31.3	-28.4	
South America	71.7	68.1	24.01	
India	16.3	5	-67.29	
Antarctica	82.1	227.3	-9.8	
North America	57.4	104.4	28.2	
Greenland	32.4	101.2	22.7	anomaly fit
Eurasia	20.9	82.3	12.2	anomaly fit
Iberia	38.2	336.4	-36.7	anomaly fit
Arabia	21.9	330.2	-27.2	anomaly fit
Spitsbergen	20.9	82.3	12.2	as Eurasia
Barentsia	20.9	82.3	12.2	as Eurasia
100 Ma				
North America	62.9	89.4	31.74	100ma
Africa	18.9	318.6	-25.35	
Madagascar	18.9	318.6	-25.35	
Australia	28.6	40.7	-27.41	
South America	72.2	45.3	26.77	
India	14.5	10.3	-70.31	
Antarctica	63.3	173.9	-13.4	
Greenland	39.9	90.2	25	anomaly fit
Eurasia	29.4	64.4	15.5	anomaly fit
Iberia	35.2	331.8	-31.4	anomaly fit
Arabia	21.1	329.9	-29.2	anomaly fit
Spitsbergen	29.4	64.4	15.5	as Eurasia

Barentsia	29.4	64.4	15.5	as Eurasia
110 Ma				
North America	66.1	77	37.27	110ma
Africa	17.7	320.5	-26.71	
Madagascar	17.7	320.5	-26.71	
Australia	34.6	52.6	-27.5	
South America	71.8	24.9	30.38	
India	13.7	10.1	-71.68	
Antarctica	49.4	164.7	-17.76	
Greenland	46.4	82.1	29.3	anomaly fit
Eurasia	39.6	55.8	20.9	anomaly fit
Iberia	27.5	327.1	-26.4	anomaly fit
Arabia	19.9	331	-30.6	anomaly fit
Spitsbergen	39.6	55.8	20.9	as Eurasia
Barentsia	39.6	55.8	20.9	as Eurasia
118.7 Ma				
North America	66.5	63.9	41.54	m0-118.7Ma
Africa	18.7	320.3	-27.37	
Madagascar	18.8	321.6	-26.67	
Australia	40.8	65.7	-28.85	
South America	68.4	9.2	33.26	
India	14.2	10.3	-72.09	
Antarctica	42	162.2	-23.45	
Greenland	49.6	72.8	33.4	anomaly fit
Eurasia	38.7	50	24.8	anomaly fit
Iberia	20.8	319.5	-22.6	anomaly fit
Arabia	20.7	330.6	-31.3	anomaly fit
Spitsbergen	38.7	50	24.8	as Eurasia
Barentsia	38.7	50	24.8	as Eurasia
130 Ma				
North America	65.9	56.9	45.42	m10
Africa	16.7	322.5	-28.52	
Madagascar	16.2	334.3	-23.96	
Australia	48.9	75.5	-32.3	
South America	67.1	10.4	34.64	
India	13.3	15.5	-75.34	
Antarctica	42.4	162.3	-30.42	
Greenland	51	67.5	37.2	anomaly fit
Eurasia	40.3	47.1	29	anomaly fit
Iberia	12.4	312.6	-20.7	anomaly fit
Arabia	18.7	332.3	-32.5	anomaly fit
Spitsbergen	40.3	47.1	29	as Eurasia
Barentsia	40.3	47.1	29	as Eurasia

Magnetic anomaly fits plus palaeomagnetic data for latitude positioning				
150 Ma				
North America	52.8	81.8	28.4	anomaly fit149ma
Africa	41	327.7	-46.7	anomaly fit
South America	76.5	26	11	anomaly fit
Iberia	43.6	325.7	-39	anomaly fit
Arabia	39.4	334.1	-51.4	anomaly fit
Madagascar	42.6	344.8	-40.4	anomaly fit
Greenland	23.7	84.7	24.3	anomaly fit
Eurasia	0	244.8	-16.7	anomaly fit
Antarctica	57	112.4	-38.1	anomaly fit
Australia	43.3	55.1	-52.1	anomaly fit
India	21.1	10.4	-94.2	anomaly fit
Spitsbergen	0	244.8	-16.7	as Eurasia
Barentsia	0.3	64.8	16.4	as Eurasia
175 Ma				
Gondwana	50.3	330.3	-38.3	Lottes & Rowley 89
North America	61.4	7.9	42.9	
Iberia	52.7	251.6	-14.5	anomaly fit
Greenland	45.7	32.7	30.5	Bullard et al. 1965
Eurasia	0	205.7	-18.9	Bullard et al. 1965
Spitsbergen	0	205.7	-18.9	as Eurasia
Barentsia	0	205.7	-18.9	as Eurasia
225 Ma				
Gondwana	35.3	318	-43.7	Lottes & Rower 89
North America	53	35.3	46.5	
Iberia	25.1	271.1	-23.4	anomaly fit
Greenland	34.9	53.4	37.8	Bullard et al. 1965
Eurasia	0	234.7	-26.2	Bullard et al. 1965
Spitsbergen	0	234.7	-26.2	as Eurasia
Barentsia	0	234.7	-26.2	as Eurasia
265 Ma (250-280)				
Gondwana	24.3	297.4	-50.7	
nampal	38.6	49.4	57.5	
Greenland	23.5	62.8	53.1	
Eurasia	0	249	-43	
Iberia	19.4	285.6	-46	Scetal
Spitsbergen	0	249	-43	as Eurasia
new foundland	38.6	49.4	57.5	as North America
acadia	38.6	49.4	57.5	as North America
Barentsia	0	249	-43	as Eurasia

Table 3
Finite rotation poles to reconstruct isochrons (magnetic anomalies). Adapted from Royer et al. (1992).

Time	Latitude	Longitude	Angle	Reference
North America to Northwest Africa				
10	80.12	50.8	2.52	Mueller et al. 1990
20	79.57	37.84	5.29	Klitgord & Schouten 1986
35.5	75.37	1.12	10.04	Müller et al. 1990
49.5	75.3	-3.88	15.25	Müller et al. 1990
59	79.68	-0.46	18.16	Müller et al. 1990
67.5	82.9	4.94	20.76	Müller et al. 1990
72.5	81.35	-9.15	22.87	Klitgord & Schouten 1986
74.3	80.76	-11.76	23.91	Klitgord & Schouten 1986
80.2	78.3	-18.35	27.06	Klitgord & Schouten 1986
84	76.55	-20.73	29.6	Klitgord & Schouten 1986
118	66.3	-19.9	54.25	Klitgord & Schouten 1986
126	66.13	-19	56.39	Klitgord & Schouten 1986
131.5	65.95	-18.5	57.4	Klitgord & Schouten 1986
141.5	66.1	-18.4	59.79	Klitgord & Schouten 1986
149.5	66.5	-18.1	61.92	Klitgord & Schouten 1986
156.5	67.15	-16	64.7	Klitgord & Schouten 1986
170	67.02	-13.17	72.1	Klitgord & Schouten 1986
175	66.95	-12.02	75.55	Klitgord & Schouten 1986
Greenland to North America				
35.5	0	0	0	
49	59.5	-92	-2.81	Royer et al 1992
56	54.91	-110.01	-4	Roest & Srivastava 1989
59	24.48	-137.25	-3.12	Roest & Srivastava 1989
61	20.61	-148.2	-3.27	Roest & Srivastava 1989
63	27.63	-149.41	-3.72	Roest & Srivastava 1989
69	43.94	-145.31	-4.92	Roest & Srivastava 1989
84	65.3	-122.45	-11	Roest & Srivastava 1989
92	66.6	-119.48	-12.2	Roest & Srivastava 1989
105	67.08	-118.96	-12.99	Roest & Srivastava 1989
118	67.5	-118.48	-13.78	Roest & Srivastava 1989
Fit	70.53	-94.34	-17.99	Calculated from Bullard et al. (1965)
South America to Central Africa				
1.9	60	-39	0.51	Cande et al. 1988
2.5	60	-39	0.77	Cande et al. 1988
3.9	60	-39	1.21	Cande et al. 1988
5.3	60	-39	1.78	Cande et al. 1988
6.7	60	-39	2.27	Cande et al. 1988
7.9	60	-39	2.76	Cande et al. 1988
8.9	60	-39	3.15	Cande et al. 1988

11.6	59.5	-38	4.05	Cande et al. 1988
14.9	59.5	-38	5.25	Cande et al. 1988
16.2	59.5	-38	5.75	Cande et al. 1988
17.6	59.5	-38	6.3	Cande et al. 1988
18.6	59.5	-38	6.7	Cande et al. 1988
19.4	59.5	-38	7.05	Cande et al. 1988
20.9	59.5	-37.75	7.6	Nuernberg & Mueller 1991
22.6	59.5	-36.5	8.45	Cande et al. 1988
23.3	59.5	-37	8.8	Nuernberg & Mueller 1991
25.5	59	-36	9.5	Cande et al. 1988
26.9	59	-36	10	Cande et al. 1988
28.2	58	-35	10.55	Cande et al. 1988
29.7	57	-35	11.05	Cande et al. 1988
31.2	57	-34.5	11.6	Nuernberg & Mueller 1991
32.5	57.5	-35	12.15	Cande et al. 1988
35.3	57.5	-34	13.38	Cande et al. 1988
37.2	57	-33.5	14.1	Cande et al. 1988
38.1	57	-33.25	14.4	Nuernberg & Mueller 1991
39.5	57	-33	15.05	Cande et al. 1988
41.3	57.5	-32.5	15.8	Cande et al. 1988
43.6	58	-32	17	Cande et al. 1988
44.7	57.5	-31.75	17.6	Cande et al. 1988
48.7	58.5	-31.5	19.07	Cande et al. 1988
51.9	59	-31.5	20.1	Cande et al. 1988
53.9	60	-32	20.75	Cande et al. 1988
55.1	60	-32	21.2	Cande et al. 1988
58.6	61.5	-32.5	22.3	Nuernberg & Mueller 1991
60.2	61.5	-32.5	22.7	Cande et al. 1988
63	62.5	-33	23.55	Cande et al. 1988
64.3	63	-33.3	24	Cande et al. 1988
65.5	63	-33.3	24.3	Cande et al. 1988
66.7	63	-33.3	24.7	Cande et al. 1988
68.5	63	-33.5	25.4	Cande et al. 1988
71.4	63	-33.5	26.6	Cande et al. 1988
74.3	63	-33.5	27.9	Cande et al. 1988
80.2	63	-34	31	Cande et al. 1988
84	61.75	-34	33.5	Cande et al. 1988
118.7	50.1	-34.6	52.78	Royer et al 1992
121	50	-34.2	53.64	Royer et al 1992
126.5	49.3	-33.8	54.29	Royer et al 1992
131.5	49.1	-33.7	55.17	Royer et al 1992
245	49.1	-33.7	55.17	Royer et al 1992
Eurasia to North America				
10	65.38	133.58	-2.44	Lawver et al. 1990
20	68.92	136.74	-4.97	Lawver et al. 1990
36	65.64	136.95	-7.51	Lawver et al. 1990
49	67.19	137.74	-10.91	Srivastava & Roest 1989

56	62.6	140.81	-12.75	Srivastava & Roest 1989
59	63.14	141.66	-14.22	Srivastava & Roest 1989
69	64.84	143.96	-16.95	Srivastava & Roest 1989
80	66.17	147.74	-19	Srivastava & Roest 1989
84	66.54	148.91	-19.7	Srivastava & Roest 1989
92	66.67	150.26	-20.37	Srivastava & Roest 1989
105	66.85	152.34	-21.49	Srivastava & Roest 1989
118	68.99	154.75	-23.05	Srivastava & Roest 1989
145	68.99	154.75	-23.05	Srivastava & Roest 1989
170	69.1	156.7	-23.64	Royer et al 1992
Fit	88	27	-38	Bullard et al. (1965)
Iberia to Eurasia				
0	0	0	0	
30	90	0	0	
Iberia to Northwest Africa				
30	31.4	-18.6	7.87	Srivastava & Tapscott 1986 fit
133.2	31.4	-18.6	7.87	Srivastava & Tapscott 1986
Iberia to North America				
133.2	70.3	-11	-51.5	calculated from Srivastava & Tapscott 1986
India to Central Indian Basin				
0	90	0	0	Royer et al 1992
10.5	-8.7	76.9	2.75	Royer et al 1992
20.5	-0.9	74.6	6.77	Royer et al 1992
70	-0.9	74.6	6.77	Royer et al 1992
India to East Antarctica				
70	13	7.2	-50.08	Royer et al 1992
80.2	8.2	11	-62.18	Royer & Sandwell 1989
84	7.8	10.9	-65.1	Royer & Sandwell 1989
India to Madagascar				
84	17.5	22.6	-55.41	Royer & Sandwell 1989
100	18.2	24.6	-61.92	Royer et al 1992
115	19.4	27.1	-59.74	Royer et al 1992
140	19.1	31.2	-61.99	calculated from Lawver & Scotese 1987
India to East Antarctica				
140	-4.4	16.7	-92.77	Lawver & Scotese 1987
Arabia to Central Africa				
0	0	0	0	
4.7	32.8	22.6	-1.89	LePichon & Gaullier 1988
13	32.2	22.6	-5.36	LePichon & Gaullier 1988
30	32.1	22.6	-6.36	LePichon & Gaullier 1988
Madagascar to Central Africa				
0	0	0	0	
115	90	0	0	
118.7	5.4	-76.2	0.9	Royer et al 1992
123	5.4	-76.2	1.96	Royer et al 1992
126.5	5.4	-76.2	3.19	Royer et al 1992
129.4	5.4	-76.2	4.2	Royer et al 1992

141.9	5.4	-76.2	8.32	Royer et al 1992
149.9	4	-71.4	11.32	Royer et al 1992
165	-3.41	-81.7	19.73	Lawver & Scotese 1987
Northwest Africa to Central Africa				
0	0	0	0	
84	0	0	0	
118.7	8.8	98.7	0.37	Royer et al 1992 (fit)
Northwest Africa to South America				
118.7	50	-35.2	-52.9	Royer et al 1992
Australia to East Antarctica				
0	90	0	0	
10.5	13.1	36.1	-6.61	Royer & Chang 1991
20.5	15.4	32.7	-11.97	Royer & Chang 1991
35.5	13.8	33.4	-20.41	Royer & Chang 1991
42.7	16.6	29.9	-23.62	Royer & Sandwell 1989
46.2	15.1	31.3	-24.5	Royer & Sandwell 1989
56.1	12.5	31.7	-25.24	Royer & Sandwell 1989
68.5	8.7	33.2	-25.83	Royer & Sandwell 1989
80.2	6.2	35.1	-26.37	Royer & Sandwell 1989
84	4.9	35.8	-26.81	Royer & Sandwell 1989
96	1	38	-28.3	Royer & Sandwell 1989
130	-2	38.9	-31.5	Royer & Sandwell 1989
East Antarctica to Central Africa				
0	0	0	0	
10.5	8.2	-49.4	1.53	Royer & Chang 1991
20.5	10.7	-47.9	2.78	Royer & Chang 1991
35.5	12	-48.4	5.46	Royer & Chang 1991
46.2	11.4	-43.7	7.81	Royer et al. 1988
50.3	10.3	-42.9	8.77	Royer et al. 1988
56.1	6.7	-40.6	9.97	Royer et al. 1988
60.8	3.8	-39.7	10.63	Royer et al. 1988
64.3	0.6	-39.2	11.32	Royer et al. 1988
66.2	-0.4	-39.4	11.59	Royer et al. 1988
68.5	1.1	-41.6	11.84	Royer et al. 1988
73.6	-1.8	-41.4	13.47	Royer et al. 1988
80.2	-4.7	-39.7	16.04	Royer et al. 1988
84	-2	-39.2	17.85	Royer et al. 1988
118.7	-4.2	-29.1	42.8	Royer et al 1992
123	-4.6	-29.1	44.17	Royer et al 1992
141.9	-7	-26.9	50.7	Royer et al 1992
149.9	-4.7	-29	52.84	Royer et al 1992
165	-7.78	-31.42	58	Lawver & Scotese 1987

Table 4
Age of magnetic anomalies

Anomaly	Age	Reference	
1y	0.00	Berggren et al. (1985)	
1c	0.37	Berggren et al. (1985)	
1o	0.73	Berggren et al. (1985)	
Jc	0.94	Berggren et al. (1985)	
2y	1.66	Berggren et al. (1985)	
2c	1.77	Berggren et al. (1985)	
2o	1.88	Berggren et al. (1985)	
2Ay	2.47	Berggren et al. (1985)	
2'c	2.94	Berggren et al. (1985)	Herron et al. (1981)
2Ac	2.94	Berggren et al. (1985)	
2Ao	3.40	Berggren et al. (1985)	
3y	3.88	Berggren et al. (1985)	
3c	4.33	Berggren et al. (1985)	
3o	4.77	Berggren et al. (1985)	
3Ay	5.35	Berggren et al. (1985)	
3Ac	5.62	Berggren et al. (1985)	
3'c	5.62	Berggren et al. (1985)	Herron et al. (1981)
3Ao	5.89	Berggren et al. (1985)	
3Bc	6.44	Berggren et al. (1985)	Royer & Schlich (1988)
3"c	6.44	Berggren et al. (1985)	Herron et al. (1981)
4y	6.70	Berggren et al. (1985)	
4c	7.05	Berggren et al. (1985)	
4o	7.41	Berggren et al. (1985)	
4Ay	7.90	Berggren et al. (1985)	
4Ac	8.20	Berggren et al. (1985)	
4'c	8.20	Berggren et al. (1985)	Assumed
4Ao	8.50	Berggren et al. (1985)	
5y	8.92	Berggren et al. (1985)	
5c	9.67	Berggren et al. (1985)	
5o	10.42	Berggren et al. (1985)	
5'c	11.06	Berggren et al. (1985)	Royer & Schlich (1988)
5Ay	11.55	Berggren et al. (1985)	
5Ac	11.84	Berggren et al. (1985)	
5Ao	12.12	Berggren et al. (1985)	
5AAy	12.83	Berggren et al. (1985)	
5AAc	12.92	Berggren et al. (1985)	
5AAo	13.01	Berggren et al. (1985)	
5ABy	13.20	Berggren et al. (1985)	
5ABc	13.33	Berggren et al. (1985)	
5ABo	13.46	Berggren et al. (1985)	
5ACy	13.69	Berggren et al. (1985)	
5ACc	13.89	Berggren et al. (1985)	
5ACo	14.08	Berggren et al. (1985)	

5ADy	14.20 Berggren et al. (1985)
5ADc	14.43 Berggren et al. (1985)
5ADo	14.66 Berggren et al. (1985)
5By	14.87 Berggren et al. (1985)
5Bc	15.07 Berggren et al. (1985)
5Bo	15.27 Berggren et al. (1985)
5Cy	16.22 Berggren et al. (1985)
5Cc	16.60 Berggren et al. (1985)
5Co	16.98 Berggren et al. (1985)
5Dy	17.57 Berggren et al. (1985)
5Dc	17.85 Berggren et al. (1985)
5Do	18.14 Berggren et al. (1985)
5Ey	18.56 Berggren et al. (1985)
5Ec	18.83 Berggren et al. (1985)
5Eo	19.09 Berggren et al. (1985)
6y	19.35 Berggren et al. (1985)
6c	19.90 Berggren et al. (1985)
6o	20.45 Berggren et al. (1985)
6Ay	20.88 Berggren et al. (1985)
6Ac	21.30 Berggren et al. (1985)
6Ao	21.71 Berggren et al. (1985)
6AAy	21.90 Berggren et al. (1985)
6AAc	22.13 Berggren et al. (1985)
6AAo	22.35 Berggren et al. (1985)
6By	22.57 Berggren et al. (1985)
6Bc	22.77 Berggren et al. (1985)
6Bo	22.97 Berggren et al. (1985)
6Cy	23.27 Berggren et al. (1985)
6Cc	23.74 Berggren et al. (1985)
6Co	24.21 Berggren et al. (1985)
7y	25.50 Berggren et al. (1985)
7c	25.74 Berggren et al. (1985)
7o	25.97 Berggren et al. (1985)
7Ay	26.38 Berggren et al. (1985)
7Ac	26.47 Berggren et al. (1985)
7Ao	26.56 Berggren et al. (1985)
8y	26.86 Berggren et al. (1985)
8c	27.30 Berggren et al. (1985)
8o	27.74 Berggren et al. (1985)
9y	28.15 Berggren et al. (1985)
9c	28.68 Berggren et al. (1985)
9o	29.21 Berggren et al. (1985)
10y	29.73 Berggren et al. (1985)
10c	30.03 Berggren et al. (1985)
10o	30.33 Berggren et al. (1985)
11y	31.23 Berggren et al. (1985)
11c	31.65 Berggren et al. (1985)

11o	32.06 Berggren et al. (1985)	
12y	32.46 Berggren et al. (1985)	
12c	32.68 Berggren et al. (1985)	
12o	32.90 Berggren et al. (1985)	
13y	35.29 Berggren et al. (1985)	
13c	35.58 Berggren et al. (1985)	
13o	35.87 Berggren et al. (1985)	
15y	37.24 Berggren et al. (1985)	
15c	37.46 Berggren et al. (1985)	
15o	37.68 Berggren et al. (1985)	
16y	38.10 Berggren et al. (1985)	
16c	38.67 Berggren et al. (1985)	
16o	39.24 Berggren et al. (1985)	
17y	39.53 Berggren et al. (1985)	
17c	40.32 Berggren et al. (1985)	
17o	41.11 Berggren et al. (1985)	
18y	41.29 Berggren et al. (1985)	
18c	42.01 Berggren et al. (1985)	
18o	42.73 Berggren et al. (1985)	
19y	43.60 Berggren et al. (1985)	
19c	43.83 Berggren et al. (1985)	
19o	44.06 Berggren et al. (1985)	
20y	44.66 Berggren et al. (1985)	
20c	45.42 Berggren et al. (1985)	
20o	46.17 Berggren et al. (1985)	
21y	48.75 Berggren et al. (1985)	
21c	49.55 Berggren et al. (1985)	
21o	50.34 Berggren et al. (1985)	
22y	51.95 Berggren et al. (1985)	
22c	52.28 Berggren et al. (1985)	
22o	52.62 Berggren et al. (1985)	
23y	53.88 Berggren et al. (1985)	
23-1c	53.95 Berggren et al. (1985)	Lonsdale (1988)
23c	54.29 Berggren et al. (1985)	
23-2c	54.39 Berggren et al. (1985)	Lonsdale (1988)
23o	54.70 Berggren et al. (1985)	
24y	55.14 Berggren et al. (1985)	
24-1c	55.25 Berggren et al. (1985)	Lonsdale (1988)
24Ac	55.25 Berggren et al. (1985)	Assumed
24c	55.64 Berggren et al. (1985)	
24-2c	55.90 Berggren et al. (1985)	Lonsdale (1988)
24Bc	55.90 Berggren et al. (1985)	Assumed
24o	56.14 Berggren et al. (1985)	
25y	58.64 Berggren et al. (1985)	
25c	58.94 Berggren et al. (1985)	
25o	59.24 Berggren et al. (1985)	
26y	60.21 Berggren et al. (1985)	

26c	60.48 Berggren et al. (1985)	
26o	60.75 Berggren et al. (1985)	
27y	63.03 Berggren et al. (1985)	
27c	63.28 Berggren et al. (1985)	
27o	63.54 Berggren et al. (1985)	
28y	64.29 Berggren et al. (1985)	
28c	64.71 Berggren et al. (1985)	
28o	65.12 Berggren et al. (1985)	
29y	65.50 Berggren et al. (1985)	
29c	65.83 Berggren et al. (1985)	
29o	66.17 Berggren et al. (1985)	
30y	66.74 Berggren et al. (1985)	
30c	67.58 Berggren et al. (1985)	
30o	68.42 Berggren et al. (1985)	
30Rc	68.47 Berggren et al. (1985)	
31y	68.52 Berggren et al. (1985)	
31c	68.96 Berggren et al. (1985)	
31o	69.40 Berggren et al. (1985)	
32y	71.37 Berggren et al. (1985)	
32Ac	71.51 Berggren et al. (1985)	Mammerickx & Sharman (1988)
32c	72.46 Berggren et al. (1985)	
32Bc	72.73 Berggren et al. (1985)	Mammerickx & Sharman (1988)
32Rc	73.87 Berggren et al. (1985)	Mammerickx & Sharman (1988)
32o	73.55 Berggren et al. (1985)	
33y	74.30 Berggren et al. (1985)	
33c	77.24 Berggren et al. (1985)	
33o	80.17 Berggren et al. (1985)	
33Rc	80.17 Berggren et al. (1985)	
34y	84.00 Berggren et al. (1985)	
34c	101.00 Berggren et al. (1985)	
34o	118.00 Berggren et al. (1985)	
M0y	118.00 Kent & Gradstein (1985)	
M0c	118.35 Kent & Gradstein (1985)	
M0o	118.70 Kent & Gradstein (1985)	
M1y	121.81 Kent & Gradstein (1985)	
M1c	122.03 Kent & Gradstein (1985)	
M1o	122.25 Kent & Gradstein (1985)	
M2y	122.25 Kent & Gradstein (1985)	
M2c	122.64 Kent & Gradstein (1985)	
M2o	123.03 Kent & Gradstein (1985)	
M3y	123.03 Kent & Gradstein (1985)	
M3c	124.19 Kent & Gradstein (1985)	
M3o	125.36 Kent & Gradstein (1985)	
M4y	125.36 Kent & Gradstein (1985)	
M4c	125.91 Kent & Gradstein (1985)	
M4o	126.46 Kent & Gradstein (1985)	
M5y	126.46 Kent & Gradstein (1985)	

M5c	126.76 Kent & Gradstein (1985)
M5o	127.05 Kent & Gradstein (1985)
M6y	127.21 Kent & Gradstein (1985)
M6c	127.28 Kent & Gradstein (1985)
M6o	127.34 Kent & Gradstein (1985)
M7y	127.52 Kent & Gradstein (1985)
M7c	127.75 Kent & Gradstein (1985)
M7o	127.97 Kent & Gradstein (1985)
M8y	128.33 Kent & Gradstein (1985)
M8c	128.47 Kent & Gradstein (1985)
M8o	128.60 Kent & Gradstein (1985)
M9y	128.91 Kent & Gradstein (1985)
M9c	129.17 Kent & Gradstein (1985)
M9o	129.43 Kent & Gradstein (1985)
M10y	129.82 Kent & Gradstein (1985)
M10c	130.01 Kent & Gradstein (1985)
M10o	130.19 Kent & Gradstein (1985)
M10Ny	131.36 Kent & Gradstein (1985)
M10Nc	131.51 Kent & Gradstein (1985)
M10Ac	131.51 Kent & Gradstein (1985)
M10No	131.65 Kent & Gradstein (1985)
M11y	132.53 Kent & Gradstein (1985)
M11c	133.01 Kent & Gradstein (1985)
M11o	133.50 Kent & Gradstein (1985)
M12y	134.75 Kent & Gradstein (1985)
M12c	135.15 Kent & Gradstein (1985)
M12o	135.56 Kent & Gradstein (1985)
M13y	136.64 Kent & Gradstein (1985)
M13c	136.87 Kent & Gradstein (1985)
M13o	137.10 Kent & Gradstein (1985)
M14y	137.39 Kent & Gradstein (1985)
M14c	137.85 Kent & Gradstein (1985)
M14o	138.30 Kent & Gradstein (1985)
M15y	139.01 Kent & Gradstein (1985)
M15c	139.29 Kent & Gradstein (1985)
M15o	139.58 Kent & Gradstein (1985)
M16y	141.20 Kent & Gradstein (1985)
M16c	141.53 Kent & Gradstein (1985)
M16o	141.85 Kent & Gradstein (1985)
M17y	142.27 Kent & Gradstein (1985)
M17c	143.01 Kent & Gradstein (1985)
M17o	143.76 Kent & Gradstein (1985)
M18y	144.33 Kent & Gradstein (1985)
M18c	144.54 Kent & Gradstein (1985)
M18o	144.75 Kent & Gradstein (1985)
M19y	145.98 Kent & Gradstein (1985)
M19c	146.21 Kent & Gradstein (1985)

M19o	146.44 Kent & Gradstein (1985)
M20y	147.47 Kent & Gradstein (1985)
M20c	147.90 Kent & Gradstein (1985)
M20o	148.33 Kent & Gradstein (1985)
M21y	149.42 Kent & Gradstein (1985)
M21c	149.65 Kent & Gradstein (1985)
M21o	149.89 Kent & Gradstein (1985)
M22y	151.69 Kent & Gradstein (1985)
M22c	152.11 Kent & Gradstein (1985)
M22o	152.53 Kent & Gradstein (1985)
M22Ac	153.35 Kent & Gradstein (1985) Fullerton et al. (1989)
M23y	153.52 Kent & Gradstein (1985)
M23c	153.84 Kent & Gradstein (1985)
M23o	154.15 Kent & Gradstein (1985)
M24y	154.88 Kent & Gradstein (1985)
M24c	154.98 Kent & Gradstein (1985)
M24o	155.08 Kent & Gradstein (1985)
M24Ac	155.61 Kent & Gradstein (1985) Fullerton et al. (1989)
M25y	156.29 Kent & Gradstein (1985)
M25c	156.42 Kent & Gradstein (1985)
M25o	156.55 Kent & Gradstein (1985)
PM26y	157.85 Kent & Gradstein (1985)
PM26c	157.93 Kent & Gradstein (1985)
PM26o	158.01 Kent & Gradstein (1985)
PM27y	158.21 Kent & Gradstein (1985)
PM27c	158.29 Kent & Gradstein (1985)
PM27o	158.37 Kent & Gradstein (1985)
PM28y	158.66 Kent & Gradstein (1985)
PM28c	158.76 Kent & Gradstein (1985)
PM28o	158.87 Kent & Gradstein (1985)
PM29y	159.80 Kent & Gradstein (1985)
PM29c	160.07 Kent & Gradstein (1985)
PM29o	160.33 Kent & Gradstein (1985)
M25y	156.29 Handschumacher et al. (1988)
M25c	156.42 Handschumacher et al. (1988)
M25o	156.55 Handschumacher et al. (1988)
M26y	158.05 Handschumacher et al. (1988)
M26c	158.17 Handschumacher et al. (1988)
M26o	158.30 Handschumacher et al. (1988)
M27y	158.52 Handschumacher et al. (1988)
M27c	158.64 Handschumacher et al. (1988)
M27o	158.76 Handschumacher et al. (1988)
M28y	158.97 Handschumacher et al. (1988)
M28c	159.08 Handschumacher et al. (1988)
M28o	159.19 Handschumacher et al. (1988)
M28Ay	159.40 Handschumacher et al. (1988)
M28Ac	159.43 Handschumacher et al. (1988)

M28Ao	159.46 Handschumacher et al. (1988)
M28By	159.71 Handschumacher et al. (1988)
M28Bc	159.72 Handschumacher et al. (1988)
M28Bo	159.74 Handschumacher et al. (1988)
M29y	159.89 Handschumacher et al. (1988)
M29c	159.95 Handschumacher et al. (1988)
M29o	160.01 Handschumacher et al. (1988)
M30y	160.49 Handschumacher et al. (1988)
M30c	160.63 Handschumacher et al. (1988)
M30o	160.78 Handschumacher et al. (1988)
M30Ay	160.82 Handschumacher et al. (1988)
M30Ac	160.86 Handschumacher et al. (1988)
M30Ao	160.90 Handschumacher et al. (1988)
M31y	161.06 Handschumacher et al. (1988)
M31c	161.13 Handschumacher et al. (1988)
M31o	161.21 Handschumacher et al. (1988)
M32y	161.60 Handschumacher et al. (1988)
M32c	161.69 Handschumacher et al. (1988)
M32o	161.78 Handschumacher et al. (1988)
M32Ay	161.83 Handschumacher et al. (1988)
M32Ac	161.86 Handschumacher et al. (1988)
M32Ao	161.89 Handschumacher et al. (1988)
M33y	162.13 Handschumacher et al. (1988)
M33c	162.23 Handschumacher et al. (1988)
M33o	162.33 Handschumacher et al. (1988)
M34y	162.61 Handschumacher et al. (1988)
M34c	162.69 Handschumacher et al. (1988)
M34o	162.77 Handschumacher et al. (1988)
M34Ay	162.84 Handschumacher et al. (1988)
M34Ac	162.90 Handschumacher et al. (1988)
M34Ao	162.95 Handschumacher et al. (1988)
M34By	163.00 Handschumacher et al. (1988)
M34Bc	163.06 Handschumacher et al. (1988)
M34Bo	163.13 Handschumacher et al. (1988)
M34Cy	163.45 Handschumacher et al. (1988)
M34Cc	163.50 Handschumacher et al. (1988)
M34Co	163.56 Handschumacher et al. (1988)
M35y	163.74 Handschumacher et al. (1988)
M35c	163.82 Handschumacher et al. (1988)
M35o	163.90 Handschumacher et al. (1988)
M35Ay	163.96 Handschumacher et al. (1988)
M35Ac	164.00 Handschumacher et al. (1988)
M35Ao	164.04 Handschumacher et al. (1988)
M35By	164.30 Handschumacher et al. (1988)
M35Bc	164.32 Handschumacher et al. (1988)
M35Bo	164.35 Handschumacher et al. (1988)
M36y	164.50 Handschumacher et al. (1988)

M36c	164.60 Handschumacher et al. (1988)
M36o	164.70 Handschumacher et al. (1988)
M37y	164.99 Handschumacher et al. (1988)
M37c	165.05 Handschumacher et al. (1988)
M37o	165.10 Handschumacher et al. (1988)
M37Ay	165.15 Handschumacher et al. (1988)
M37Ac	165.21 Handschumacher et al. (1988)
M37Ao	165.26 Handschumacher et al. (1988)
M37By	165.33 Handschumacher et al. (1988)
M37Bc	165.38 Handschumacher et al. (1988)
M37Bo	165.42 Handschumacher et al. (1988)
M37Cy	165.64 Handschumacher et al. (1988)
M37Cc	165.65 Handschumacher et al. (1988)
M37Co	165.66 Handschumacher et al. (1988)
M38y	165.85 Handschumacher et al. (1988)
M38c	166.16 Handschumacher et al. (1988)
M38o	166.47 Handschumacher et al. (1988)

Table 5
Compilation of normal polarity chrons with start & end interval ages (Ma). After Cande & Kent (1995) and Ogg (1995).

Start	End	Chron
0	0.78	C1n
0.99	1.07	C1r.1n
1.77	1.95	C2n
2.14	2.15	C2r.1n
2.581	3.04	C2An.1n
3.11	3.22	C2An.2n
3.33	3.58	C2An.3n
4.18	4.29	C3n.1n
4.48	4.62	C3n.2n
4.8	4.89	C3n.3n
4.98	5.23	C3n.4n
5.894	6.137	C3An.1n
6.269	6.567	C3An.2n
6.935	7.091	C3Bn
7.135	7.17	C3Br.1n
7.341	7.375	C3Br.2n
7.432	7.562	C4n.1n
7.65	8.072	C4n.2n
8.225	8.257	C4r.1n
8.699	9.025	C4An
9.23	9.308	C4Ar.1n
9.58	9.642	C4Ar.2n
9.74	9.88	C5n.1n

9.92	10.949	C5n.2n
11.052	11.099	C5r.1n
11.476	11.531	C5r.2n
11.935	12.078	C5An.1n
12.184	12.401	C5An.2n
12.678	12.708	C5Ar.1n
12.775	12.819	C5Ar.2n
12.991	13.139	C5AAn
13.302	13.51	C5ABn
13.703	14.076	C5ACn
14.178	14.612	C5ADn
14.8	14.888	C5Bn.1n
15.034	15.155	C5Bn.2n
16.014	16.293	C5Cn.1n
16.327	16.488	C5Cn.2n
16.556	16.726	C5Cn.3n
17.277	17.615	C5Dn
18.281	18.781	C5En
19.048	20.131	C6n
20.518	20.725	C6An.1n
20.996	21.32	C6An.2n
21.768	21.859	C6AAn
22.151	22.248	C6AAr.1n
22.459	22.493	C6AAr.2n
22.588	22.75	C6Bn.1n
22.804	23.069	C6Bn.2n
23.353	23.535	C6Cn.1n
23.677	23.8	C6Cn.2n
23.999	24.118	C6Cn.3n
24.73	24.781	C7n.1n
24.835	25.183	C7n.2n
25.496	25.648	C7An
25.823	25.951	C8n.1n
25.992	26.554	C8n.2n
27.027	27.972	C9n
28.283	28.512	C10n.1n
28.578	28.745	C10n.2n
29.401	29.662	C11n.1n
29.765	30.098	C11n.2n
30.479	30.939	C12n
33.058	33.545	C13n
34.655	34.94	C15n
35.343	35.526	C16n.1n
35.685	36.341	C16n.2n
36.618	37.473	C17n.1n
37.604	37.848	C17n.2n
37.92	38.113	C17n.3n

38.426	39.552	C18n.1n
39.631	40.13	C18n.2n
41.353	41.617	C19n
42.536	43.789	C20n
46.264	47.906	C21n
49.037	49.714	C22n
50.778	50.946	C23n.1n
51.047	51.743	C23n.2n
52.364	52.663	C24n.1n
52.757	52.801	C24n.2n
52.903	53.347	C24n.3n
55.904	56.391	C25n
57.554	57.911	C26n
60.92	61.276	C27n
62.499	63.634	C28n
63.976	64.745	C29n
65.578	67.61	C30n
67.735	68.737	C31n
71.071	71.338	C32n.1n
71.587	73.004	C32n.2n
73.291	73.374	C32r.1n
73.619	79.075	C33n
83	118	C34n
118.7	121.81	M1n
122.25	123.03	M3n
125.36	126.46	M5n
127.05	127.21	M6n
127.34	127.52	M7n
127.97	128.33	M8n
128.6	128.91	M9n
129.43	129.82	M10n
130.19	130.57	M10Nn.1n
130.63	131	M10Nn.2n
131.01	131.36	M10Nn.3n
131.65	132.53	M11n
133.03	133.08	M11r.1n
133.5	133.9	M11An.1n
133.92	134.31	M11An.2n
134.42	134.75	M12n
135.56	135.66	M12r.1n1
135.88	136.24	M12An
136.37	136.64	M13n
137.1	137.39	M14n
138.3	139.09	M15n
139.58	141.2	M16n
141.85	142.27	M17n
143.76	144.33	M18n

144.75	144.88	M19n.1n
144.96	145.98	M19n.2n
146.44	146.75	M20n.1n
146.81	147.47	M20n.2n
148.33	149.42	M21n
149.89	151.46	M22n.1n
151.51	151.56	M22n.2n
151.61	151.69	M22n.3n
152.53	152.66	M22An
152.84	153.21	M23n
153.49	153.52	M23r.1n
154.15	154.48	M24n
154.85	154.88	M24r.1n
155.08	155.21	M24An
155.48	155.84	M24Bn
156	156.29	M25n
156.55	156.72	M25An.1n
156.81	156.92	M25An.2n
157	157.16	M25An.3n
157.28	157.39	M26n.1n
157.47	157.56	M26n.2n
157.64	157.72	M26n.3n
157.78	157.99	M26n.4n
158.23	158.44	M27n
158.67	158.88	M28n
159.08	159.28	M29n.1n
159.35	159.58	M29n.2n
159.61	159.76	M29n.3n
159.87	160.33	M30n
160.61	160.65	M30r.1n
160.73	160.87	M31n
161.02	161.39	M32n
161.57	161.62	M32r.1n
161.68	161.91	M33n
162.1	162.37	M34n
162.52	162.59	M34r.1n
162.69	162.74	M34r.2n
162.86	163.17	M35n.1n
163.28	163.45	M35n.2n
163.61	163.66	M35r.1n
163.74	163.99	M36n.1n
164.04	164.18	M36n.2n
164.37	164.65	M37n
164.75	164.8	M37r.1n
164.91	164.98	M37r.2n
165.07	165.27	M38n.1n
165.29	165.48	M38n.2n

FIGURES 1-32

CAPTION FOR FIGURE 13

Early Triassic, Buntsandsstein, Palaeogeography (c. 243 Ma). Facies distributions after Ziegler (1990) overlain with palaeolatitude lines (15-25°N) derived from palaeomagnetic data. Mean ages from local volcanics (dykes) are as follows: 241±11=Sotra dykes; 238±4=Sunnhordaland dykes; 241±11=Skår volcanics; 243±5=Lunner and Bøverbru dykes. These dykes are syn- to post-rift and discussed in detail by Eide & Torsvik (1998). Original age-data also summarised in Torsvik & Eide (1998).

CAPTION FOR FIGURE 18

Mid-Jurassic, Bajocian-Bathonian, Palaeogeography (c. 176-164 Ma). Facies distributions after Ziegler (1990) overlain with palaeolatitude lines (40-55°N) derived from palaeomagnetic data. Onshore, mean ages from local volcanics are as follows: 162±4=Sunnhordaland dykes (youngest generation); 179±4=Gobnehall volcanics. The Dalsfjord Fault, western Norway, shows important reactivation at this time (163±4 Ma is a maximum age). Fission-track exhumation ages are concentrated in this time-slice. Dykes are probably syn-rift and discussed in detail by Eide & Torsvik (1998). Original age-data also summarised in Torsvik & Eide (1998).

Early Ordovician (Late Tremadoc-Early Arenig,
c. 480-490 Ma)

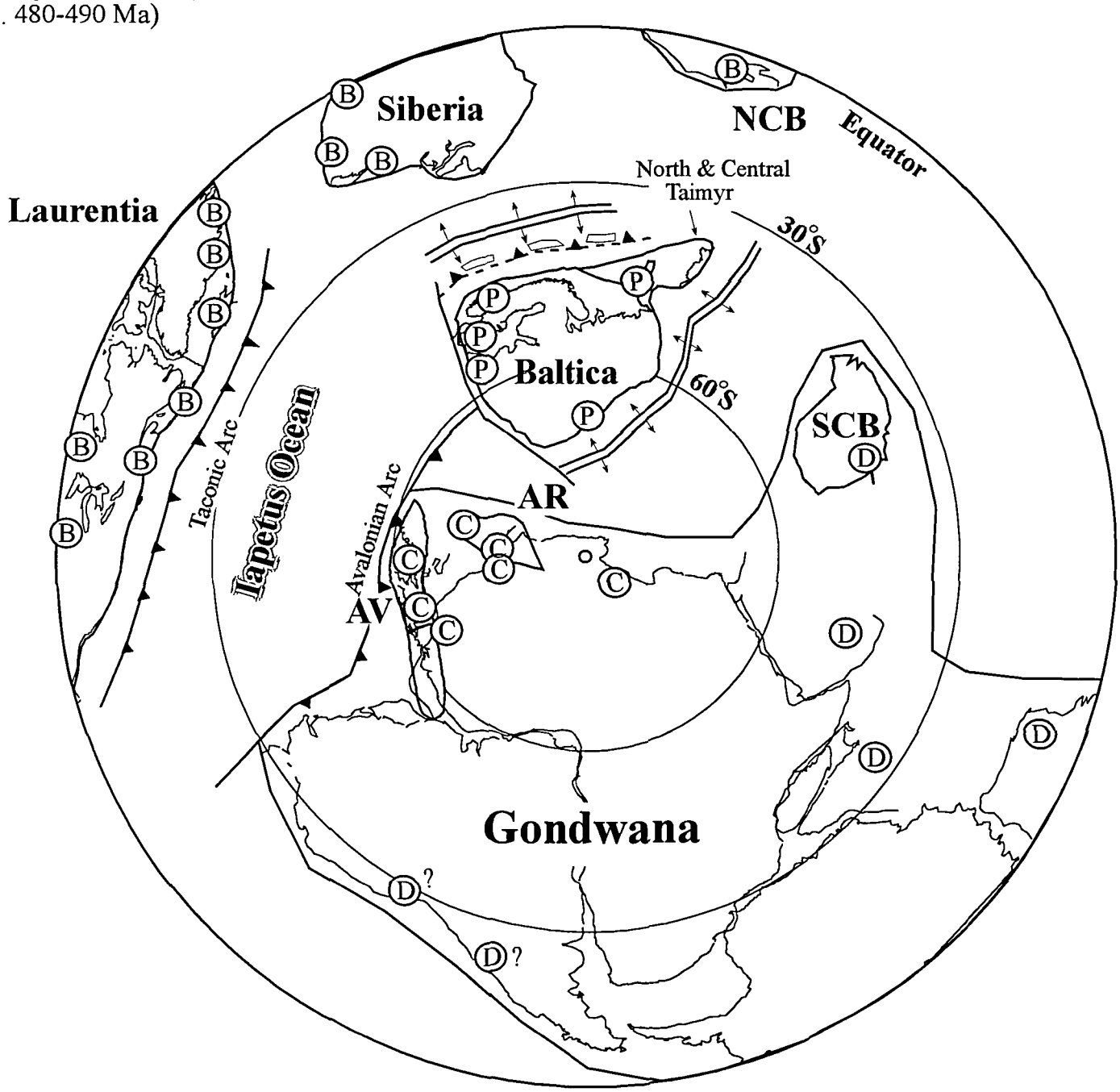

FIGURE 1
Early Ordovician, Late Tremadoc-Early Arenig (c. 480-490 Ma), reconstruction (cf. text).
Arenig-Llanvirn platform trilobites: B=*Bathyurid* P=*Ptychopygine/Megalaspid* C=*Calymenacean*
D=*Dalmanitacean.* NCB=North China Block, SCB=South China Block, AV=Avalonia,
AR=European Massifs, including the Armorican, Iberian and Bohemian Massifs.

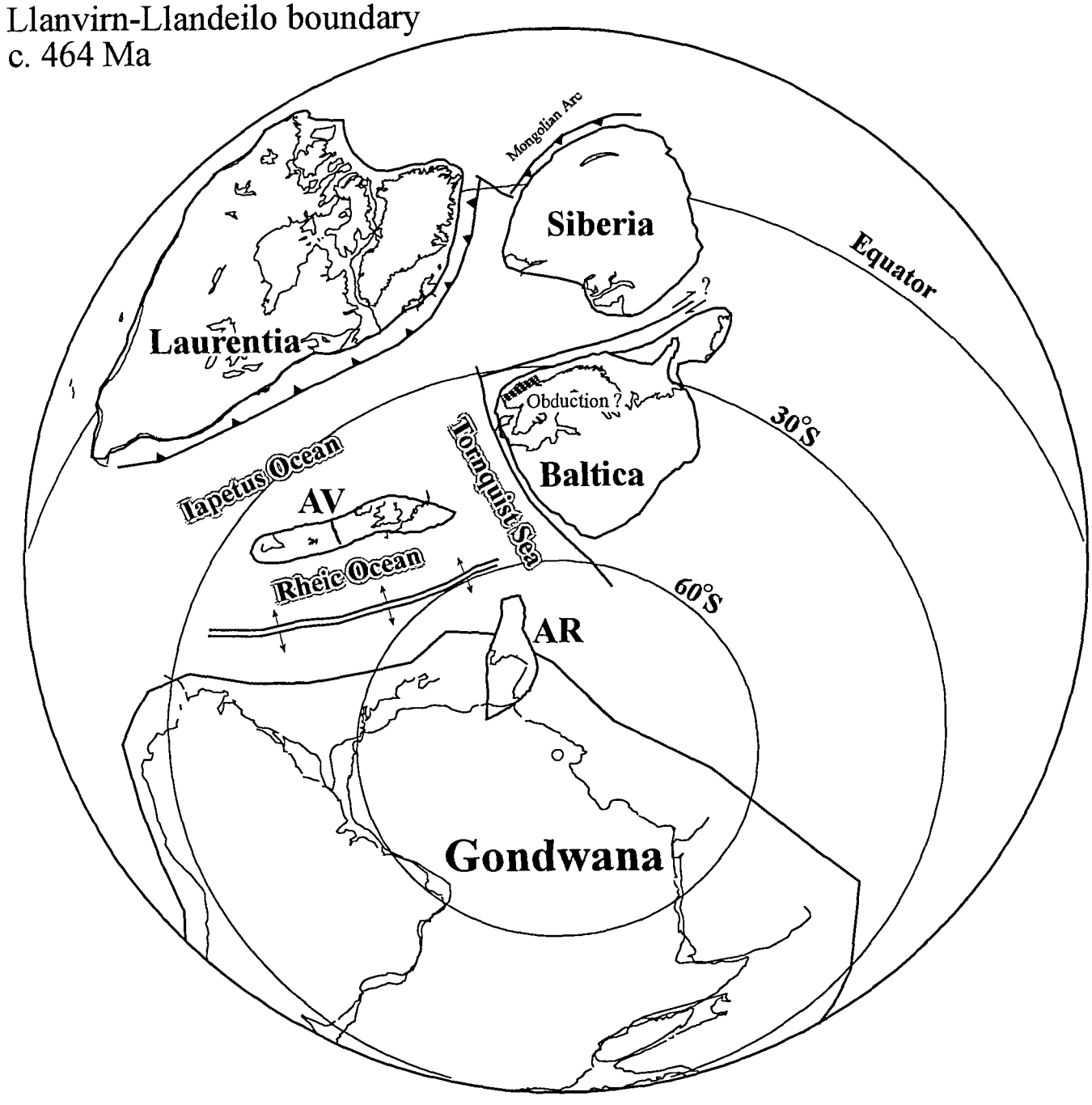

FIGURE 2
Mid-Ordovician reconstruction (see text)

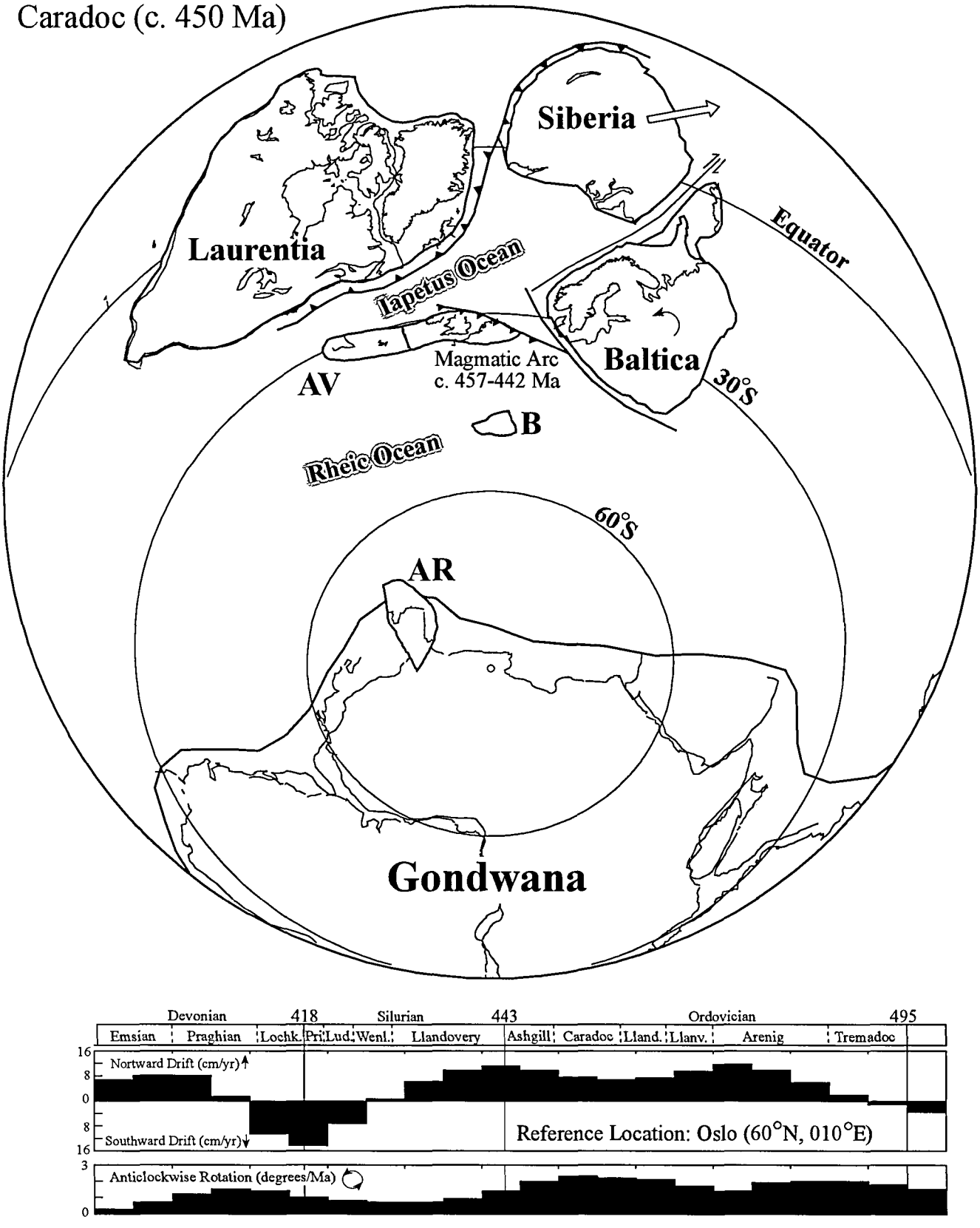

FIGURE 3

Late Ordovician, Caradoc (c. 450 Ma) reconstruction.

Bottom diagram: Latitudinal drift (cm/year) and angular rotation rates (degrees/Ma) for Baltica (reference location: Oslo, c. 60 °N, 10 °E) during Ordovician to Devonian times. Time-scale after Tucker & McKerrow (1995) and Tucker et al. (1998). AR as in Fig. 1 except Bohemian Massif. B=Bohemian Massif.

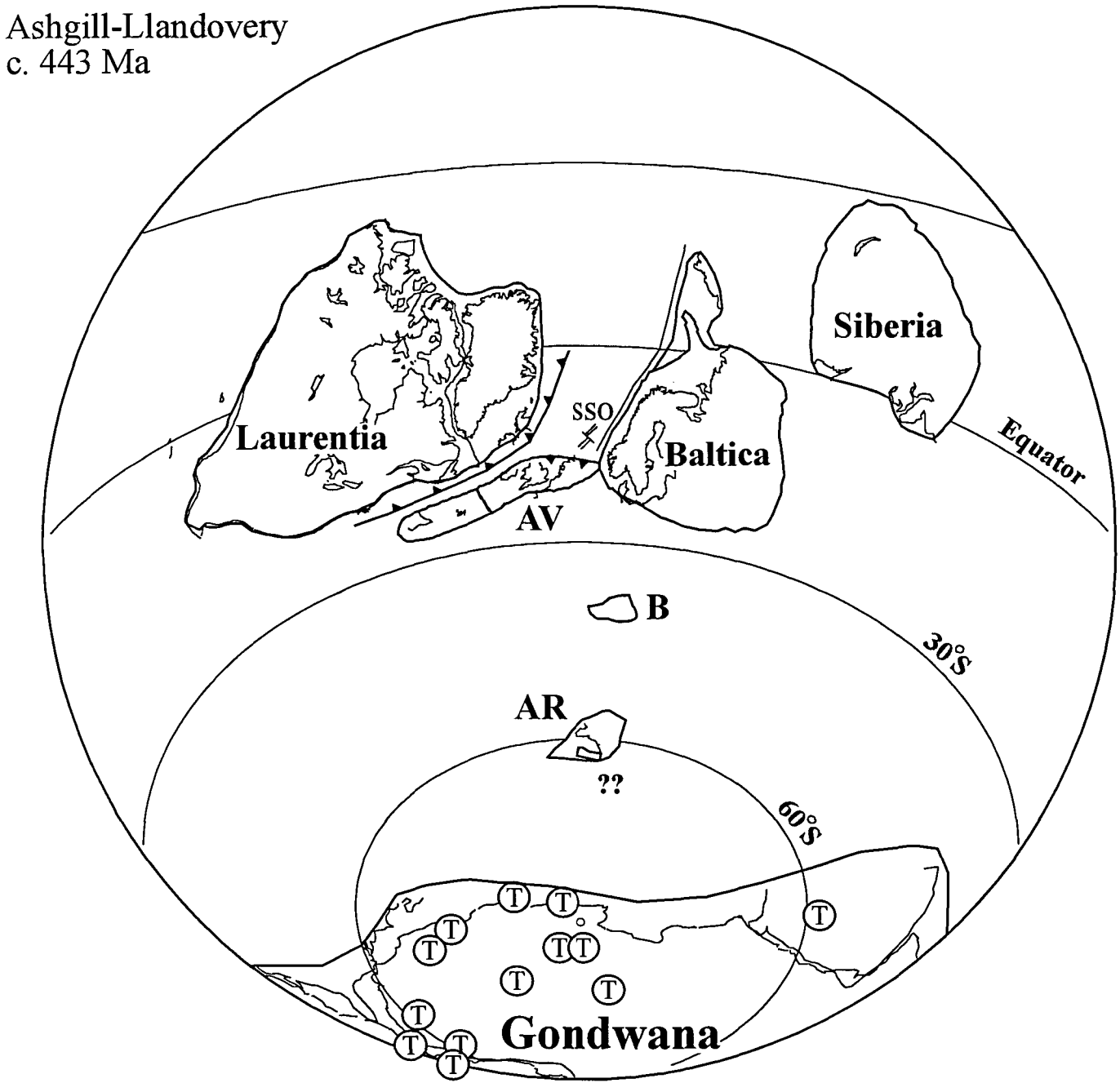

FIGURE 4
Late Ordovician-early Silurian, Asgill-Llandovery (c. 443 Ma) reconstruction.
T=Tillites (after Scotese and Barrett 1990). SSO=Solund-Stavfjord Ophiolite probably relating to back-arc spreading, and demonstrating that Iapetus oceanic crust formed adjacent to Western Norway as late as Late Ordovician time.

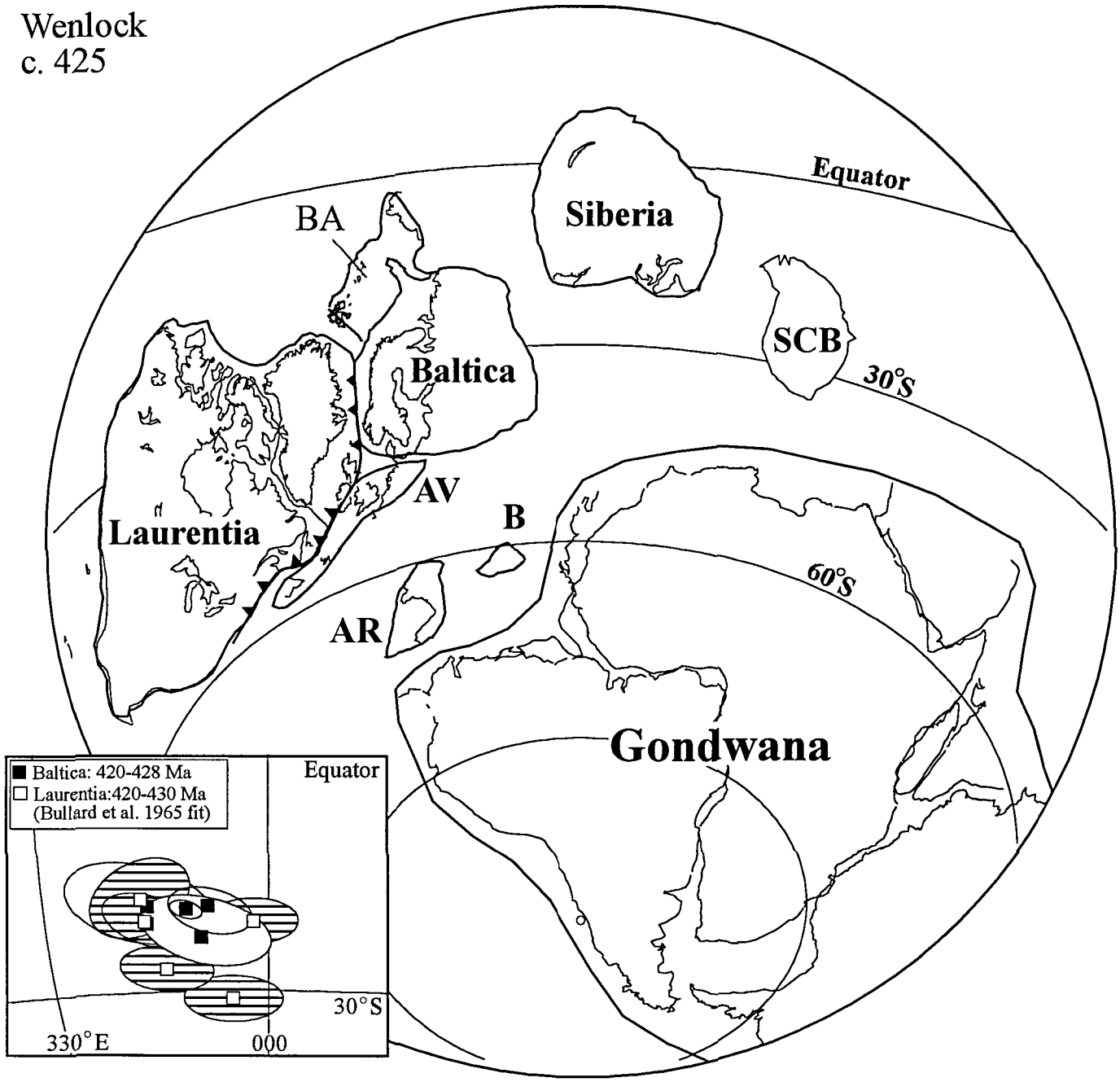

FIGURE 5
Mid-Silurian, Wenlock (c. 425 Ma) reconstruction. Inset: 420-430 Ma palaeomagnetic poles from Baltica and Laurentia (North America and Scotland) in a Bullard et al. (1965) fit. Notice the overlap which demonstrate that Iapetus is closed or below the resolution power of palaeomagnetic data. BA=Barentsia:reliable pre-Devonian palaeomagnetic data for Barentsia (NE Svalbard and Barents Shelf) are non-existent, hence this palaeo-continent with strong Laurentian affinities (Gee 1996) is typically ignored in most reconstructions. Barentsia is likely to have collided with Greenland in the end of the Llandovery (McKerrow et al. 1991), and is therefore included in mid-Silurian reconstruction and onwards.

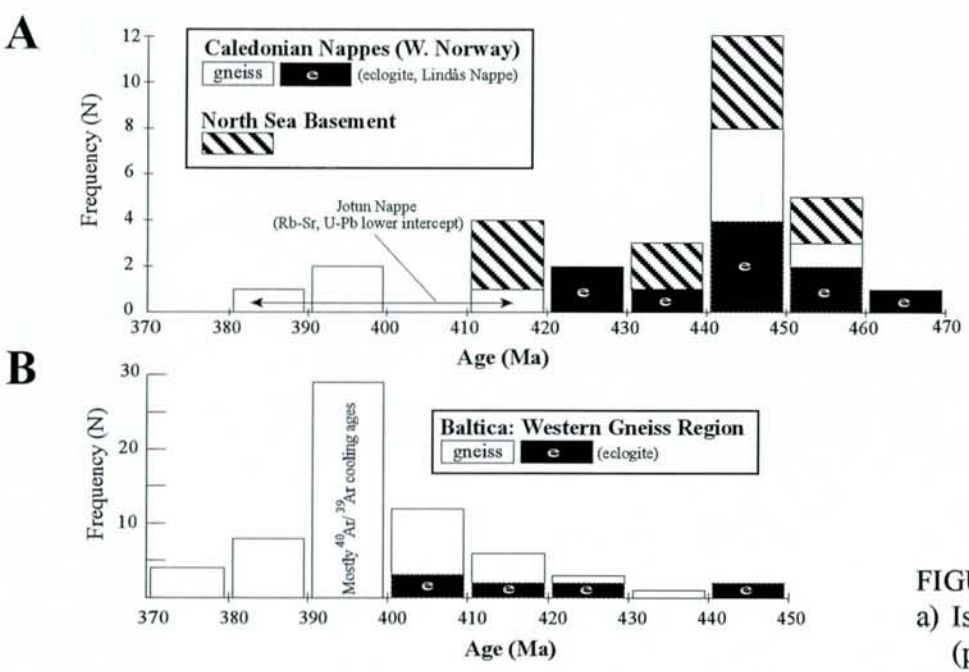

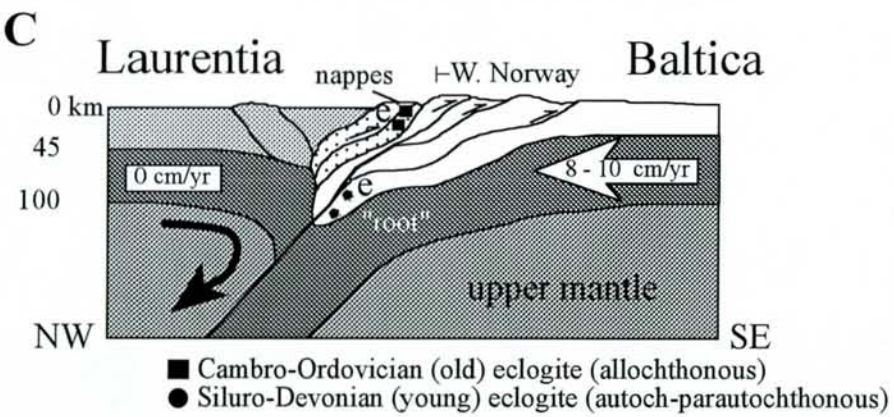

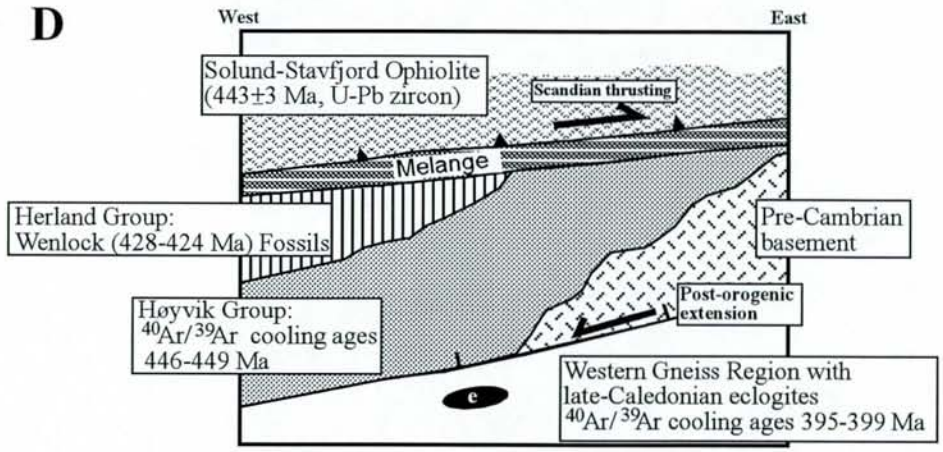

FIGURE 6

a) Isotope ages from Caledonian Nappes in Western Norway and North Sea Basement (probably allochtonous) which show a similar age range. Eclogite ages marked with e.

b) Isotope ages from the Western Gneiss Region (Baltica). Shortly after collision between Baltica and Laurentia (Fig. 5), geochronologic and structural evidence indicate the rocks were being exhumed by extensional collapse (main event c. 390-400 Ma); the welded continents moved southward at this time (compare Fig. 5 and 7) as the subducted cold lithospheric slab (Fig. 6c) began to delaminate.

c) Schematic cross sections for the collision-exhumation-detachment sequence for Baltica and Laurentia in mid-Silurian times (modified from Eide & Torsvik 1996). White horizontal arrows indicate the direction and speed of the plates. Black dots and squares in the Baltican crust represent probable levels of formation and subsequent exhumation of eclogites found in western Norway; ''root'' refers to the entire lithospheric slab underlying the oceanic and continental crust. The main collisional event between Baltica and Laurentia occurred at c. 425 Ma and was marked by deep subduction (up to 120 km) of Baltican crust beneath Laurentia with concomitant eastward translation of nappes over the Baltican margin. Deep subduction was a function both of rapid motion of Baltica toward stationary Laurentia and precedence of prolonged subduction of large volumes of cold lithosphere.

d) Schematic tectono-stratigraphy (not to scale) in the Sunnfjord region, Western Norway (after Andersen et al. 1990, Torsvik et al. 1997).

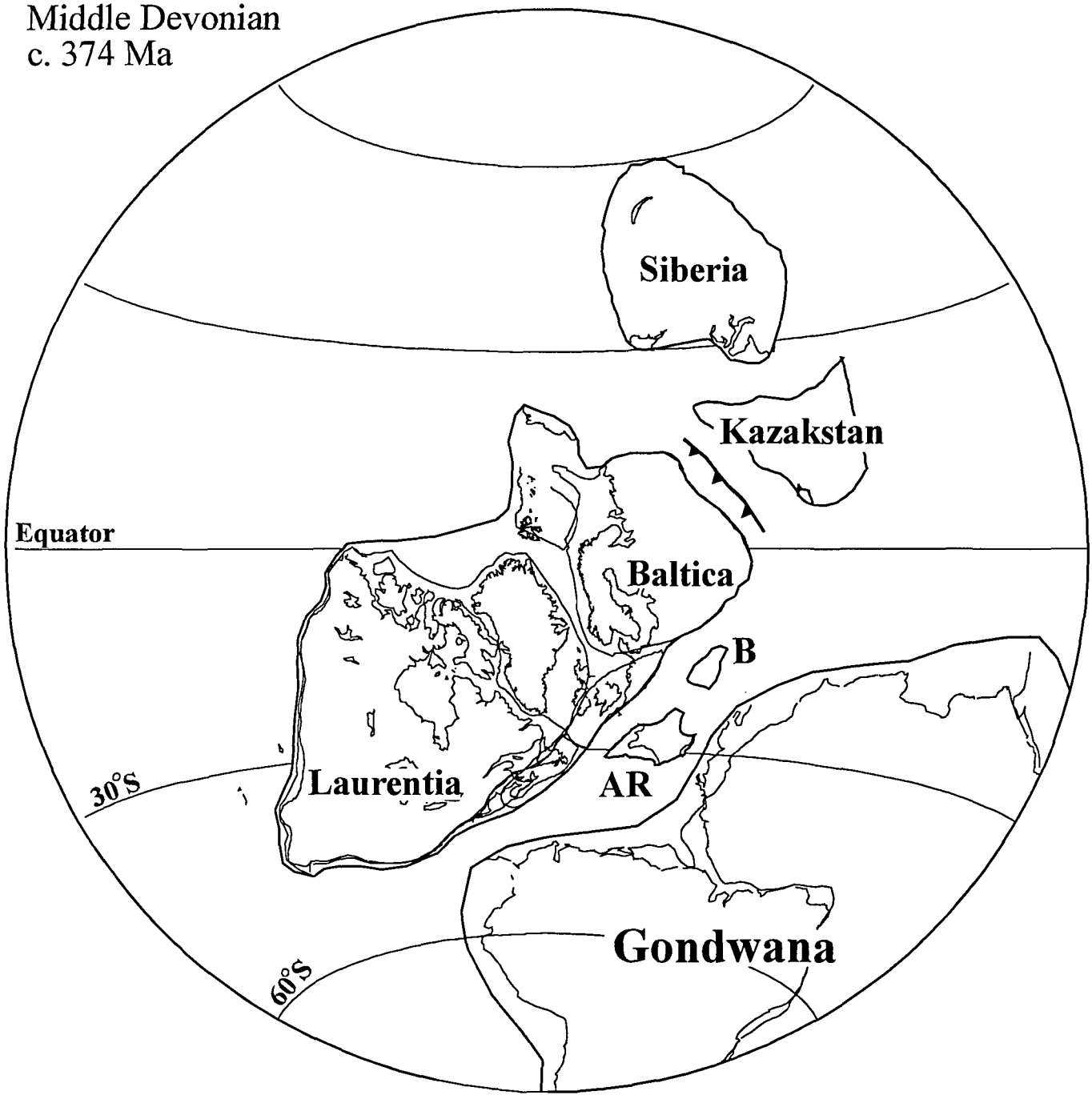

FIGURE 7
Mid-Devonian reconstruction (see text).

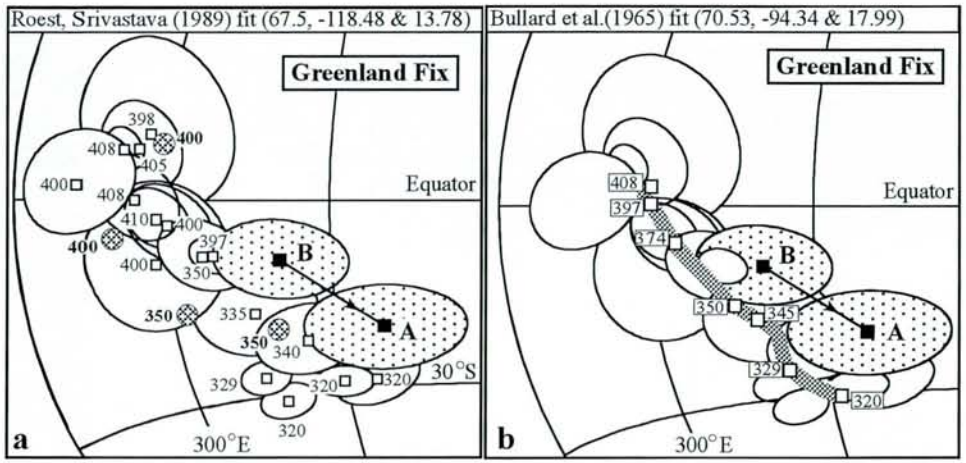

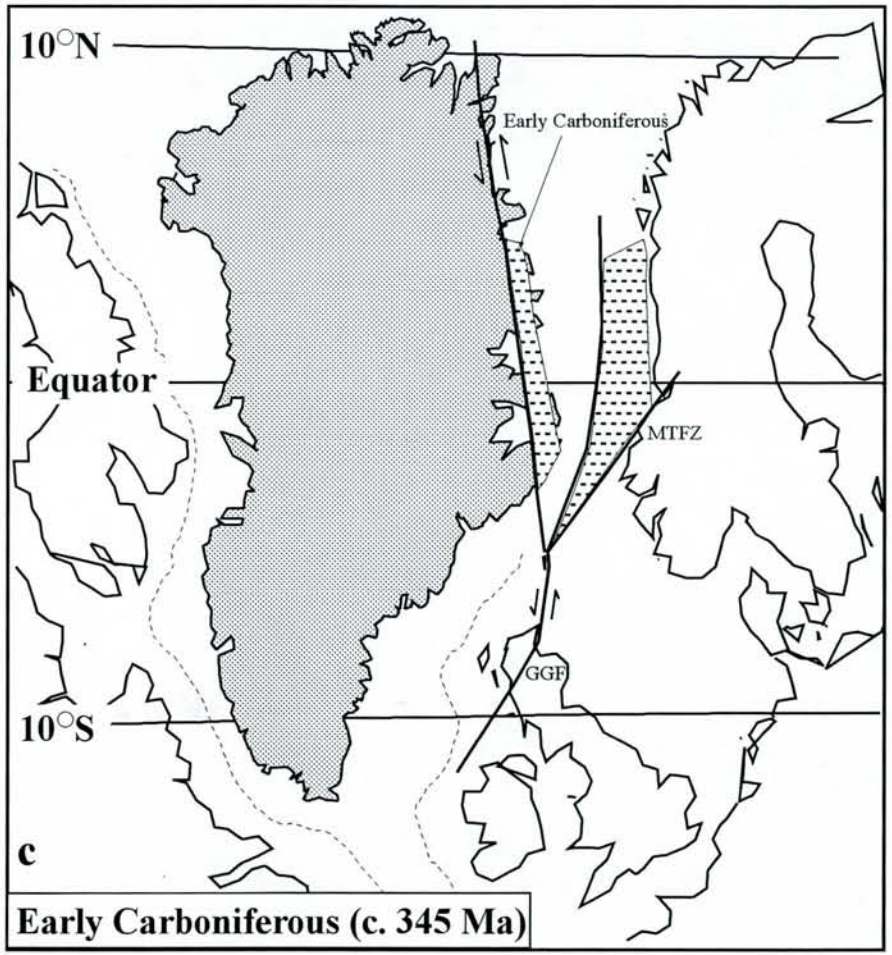

FIGURE 8

a) Devonian and Carboniferous poles from Laurentia (North America and Scotland; open squares with 95% confidence ovals) and Baltica (patterned larger circles with bold age numbers) in North American coordinates and subsequently rotated into Greenland coordinates (Labrador Sea closed) using fit of Roest and Srivastava (1989). 410-320 Ma reference poles listed in Torsvik et al. 1996 (except entry no. 20 in Table 1). Poles A (Upper Devonian, Frasnian) and B (Lower Carboniferous, 337-342 Ma) from Greenland listed in Hartz et al. (1997). b) As in a, but using a Bullard et al. (1965) fit for Labrador Sea reconstruction (euler-pole and rotation angle calculated from their Greenland-Europe and Europe-North America fits). For diagram simplicity only shown with Laurentia error ellipses and smooth spline path derived from Laurentia and Baltica data (smoothing parameter = 200; graded according to Q-factor; cf. procedure in Torsvik et al., 1996). In both fits, Greenland poles (A and B) plot to the east but overlap with Devonian and Carboniferous poles. The misfit is least noted with the original Bullard et al. (1965) fit.

c) Early Carboniferous reconstruction based on the combined Laurentia and Baltica smooth path in (b)

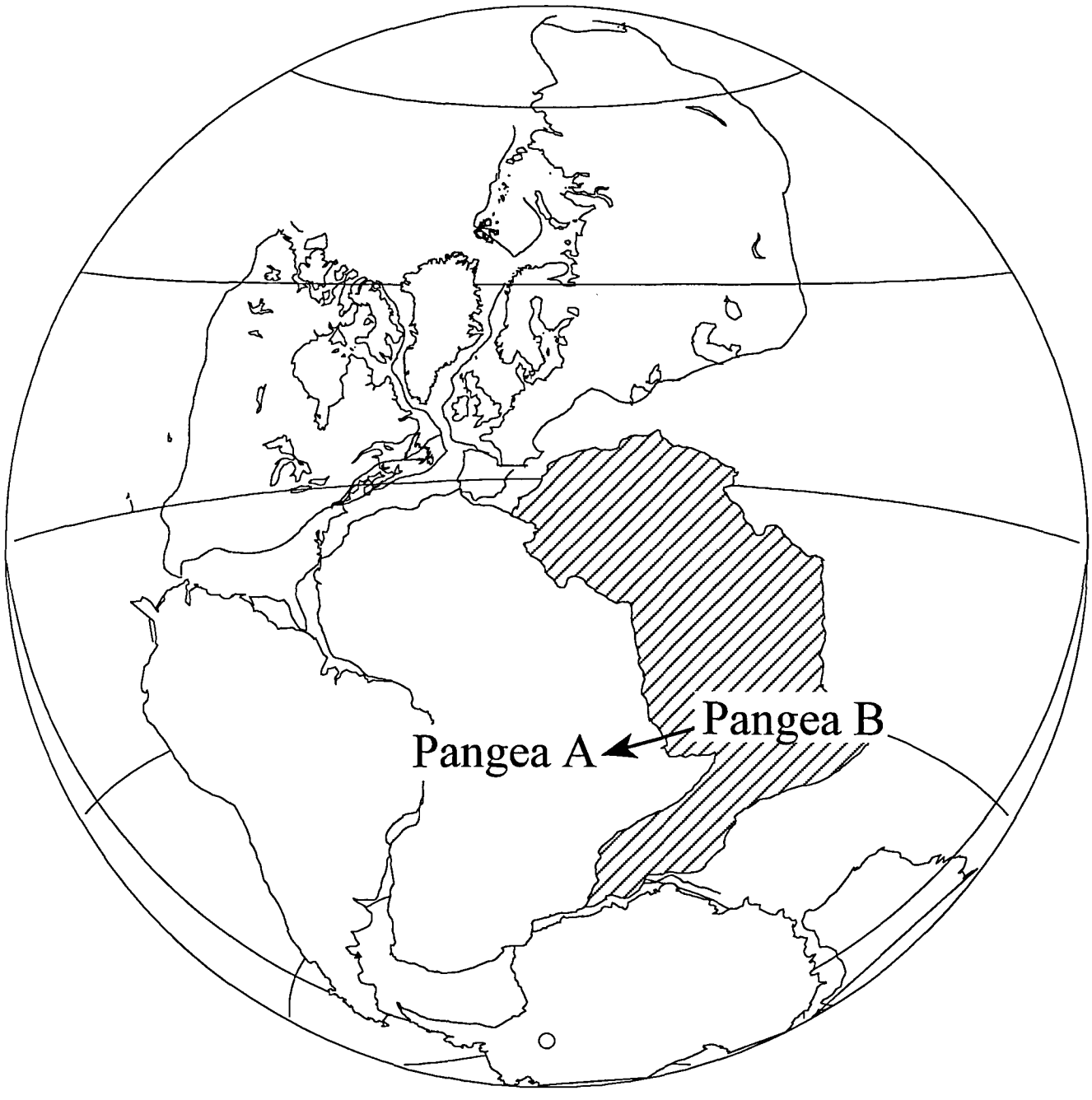

FIGURE 9
Pangea as in Fig. 11a (Pangea A), but showing the position of Africa/Gondwana (Pangea B) according to Torq et al. (1997) in *earliest Triassic* times (relative fit Gondwana-Laurentia fit:38.09N, 357.49E, angle=69.9)

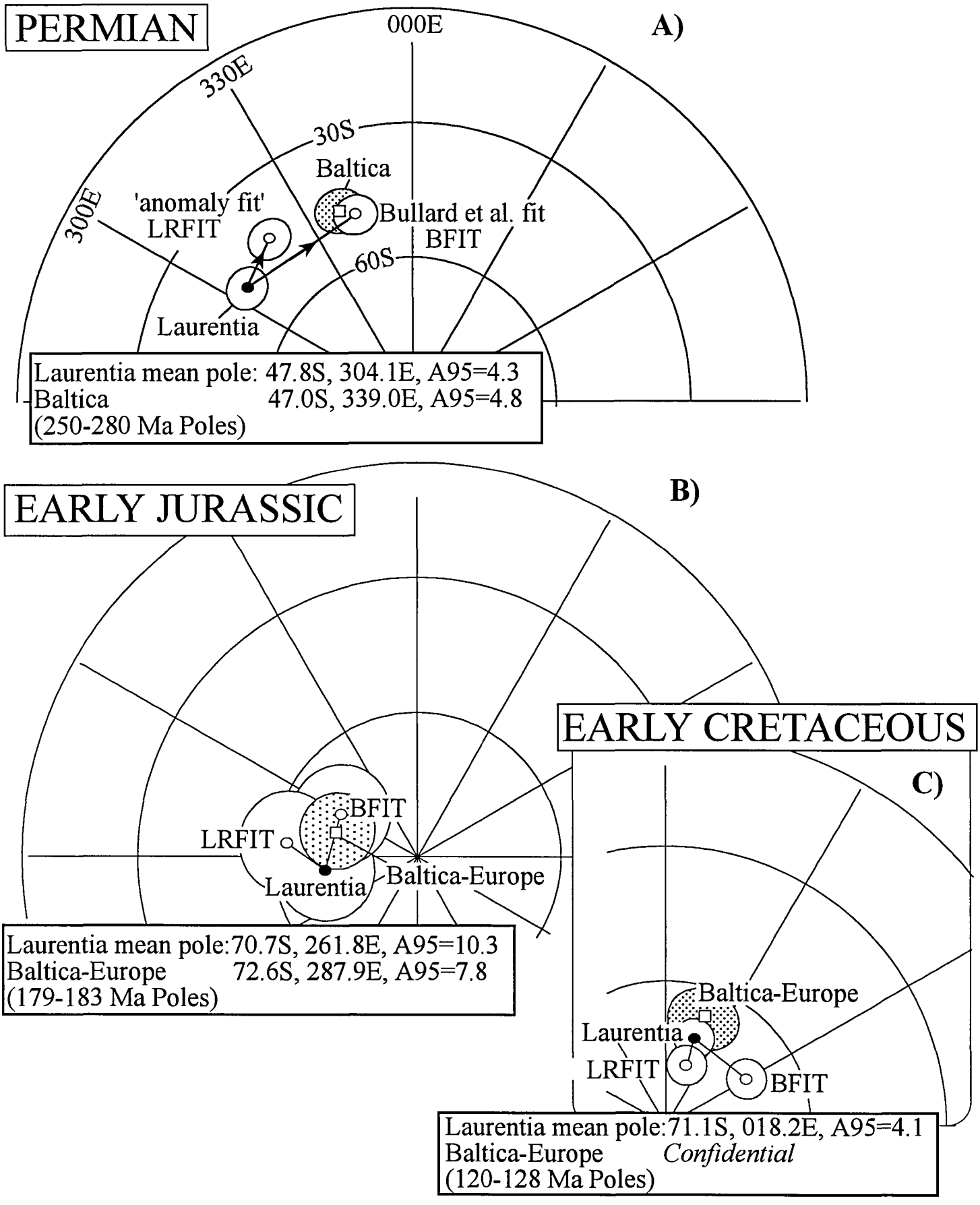

FIGURE 10
Comparison of palaeomagnetic data from Laurentia and Baltica (/Europe) using Bullard et al. (88N, 27E & 38 - BFIT) or the oldest magnetic'anomaly fits (Permian: 69.0N, 156.7E & 23.64, E. Jurassic: 69.1N, 156.7E & 23.64, E. Cretaceous: 68.99N, 154.75E & 23.05 - 'LRFIT'). Note that the Bullard et al. fit is better in early Jurassic and older times (see text for details).

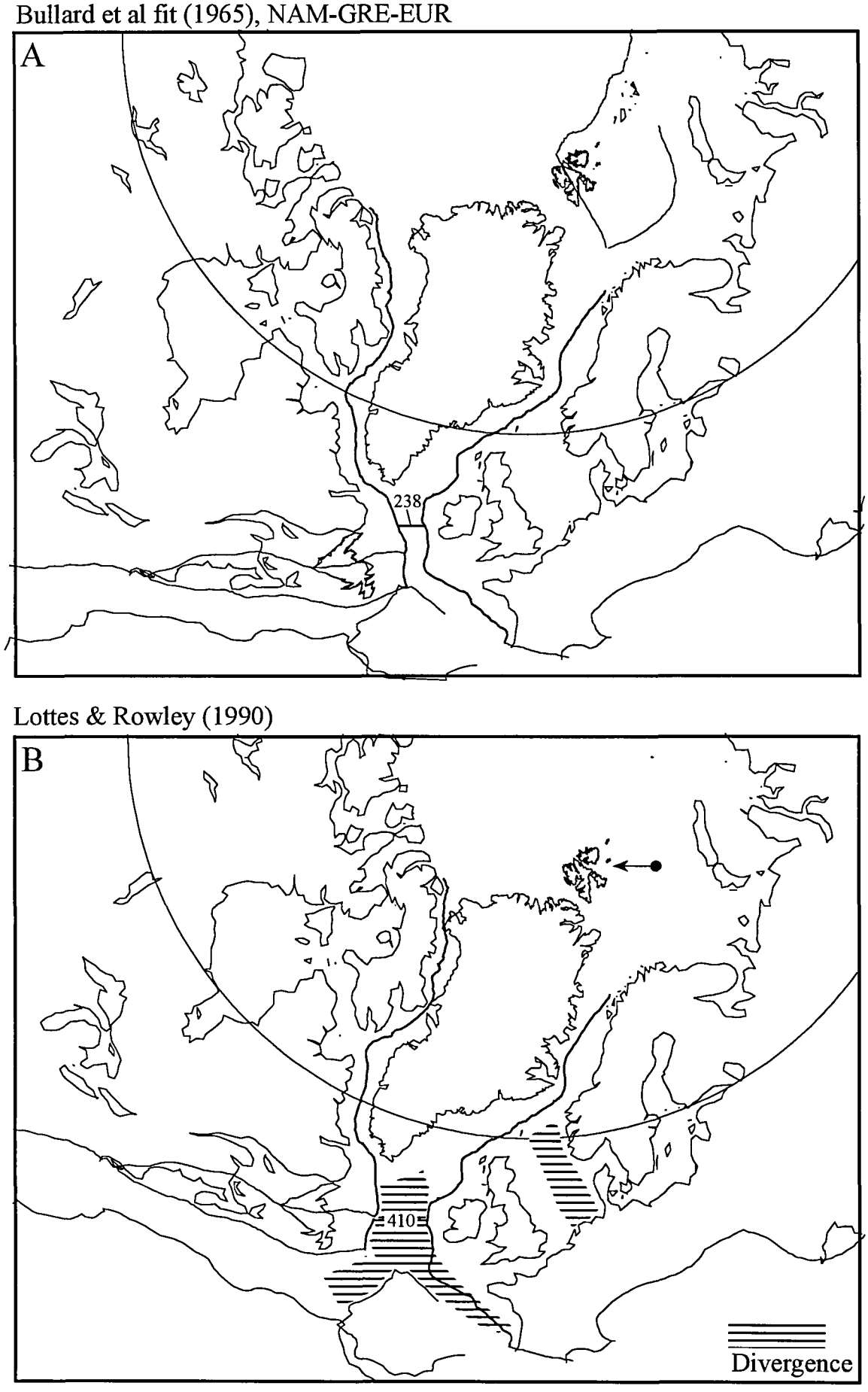

FIGURE 11
Comparison of (a) Bullard et al. (1965)(BFIT) and (b) Lottes & Rowley (1990) fit (LRFIT) for the North Atlantic. The latter fit is better for the Cretaceous, but the Bullard et al. fit is superior for Permian times. It is likely that the North Atlantic fits were gradually translated from (a) to (b) during Permo-Triassic and Jurassic-early Cretaceous rifting events (pre-North Atlantic drift). In the Rockall Area we estimate pre-drift extension (from (a) to (b)) of c. 200 kilometers (asymmetric), while Permo-Triassic and younger extension in the North Sea probably is on the order of c. 100 kilometers.

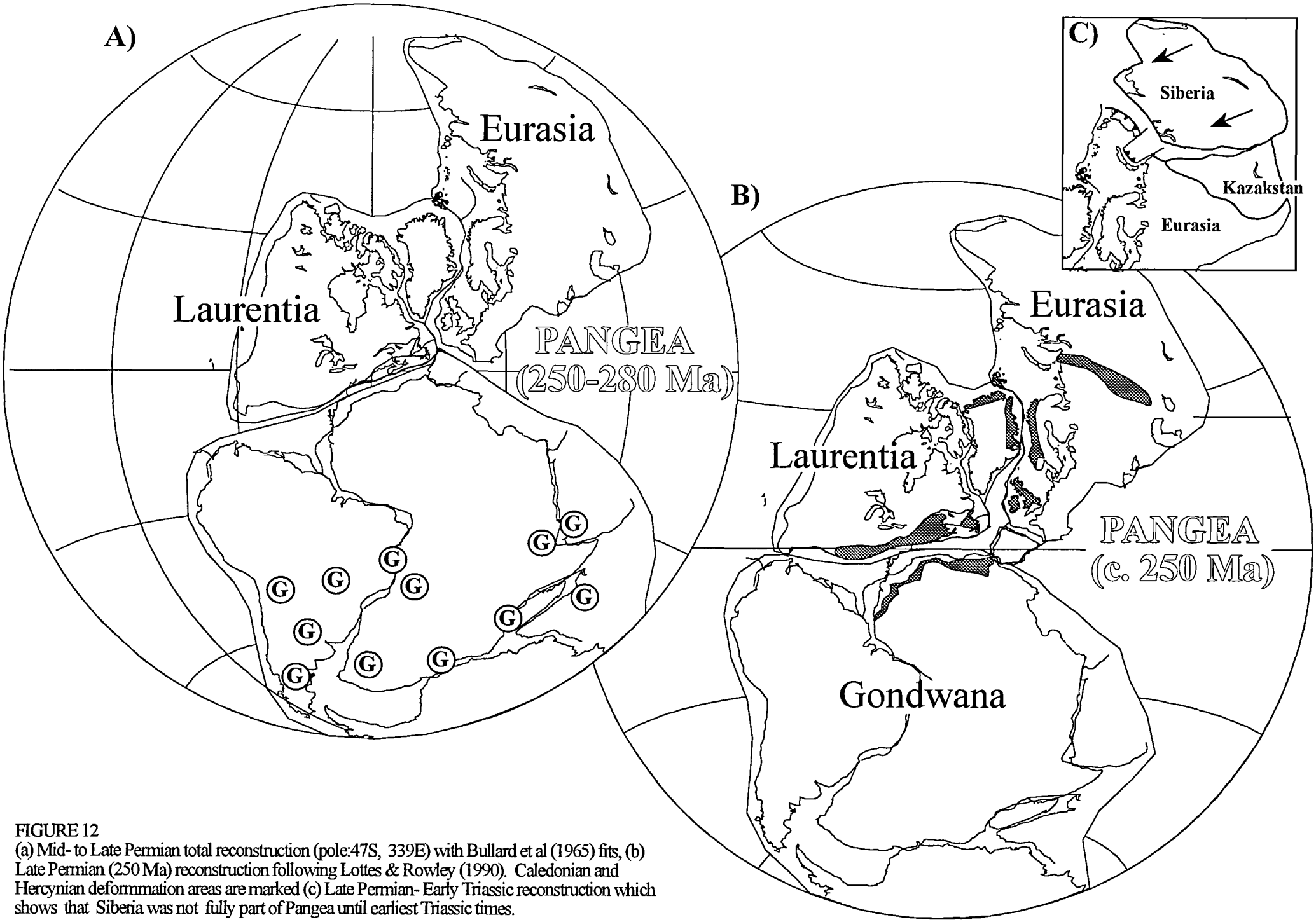

FIGURE 12
(a) Mid- to Late Permian total reconstruction (pole:47S, 339E) with Bullard et al (1965) fits, (b) Late Permian (250 Ma) reconstruction following Lottes & Rowley (1990). Caledonian and Hercynian deformmation areas are marked (c) Late Permian- Early Triassic reconstruction which shows that Siberia was not fully part of Pangea until earliest Triassic times.

Early Triassic, Buntsandsstein, Palaeogeography (243 Ma)

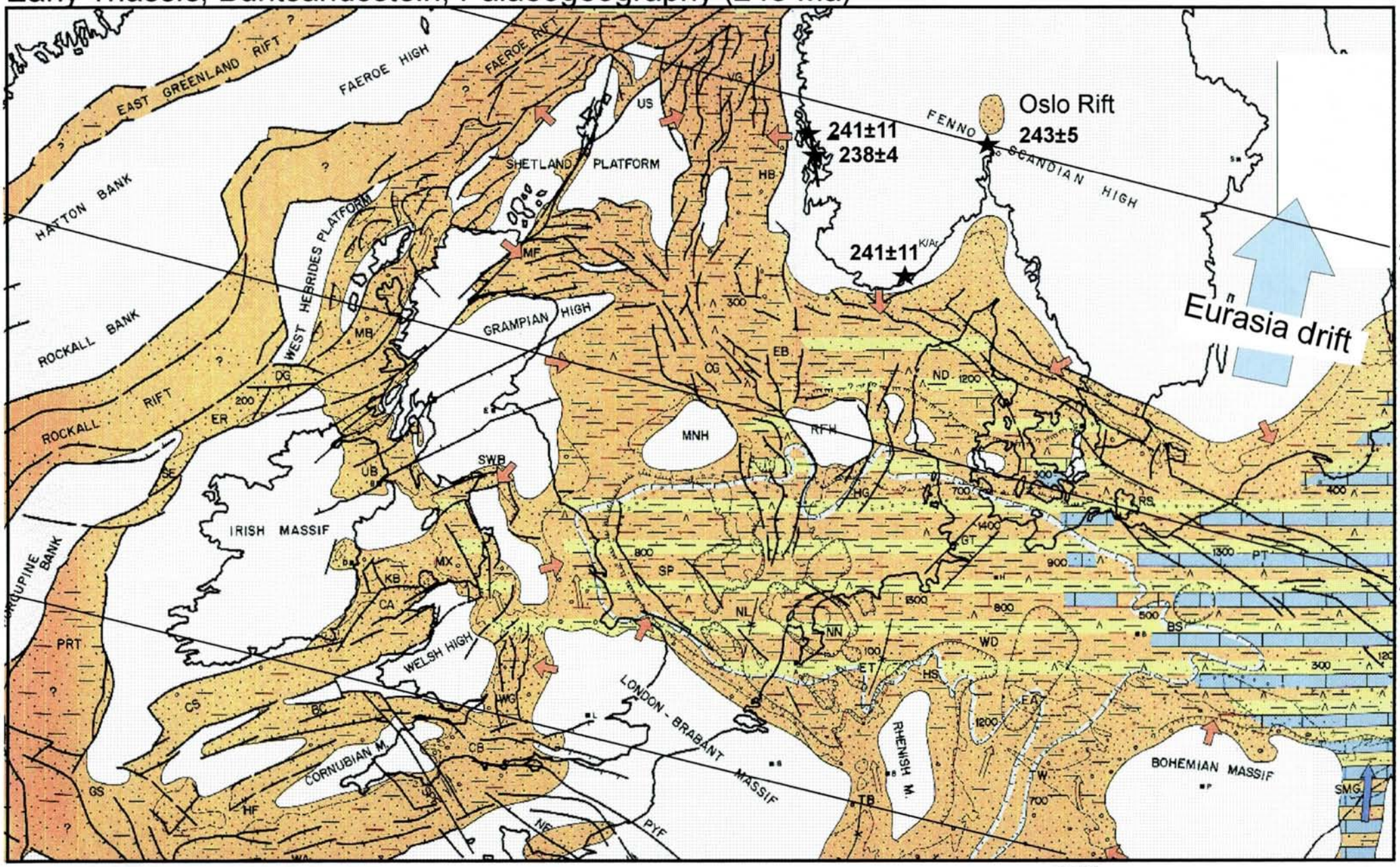

Continental, lacustrine

Deltaic, coastal and shallow-marine clastics

Cratonic, mainly low relief

Carbonates, mainly shallow-marine

★ Volcanics, local

Coal

Salt

FIGURE 13

CAPTION FOR FIGURE 13

Early Triassic, Buntsandsstein, Palaeogeography (c. 243 Ma). Facies distributions after Ziegler (1990) overlain with palaeolatitude lines (15-25°N) derived from palaeomagnetic data. Mean ages from local volcanics (dykes) are as follows: 241±11=Sotra dykes; 238±4=Sunnhordaland dykes; 241±11=Skår volcanics; 243±5=Lunner and Bøverbru dykes. These dykes are syn- to post-rift and discussed in detail by Eide & Torsvik (1998). Original age-data also summarised in Torsvik & Eide (1998).

FIGURE 14a
Middle Triassic reconstruction using an interpolatated European pole (63.8N & 144.7E, from path in Fig. 14b). North Atlatic using BFIT; others LRFIT.

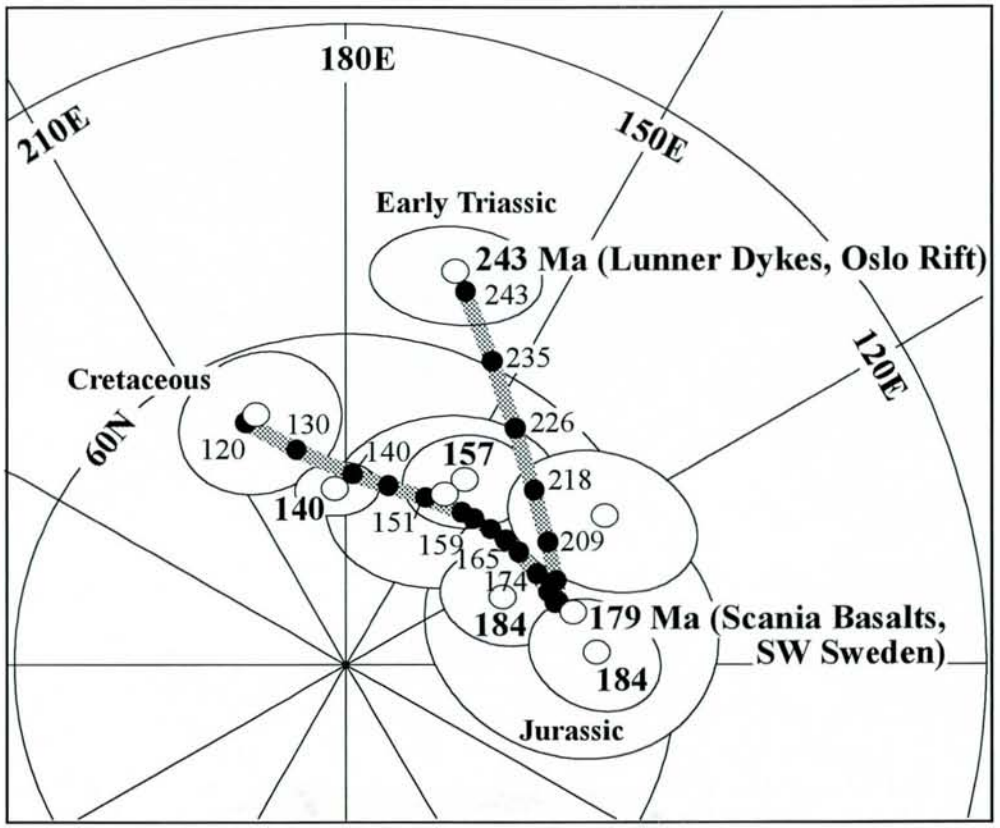

FIGURE 14b
High quality and well-dated palaeomagnetic north-poles (with 95% confidence ellipses) for Baltica-Europe and a smooth APW path. Numbers in million years. Large bold numbers refer to input poles (Torsvik, in progress). Lunner dykes (243 Ma) and Scania basalts (179 Ma) dated during the course of this project.

Age of the Ocean Floor

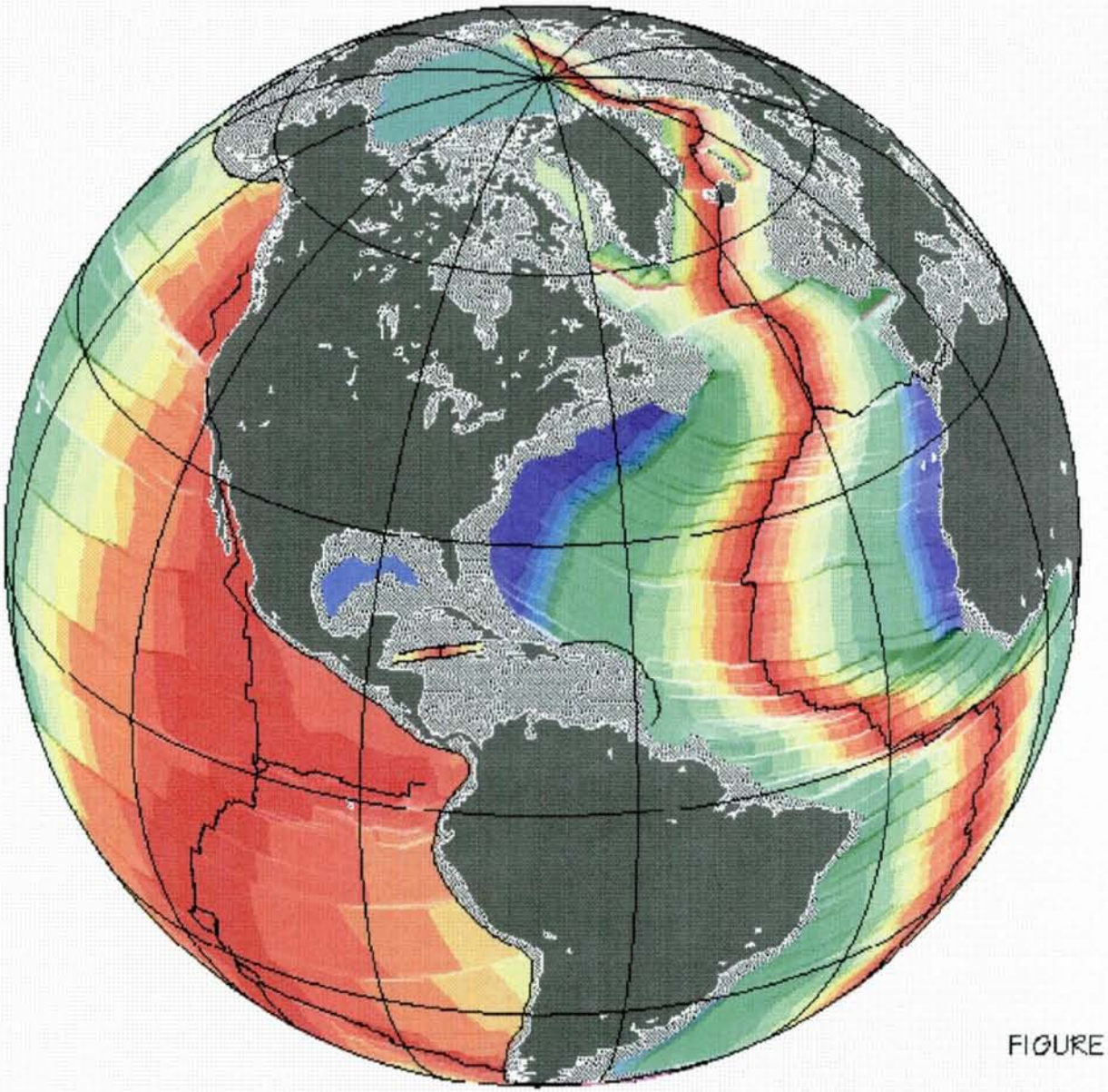

FIGURE 15

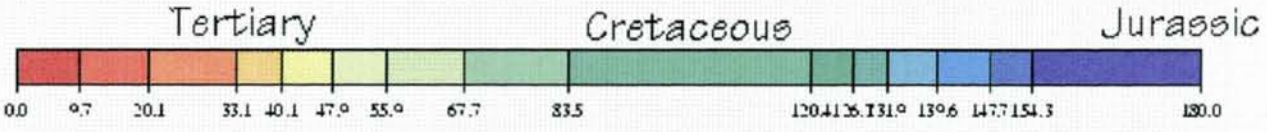

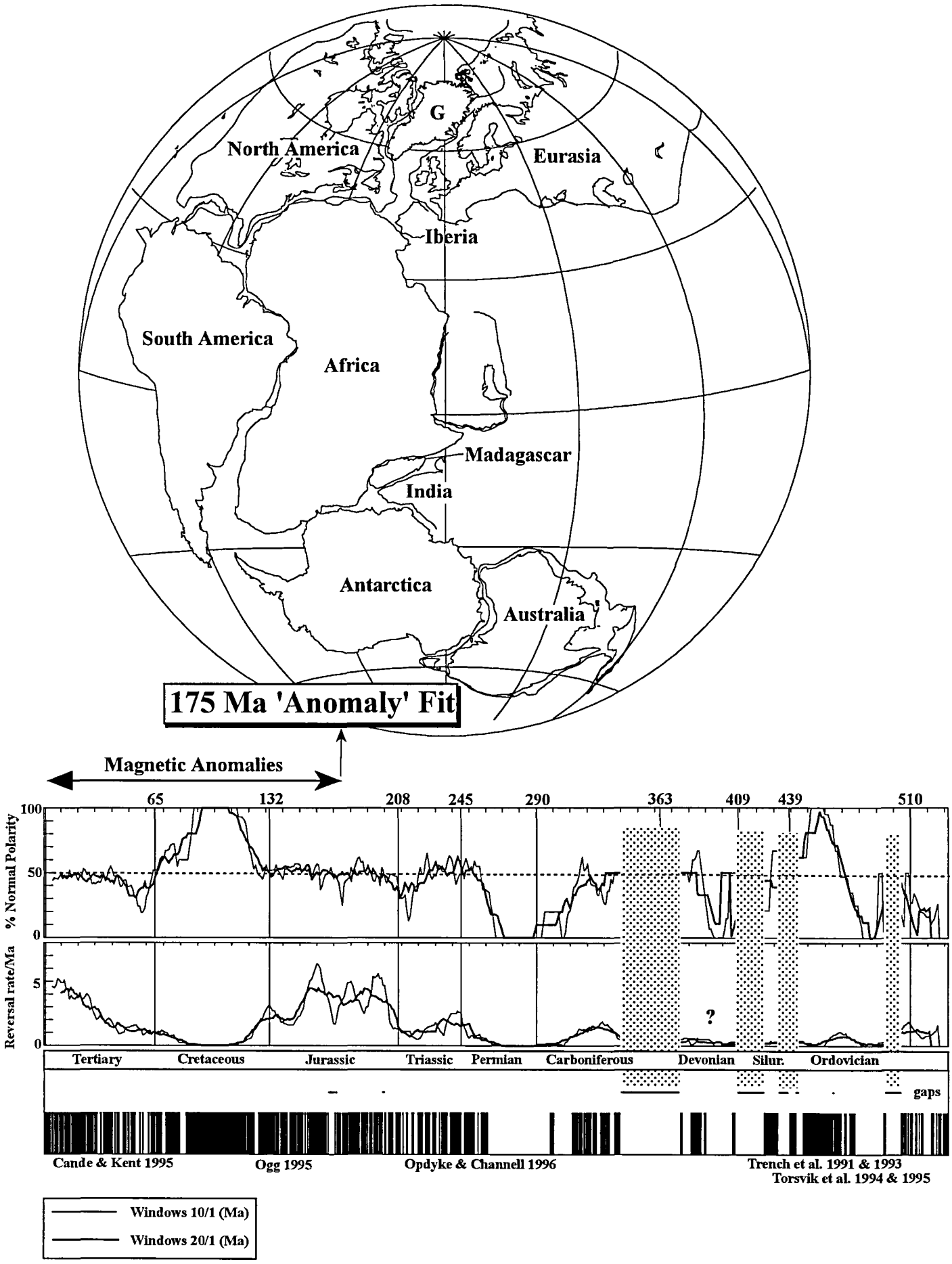

FIGURE 16 Estimates of polarity ratio (expressed in % Normal Polarity) and reversal rates (/Ma) from Lower Cambrian to the present. Data compiled from magnetic anomalies and magnetostratigraphic compilations (see Eide & Torsvik 1996). Calculations are based on a 1 Ma sliding time-window (window length, 10 and 20 Ma). Gaps or uncertainties in the polarity record are shaded. Reconstruction (Eurasia fixed), based on the oldest available magnetic anomalies, is shown at the top.

Late Jurassic
Kimmeridgian-Volgian (150 Ma)

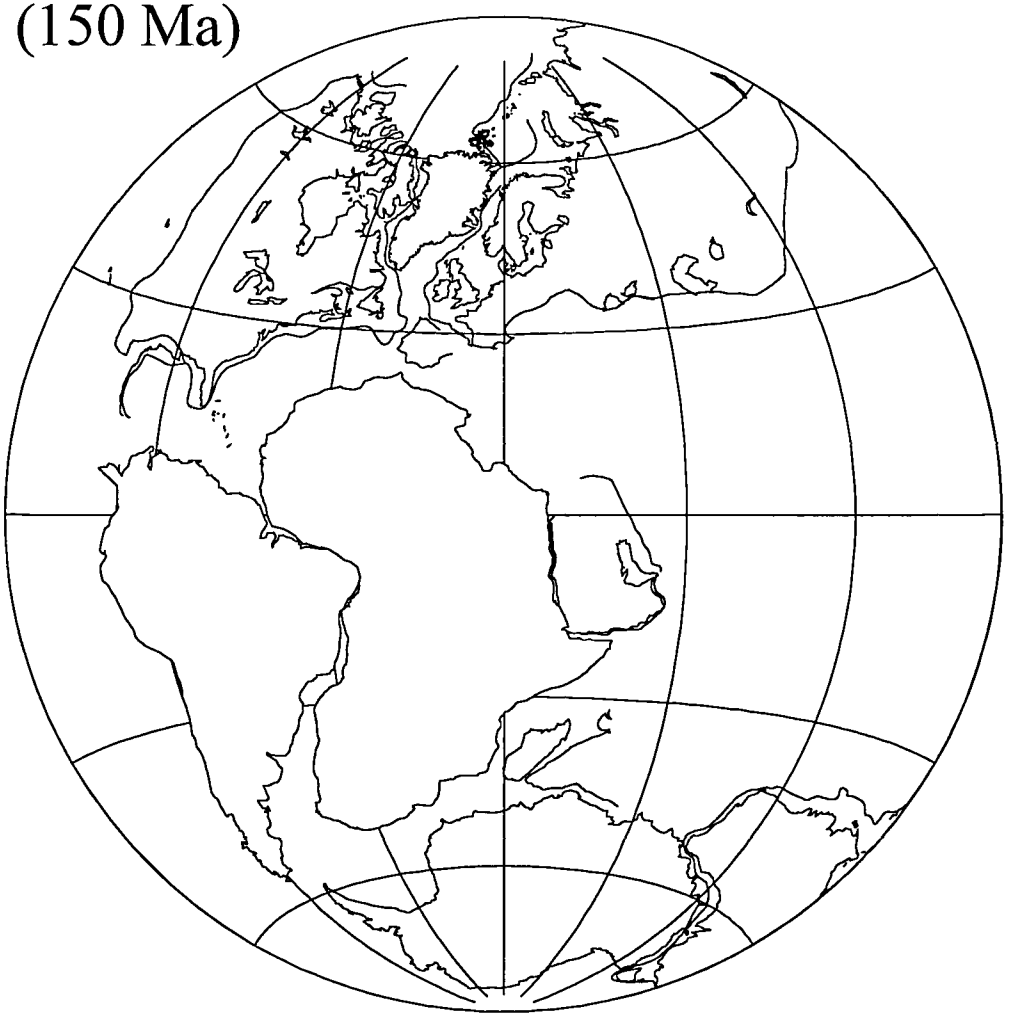

FIGURE 17b
Late Jurassic reconstruction based on an European pole of 73.3N & 154.8E (Fig. 14b) and magnetic anomaly fits.

Middle Jurassic
Bajocian (175 Ma)

FIGURE 17a
Middle Jurassic reconstruction using an Eurpean pole of 71.1N & 115.7E (Fig. 14b). BRFIT for NAM-GRE-EU. Other elements are LRFIT's.

CAPTION FOR FIGURE 18

Mid-Jurassic, Bajocian-Bathonian, Palaeogeography (c. 176-164 Ma). Facies distributions after Ziegler (1990) overlain with palaeolatitude lines (40-55°N) derived from palaeomagnetic data. Onshore, mean ages from local volcanics are as follows: 162±4=Sunnhordaland dykes (youngest generation); 179±4=Gobnehall volcanics. The Dalsfjord Fault, western Norway, shows important reactivation at this time (163±4 Ma is a maximum age). Fission-track exhumation ages are concentrated in this time-slice. Dykes are probably syn-rift and discussed in detail by Eide & Torsvik (1998). Original age-data also summarised in Torsvik & Eide (1998).

Mid-Jurassic, Bajocian-Bathonian (176.5±4.0 -164.4±3.8 Ma), Palaeogeography

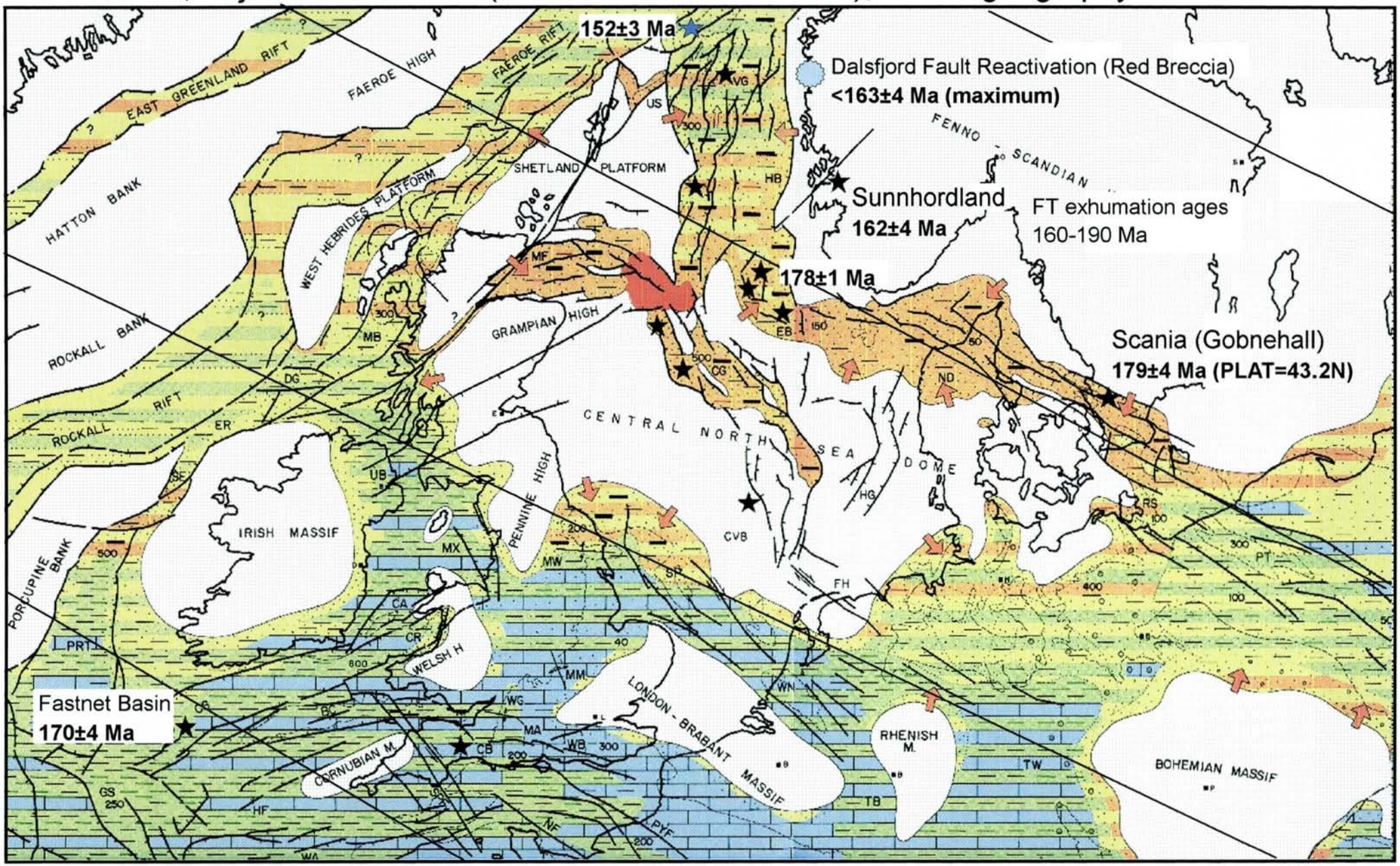

Continental, lacustrine

Deltaic, coastal and shallow-marine clastics

Shallow-marine, mainly shales

Carbonates, mainly shallow-marine

Cratonic, mainly low relief

Major extrusives

Volcanics, local

Coal

FIGURE 18

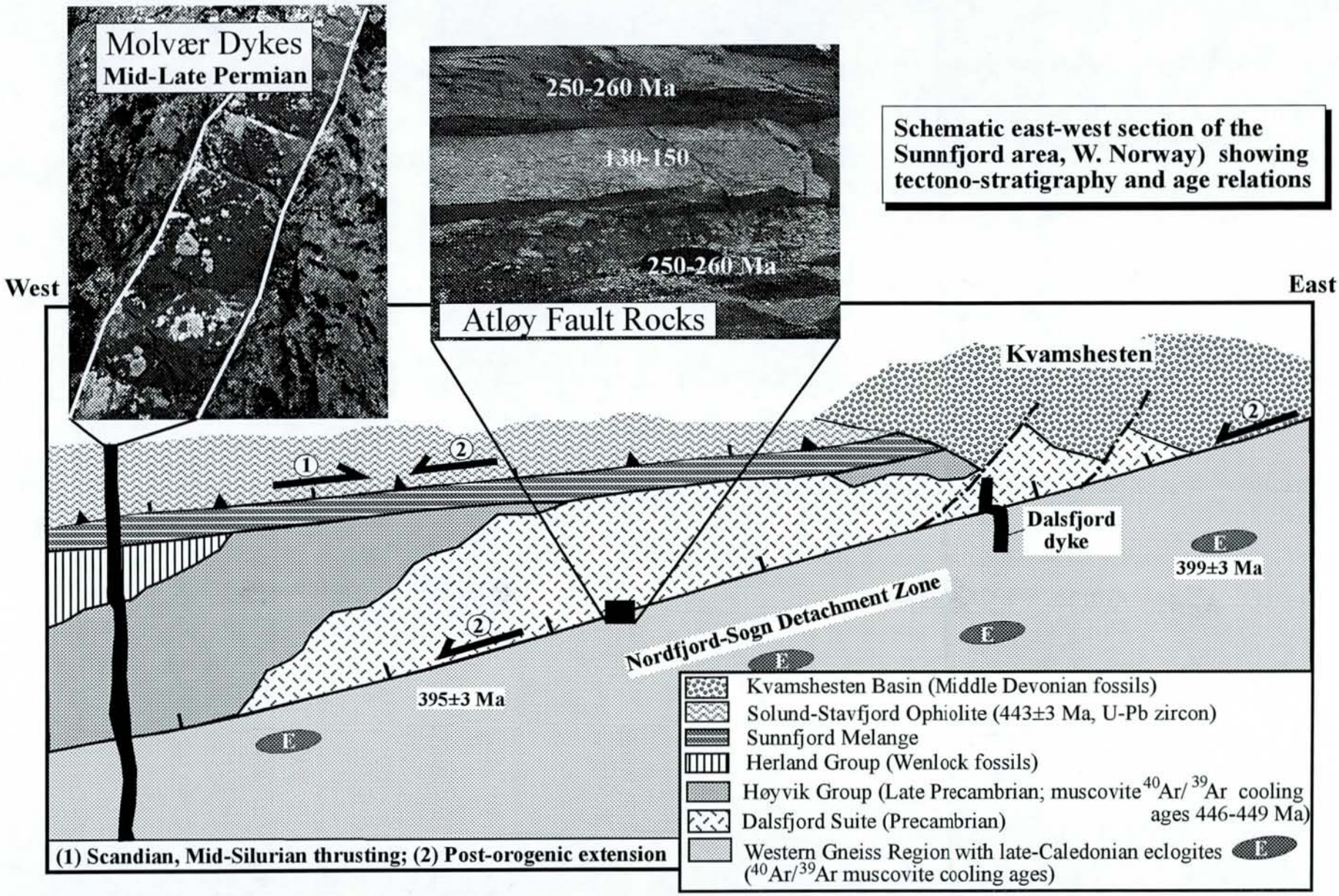

FIGURE 19

Schematic (not to scale) east-west section of the Kvamshesten Devonian Basin and substrate in Western Norway . The profile illustrates the tectono-stratigraphy and the approximate position of the Molvær and Dalsfjord dykes. Notice that syn-depositional Devonian faults are truncated by the reactivated Nordfjord-Sogn Detachment, and that the Dalsfjord dyke is deformed by the fault.

The Molvær dyke is mid-late Permian in age (Torsvik et al. 1997).

$^{40}Ar/^{39}Ar$ cooling ages of white micas are from Andersen et al. (1998) and Eide et al. (1997).

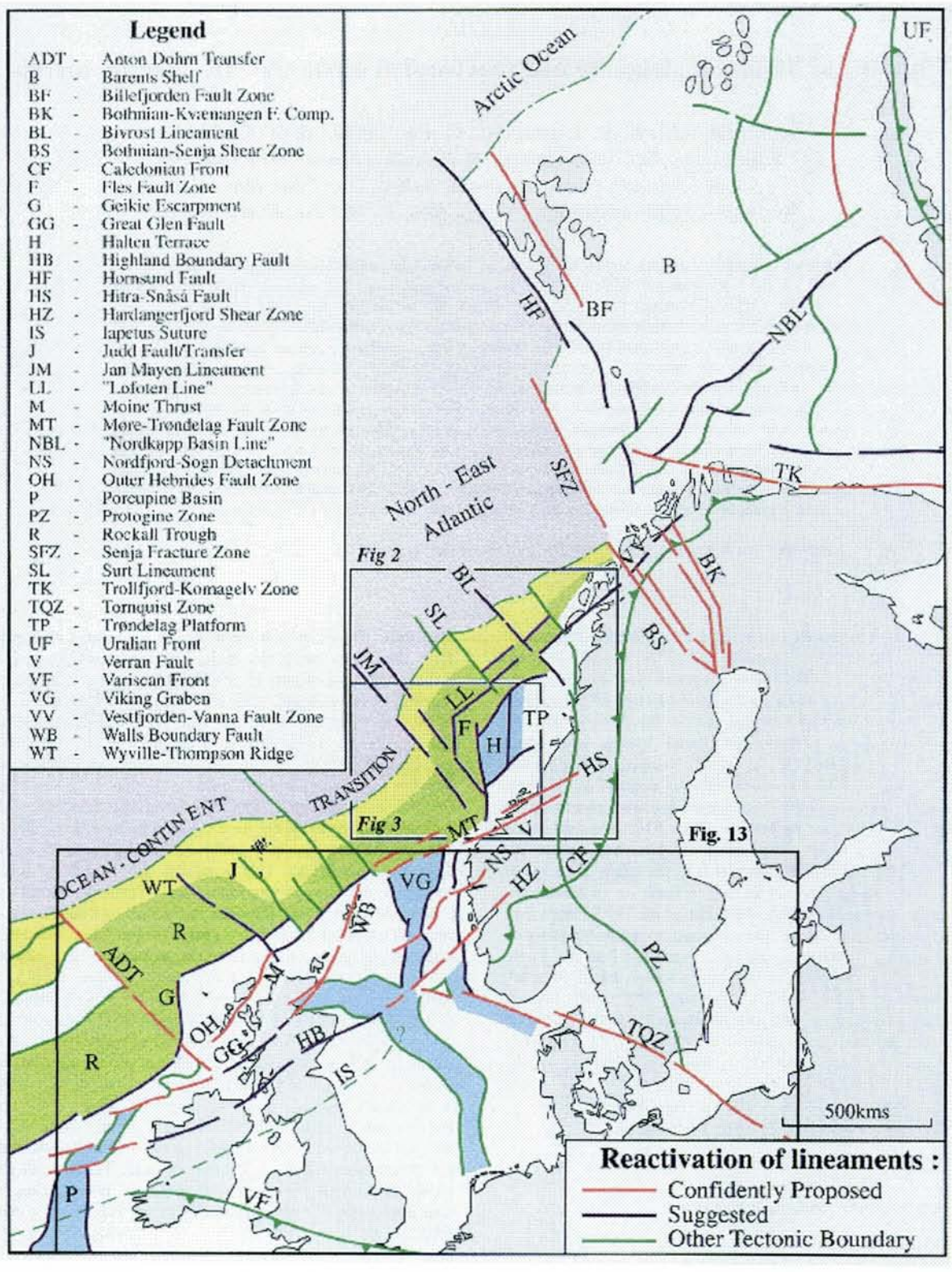

FIGURE 20
Interpreted lineaments for the North Atlantic and Barents Sea (after Dore et al. 1997). Basins are: blue (Jurassic), green (Cretaceous), yellow (Cenozoic). Reactivation lineaments are considered to be basement reactivated.

Early Cretaceous, Hauterivian-Barremian

HOT SPOT REFERENCE (130 Ma)

FIGURE 21a
Early Cretaceous Hot-spot (/magnetic anomaly) reconstruction.

PALEOMAGNETIC REFERENCE (120-128 Ma)

(NAM Pole: 71.1S, 018.2E)

FIGURE 21b
Early Cretaceous palaeomagnetic (/magnetic anomaly) reconstruction.

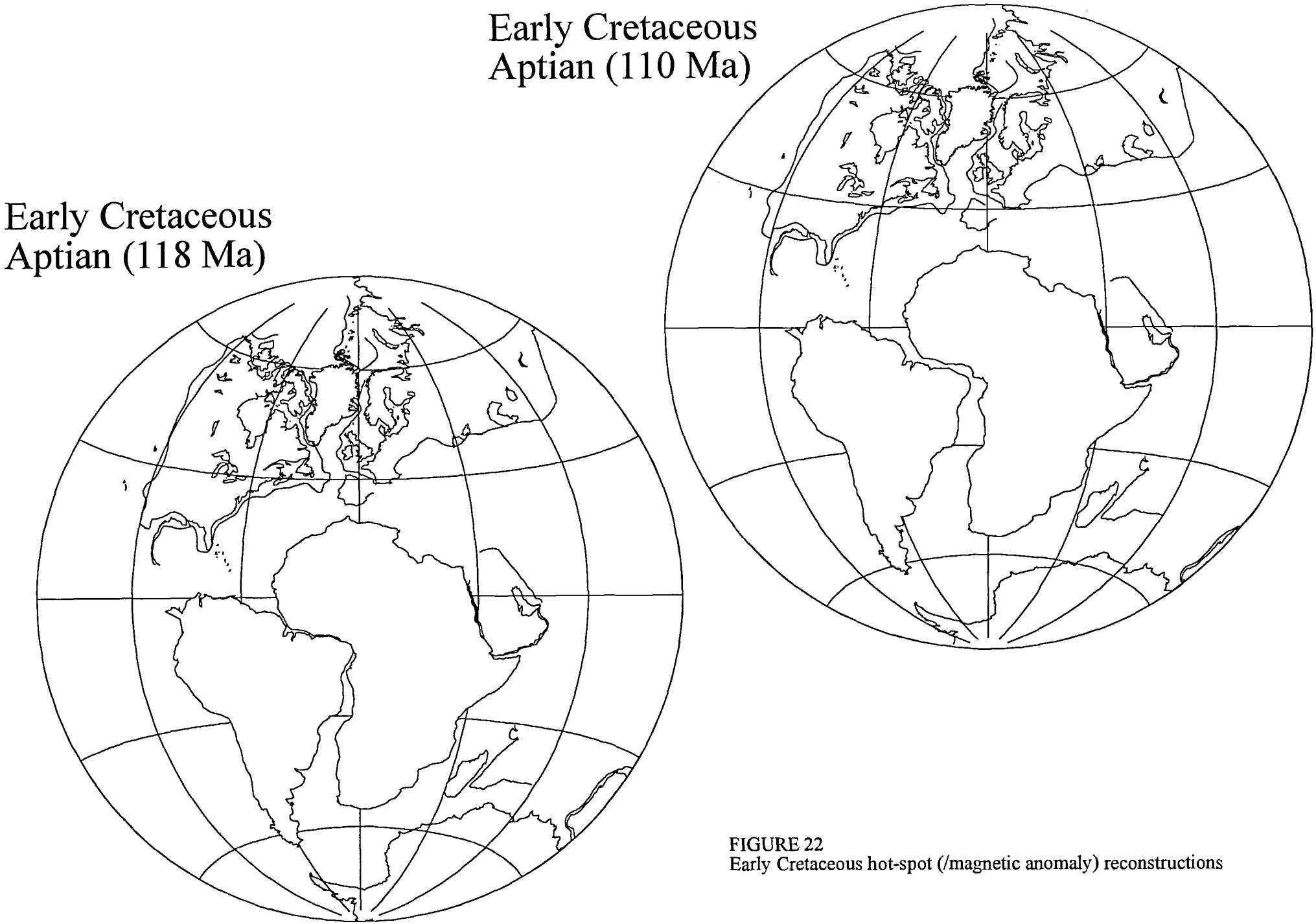

FIGURE 22
Early Cretaceous hot-spot (/magnetic anomaly) reconstructions

Late Cretaceous
Turonian (90 Ma)

Early Cretaceous
Albian (100 Ma)

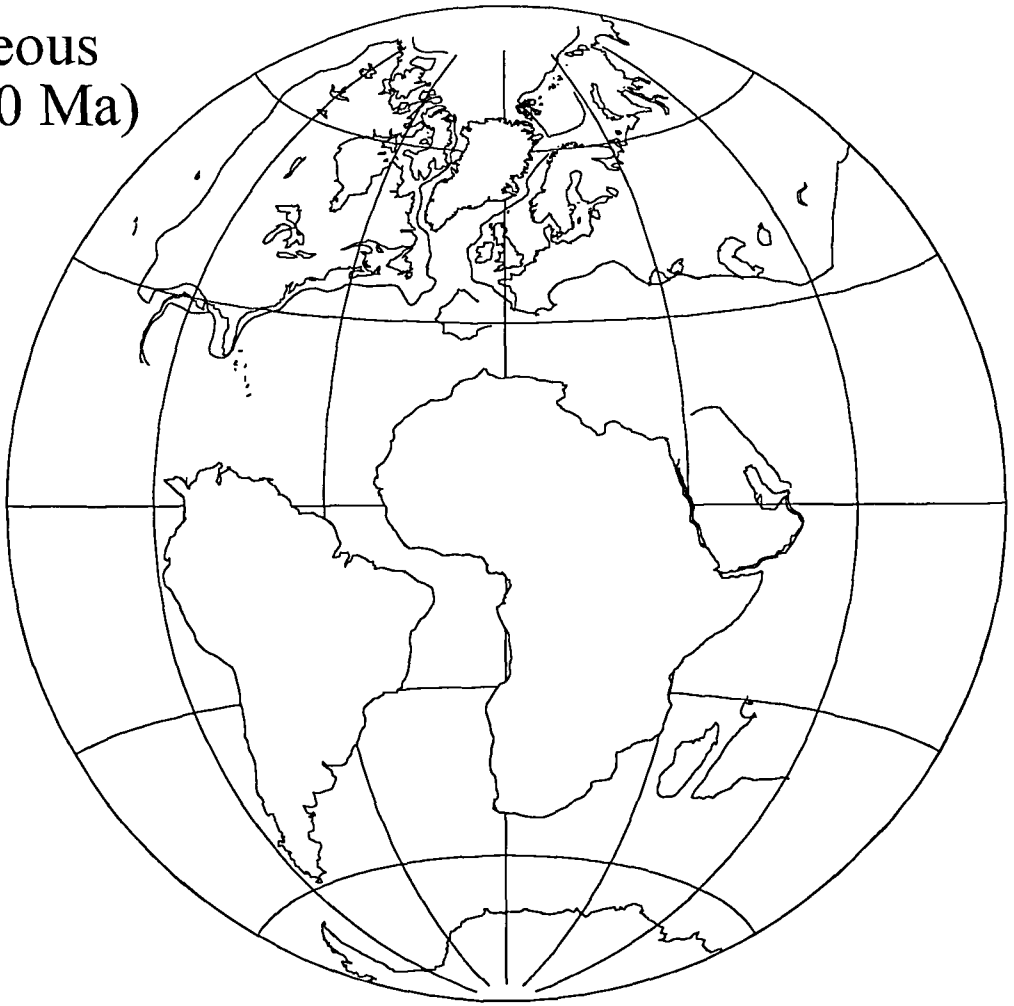

FIGURE 23
Early and Late Cretaceous hot-spot (/magnetic anomaly) reconstructions

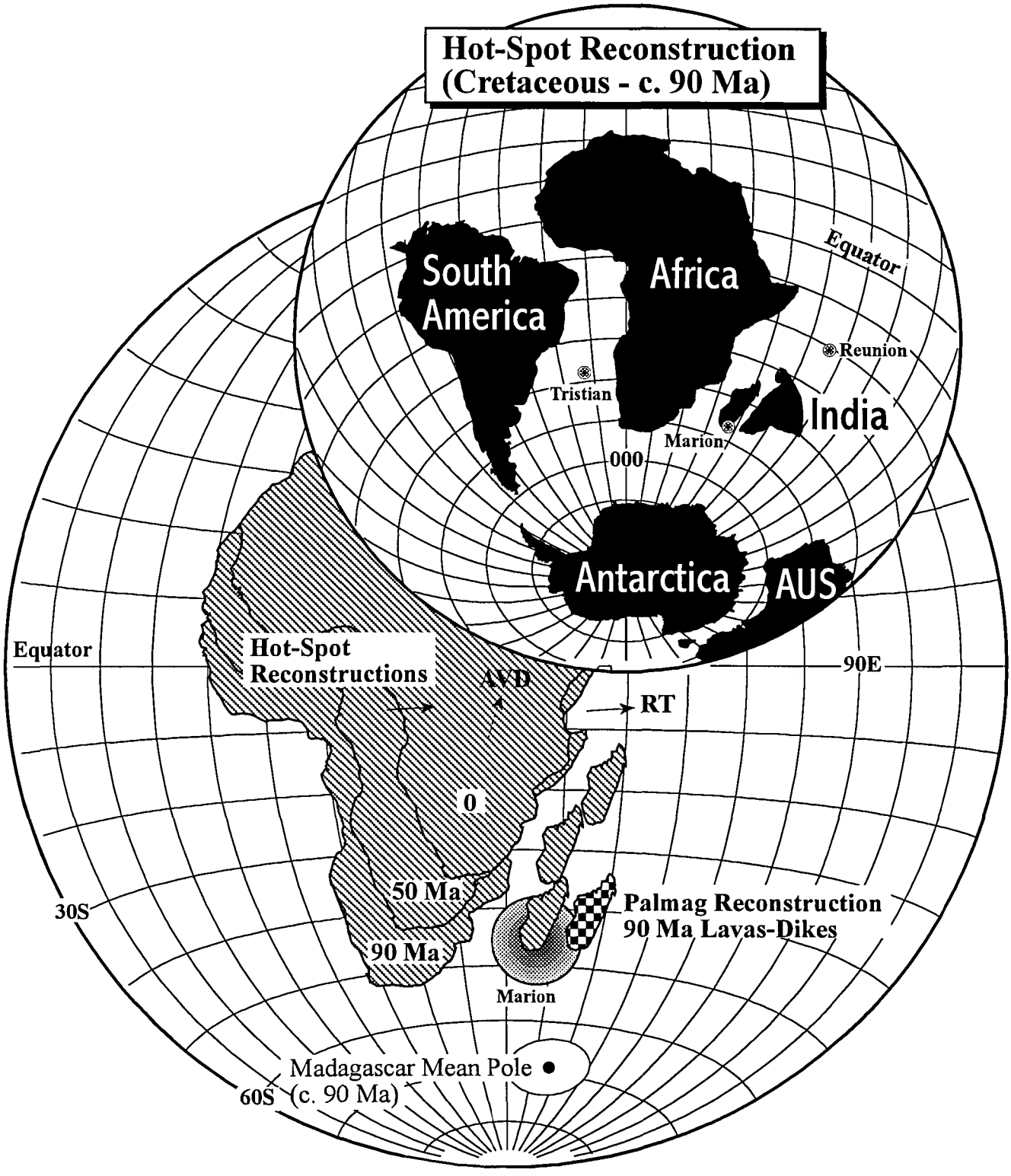

FIGURE 24
Example of the perfect fit between a hot-spot reconstruction and a palaeomagnetic reconstruction of Madagascar (Torsvik et al. 1998) at 90 Ma. This illustrates that the Marion hot-spot was the instegator for separation of the Mad-India amalgam.

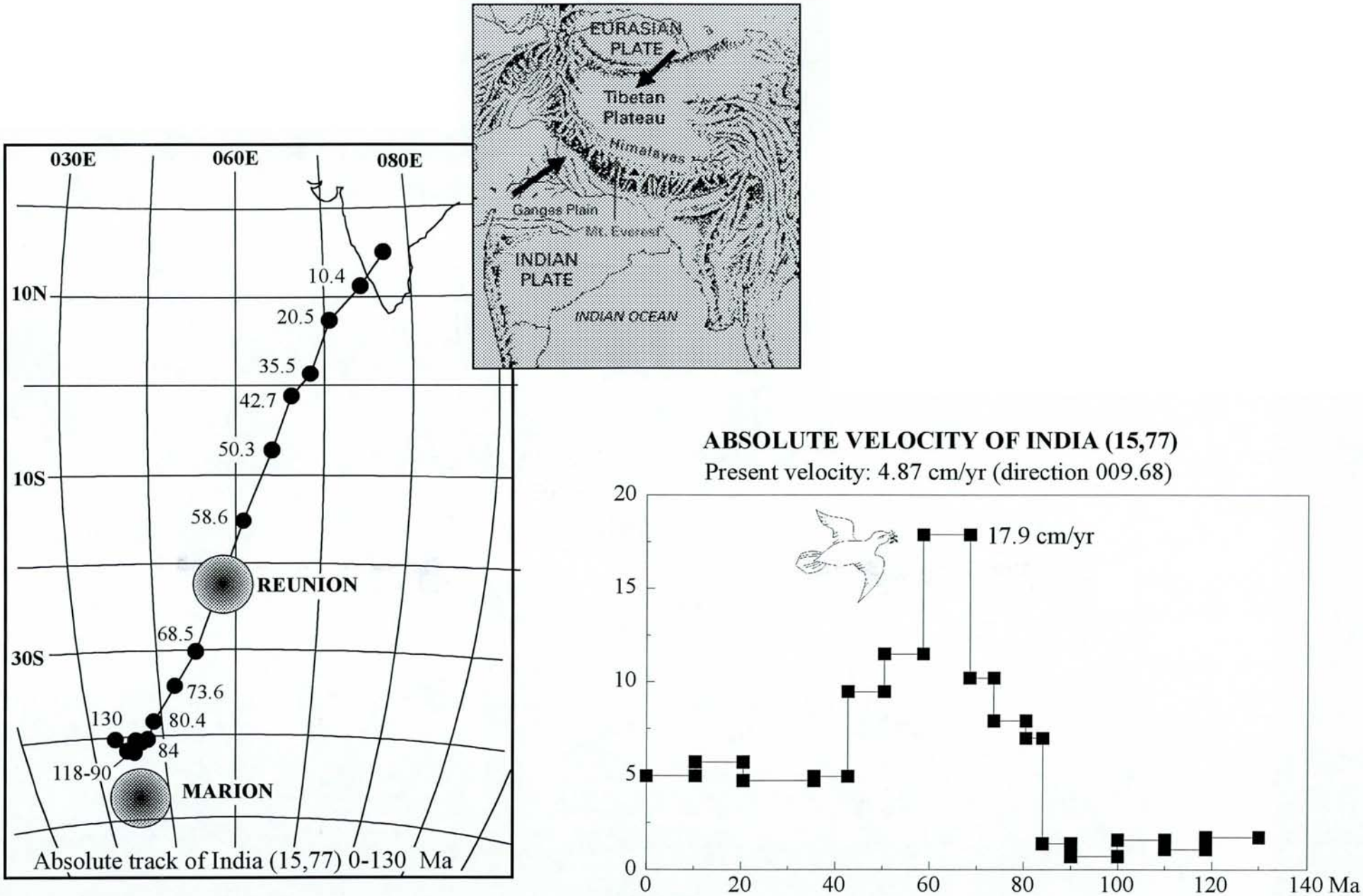

FIGURE 25
Left diagram: Absolute track of India (15N & 077E). Right diagram: Calculated absolute velocities for India over the last 130 Ma. Notice the peak at the K-T boundary when India separated from the Seychelles over the Reunion hot-spot.

Late Cretaceous
Campanian (80 Ma)

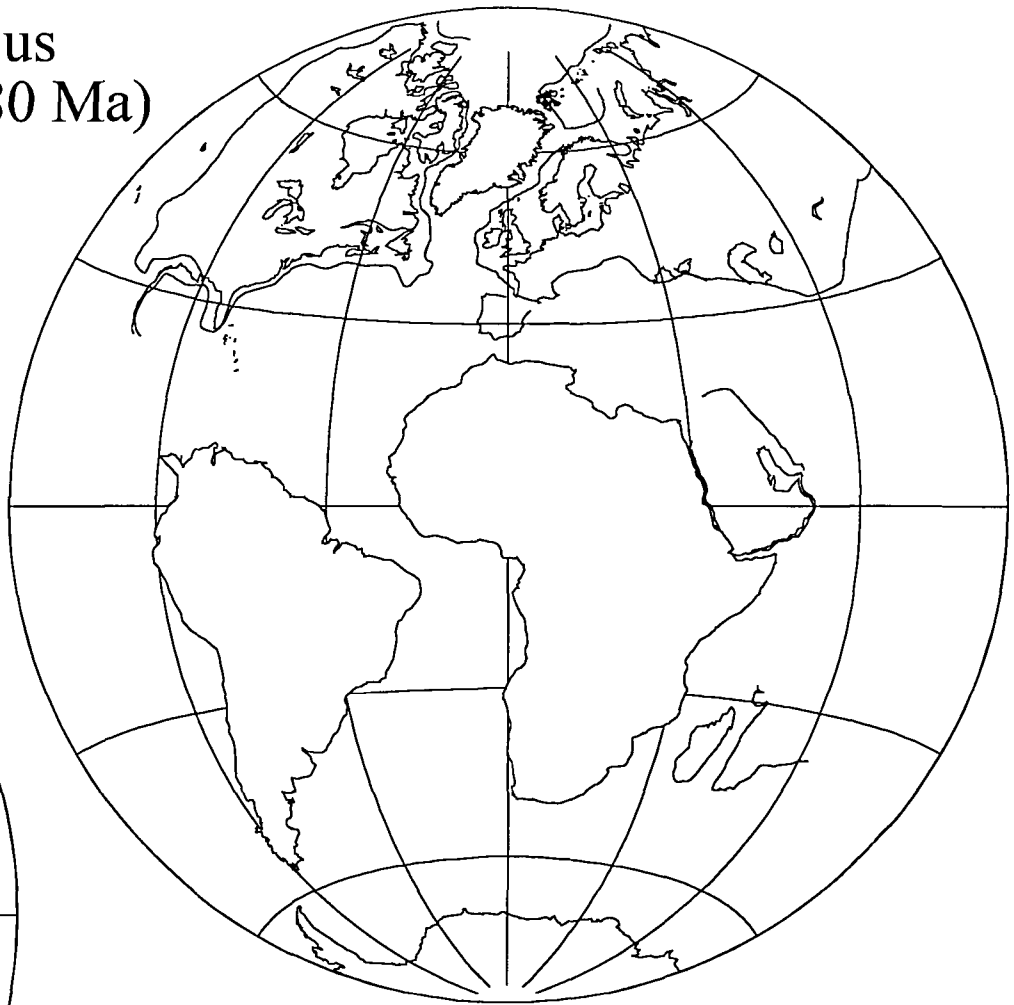

Late Cretaceous
Santonian (84 Ma)

FIGURE 26
Late Cretaceous hot-spot (/magnetic anomaly) reconstructions.

Late Cretaceous
Maastrichtian (68 Ma)

Late Cretaceous
Campanian (74 Ma)

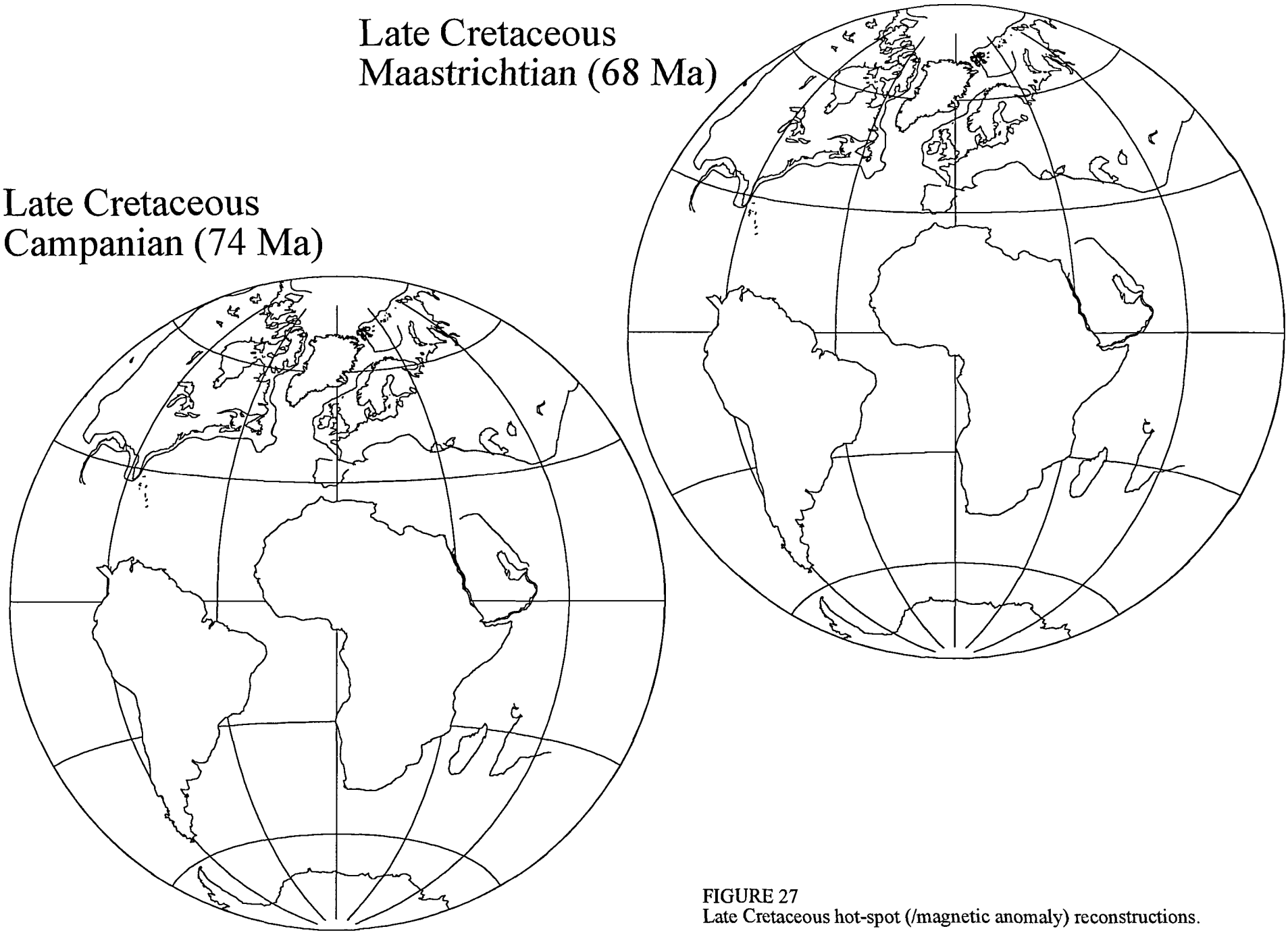

FIGURE 27
Late Cretaceous hot-spot (/magnetic anomaly) reconstructions.

Tertiary
Eocene (50 Ma)

Tertiary
Paleocene (58 Ma)

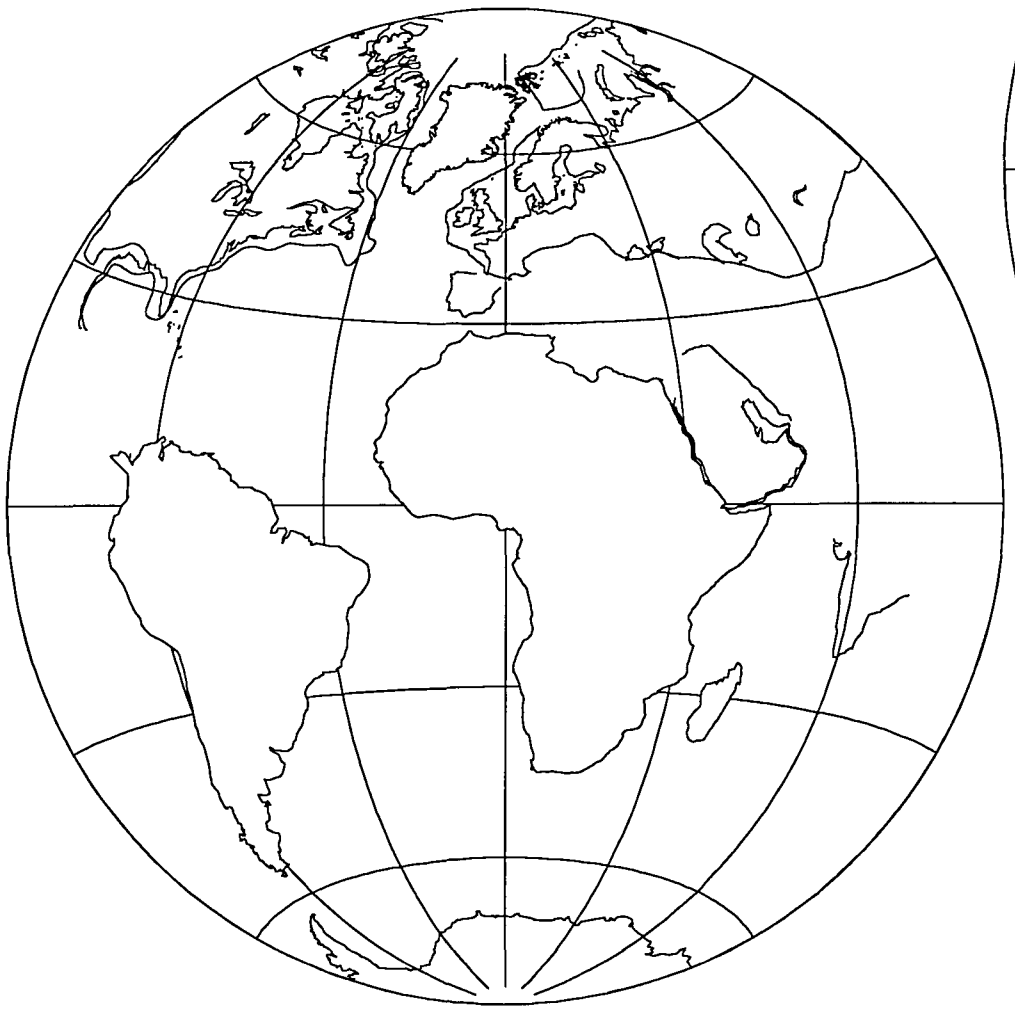

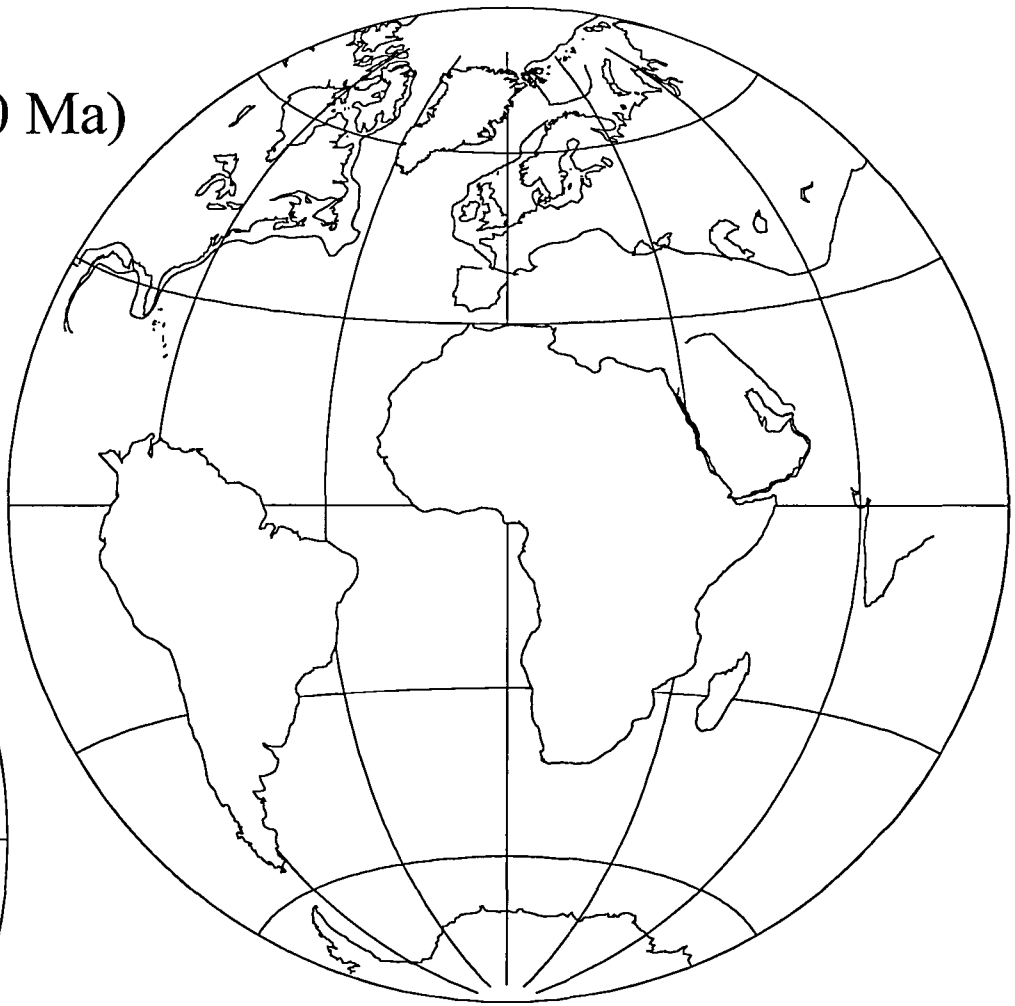

FIGURE 28
Paleocene and Eocene hot-spot (/magnetic anomaly) reconstructions.

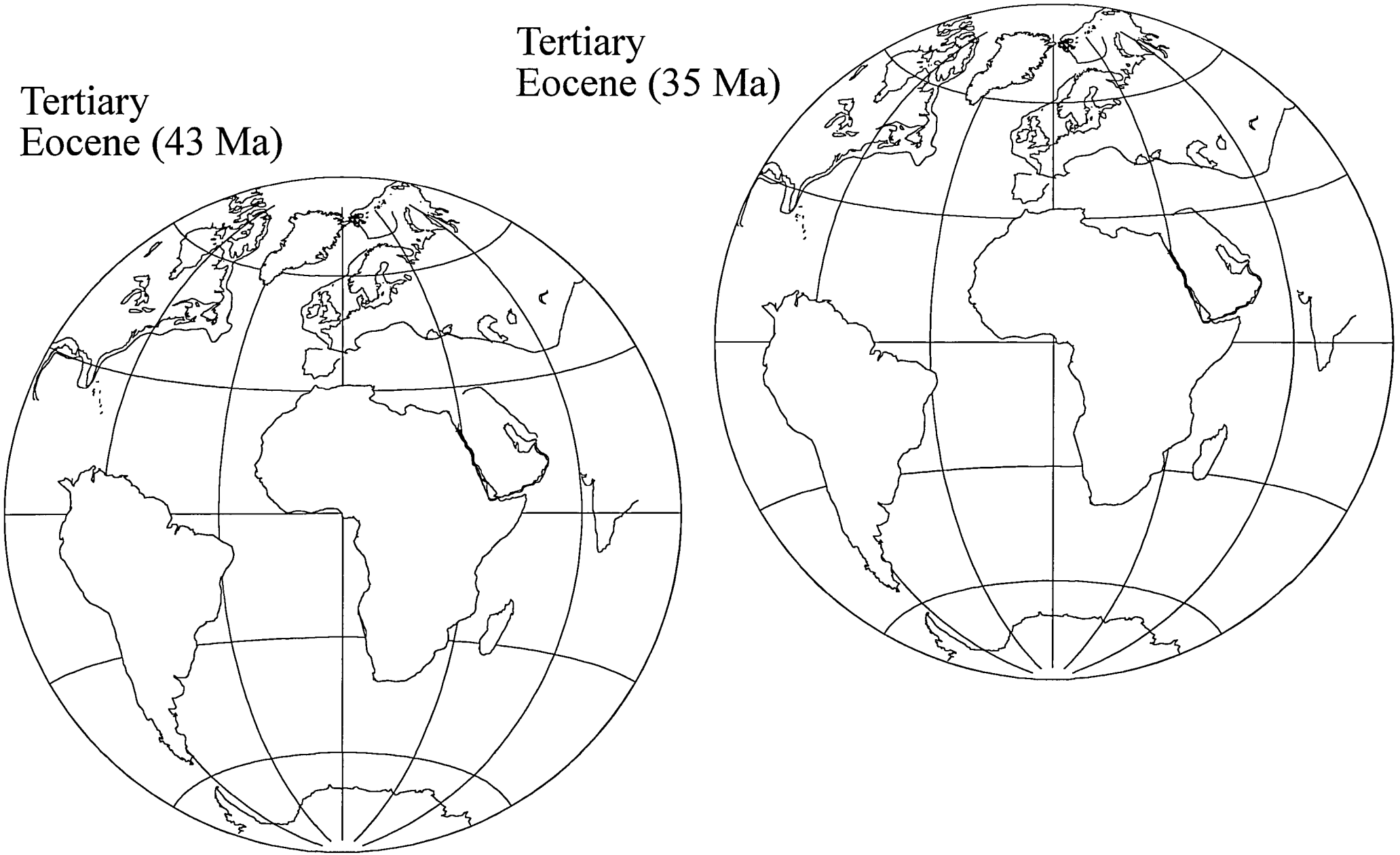

FIGURE 29
Eocene hot Spot (/magnetic anomaly) rReconstructions.

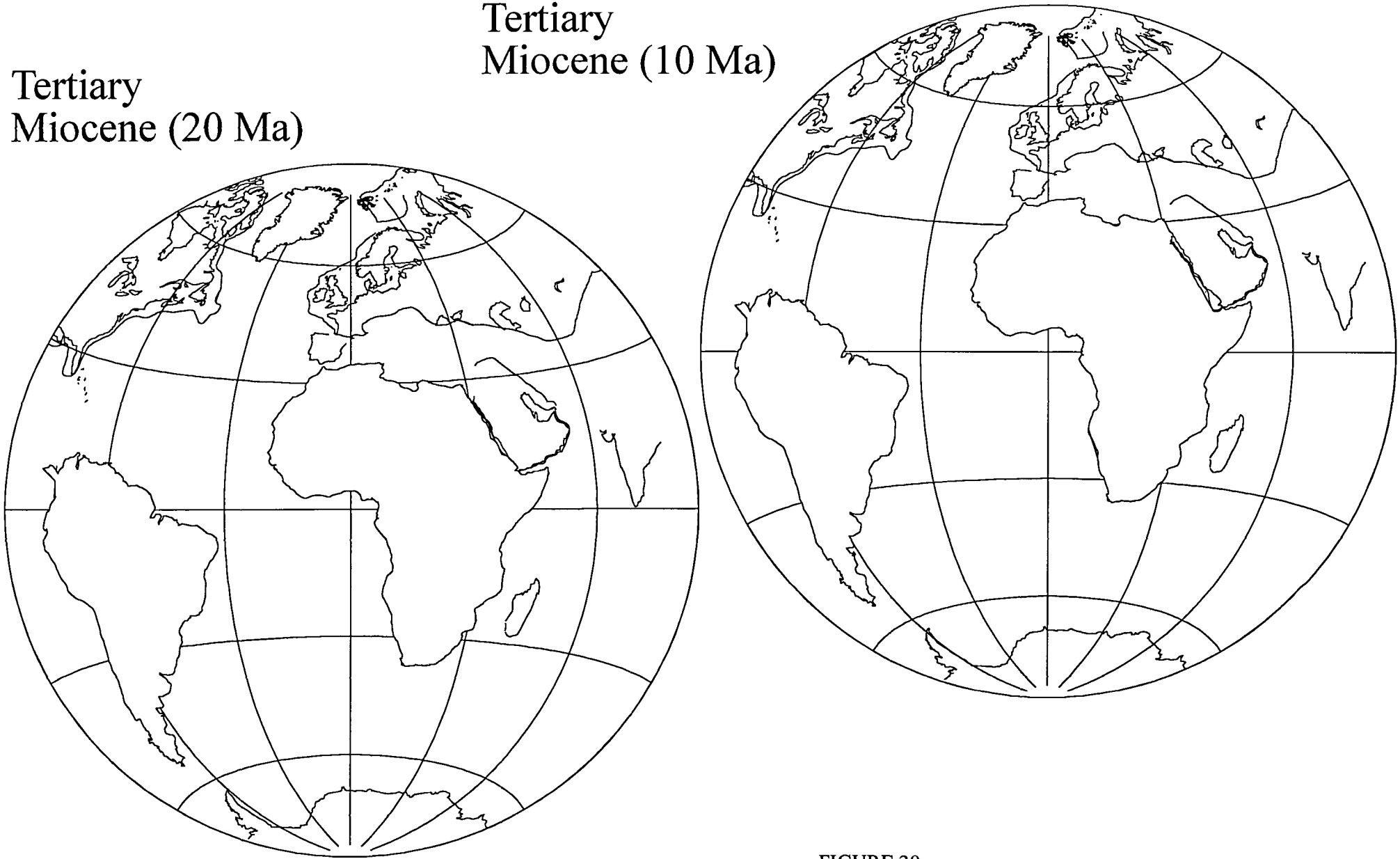

FIGURE 30
Miocene hot-Spot (/magnetic anomaly) reconstructions.

A)

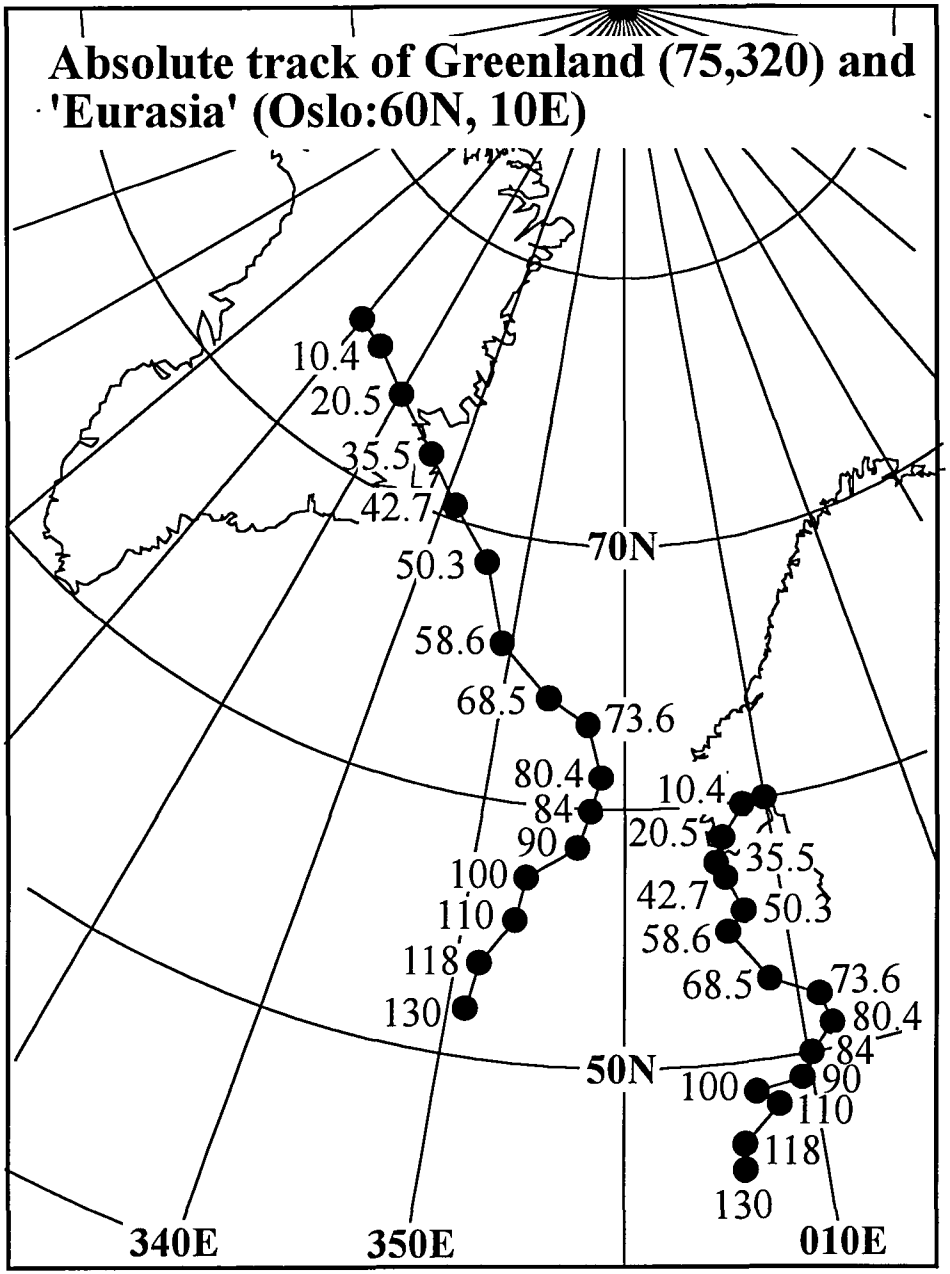

B)

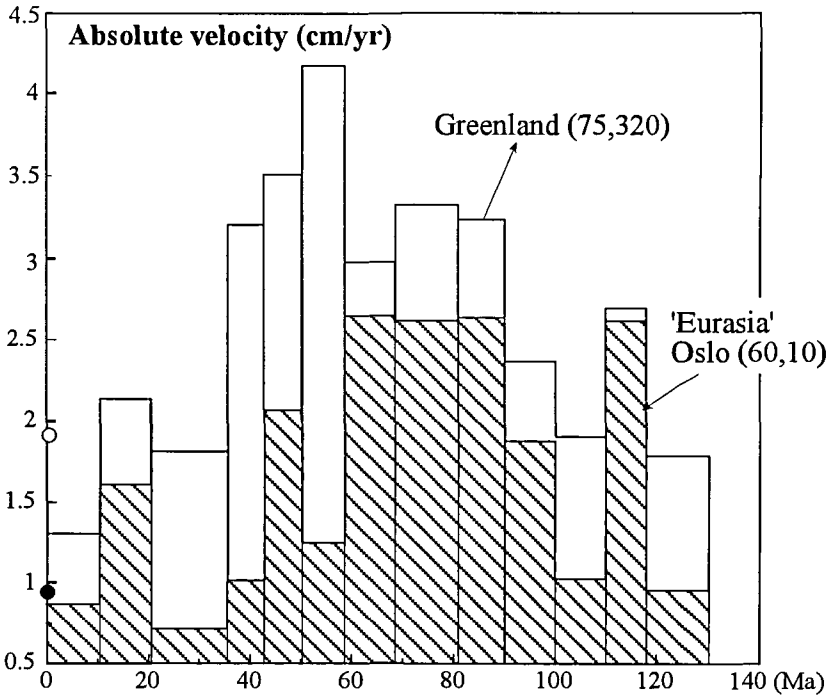

Absolute velocity in hot-spot reference frame (NUVEL-1):
○ Greenland (75,320):1.86 cm/yr (direction=251.7)
● 'EUR'/Oslo (60,10):0.93 cm/yr (direction=235.5)

FIGURE 31
(a) Absolute track of Greenland and 'Eurasia' in a hot-spot/magnetic anomaly frame
(b) Calculated aboslute velocities.

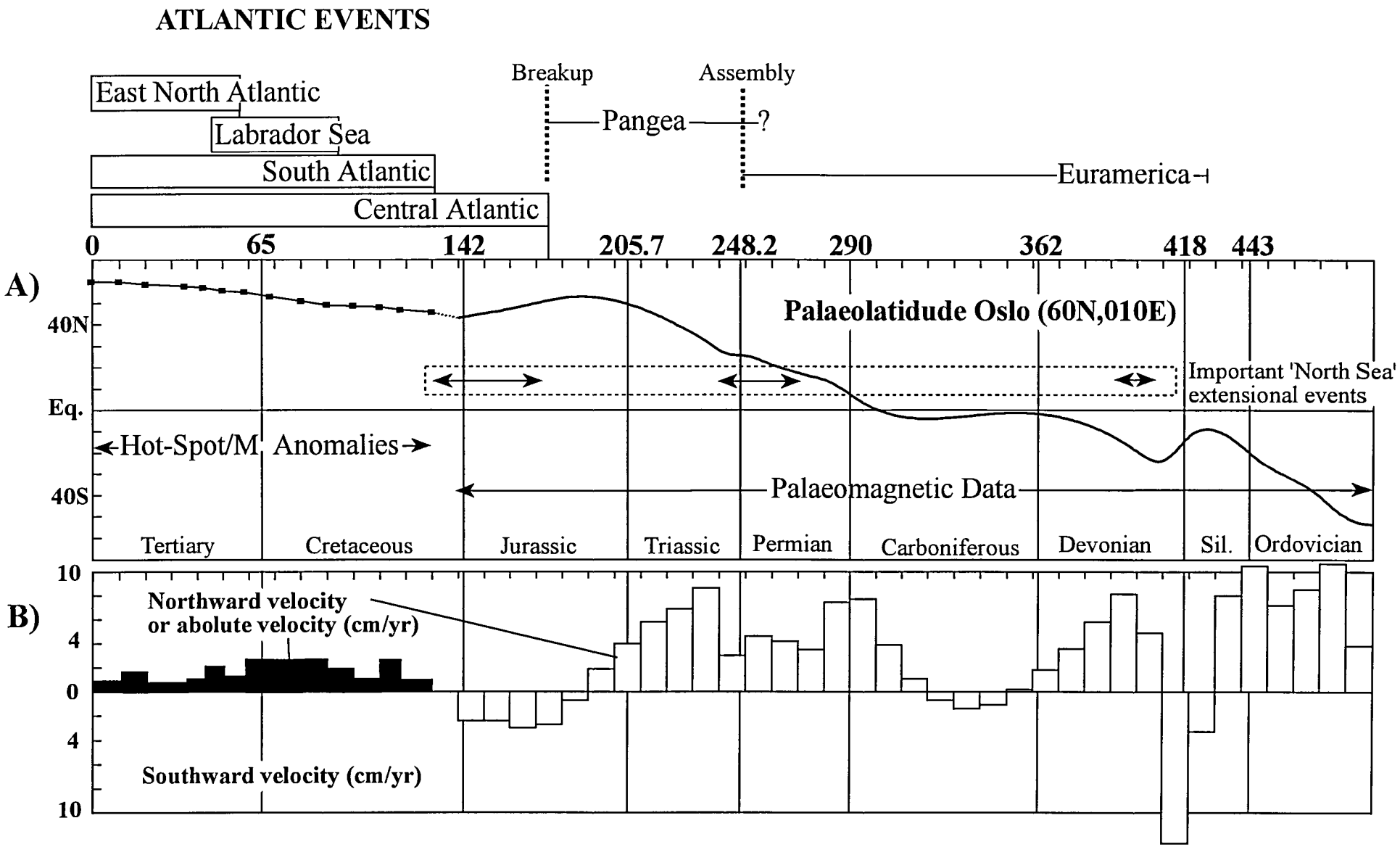

FIGURE 32
(A) Absolute track of Oslo (part of Baltica/Eurasia), (B) Absolute velocities for Oslo. Latitudinal position of Oslo in the interval 490-140 Ma is based on palaeomagnetic data. Absolute velocities 130-0 Ma based on hot-spot/magnetic anomaly data.